Development and analysis of recombinant fluorescent probes for use in live cell imaging of filamentous fungi

Kirsten Altenbach

PhD thesis

University of Edinburgh

2010

Declaration

This thesis has been composed by myself and the work, of which it is a record, has been carried out by myself. All sources of information have been acknowledged by means of reference.

Kirsten Altenbach
October 2010

Abstract

The molecular cloning and subsequent engineering of the green fluorescent protein (GFP) of the jellyfish *Aequoria victoria* allowed a novel approach to the investigation of cell signalling. GFP and its mutants can now not only be used to target specific organelles in living cells but also function as a basis for a variety of sensors for biologically important ions and molecular interactions.

GFP-based Ca^{2+}- sensors have been successfully used for studies in mammalian and plant cells. In filamentous fungi, however, they have not yet been reported to work. Since only little is known about calcium signalling in filamentous fungi, this project aimed to improve existing GFP-based Ca^{2+}- sensors by exchanging the original fluorophores for improved versions and expressing those in the filamentous fungus *Aspergillus niger*.

During this project, the donor and acceptor fluorophores of 3 existing Ca^{2+}-FRET-probes based on cameleons and troponin C-sensors, have been changed, 2 novel positive FRET controls have been designed and these , as well as donor and acceptor fluorophores alone, have been expressed in the filamentous fungus *Aspergillus niger*. The probes were assessed using different imaging techniques, such as conventional confocal laser scanning microscopy (CLSM), fluorescence lifetime imaging microscopy (FLIM) and spectral imaging using a Leica TSC SP5 confocal and IRIS, a novel spectral imaging device designed at Heriot Watt University. Problems were encountered that prevented FRET analysis using CLSM and IRIS. These were due mainly to the difference in expression level of the constructs and the distribution of the emission bandpasses of the IRIS system. Analysis of the spectral data obtained on the Leica confocal system and analysis of the FLIM results, however, revealed significant differences between the donor only and the positive FRET controls.

Spectra of the positive FRET controls and the Ca^{2+}-sensitive probes showed emission peaks of both the donor and the acceptor fluorophores upon excitation of the donor fluorophore alone while analysis of the FLIM results revealed an additional decay component in the positive FRET controls. Both results are very strong indicators that we can detect FRET in living hyphae of *Aspergillus niger* transformed with the probes designed during this project.

Contents

Chapter 1

Introduction

Fluorescent indicators have been developed for a variety of biologically important ions like calcium, hydrogen, magnesium, sodium, potassium and chloride and are used to investigate their role in different cell functions. The most successful and widely used probes have been designed for *in vivo* measurement of intracellular calcium concentrations and pH. Apart from showing a high selectivity for the ion of interest, ideal probes allow for accurate quantification of the ion concentration, provide a high spatial and temporal resolution and interfere as little as possible with normal cell functions.

1.1 Introduction to the research reported in this thesis

Since existing genetically encoded probes for imaging of intracellular Ca^{2+} concentration and pH had previously not been demonstrated in filamentous fungi, the aims of this project were to:

- develop novel genetically encoded probes based on existing Ca^{2+}-FRET sensors for imaging changes in intracellular Ca^{2+}-levels in filamentous fungi
- develop positive FRET controls based on the donor and acceptor fluorophores employed in the actual sensors
- express the developed probes and control constructs in *Aspergillus niger* for live cell FRET imaging
- assess different imaging techniques with regard to their suitability for live cell imaging and FRET analysis of the probes
- attempt to construct an *in vivo* calibration curve for the different Ca^{2+}-sensors
- analyse the genetically encoded pH-sensor RaVC using confocal microscopy

1.2 Fungal pH and pH-sensitive probes

In living cells, many cellular processes, including DNA transcription, protein synthesis and enzyme activities, are pH controlled. Many organisms, especially when able to grow over a wide pH range, tailor their gene expression to the pH of their environment. In *Aspergillus nidulans* for example, the genes subject to regulation by ambient pH can be classified into three categories (Peñalva and Arst, 2002): those encoding secreted enzymes; those encoding permeases; and those encoding enzymes involved in synthesis of exported metabolites.

1.2.1 Measuring pH in living cells

Methods for measuring intracellular pH have included the use of H^+-sensitive microelectrodes (Gerson and Burton, 1976), ^{31}P NMR (Barton et al., 1980; den Hollander et al., 1981; Hesse et al., 2000; Hesse et al., 2002; Plumridge at al., 2004), radiolabeled membrane-permeable weak acids (Gillies and Deamer, 1979; Schuldiner and Rozengurt, 1982; Anand and Prasad, 1989) and pH-sensitive fluorescent dyes (Haworth et al., 1991; Peña et al., 1995; Parton et al., 1997).
These methods require more or less extensive manipulation of the cells, which raises the question of how accurate the pH values detected with these methods really are.

A less invasive approach is possible by using pH-sensors based on green fluorescent protein (GFP). GFP is a 26.9 kDa protein first isolated from the jellyfish *Aequorea victorea* by Shimomura et al. in 1962. Its chromophore consists of 3 amino acids: Ser65, Tyr66 and Gly67 and is located in the centre of a barrel structure consisting of 11 β-strands (Ormö et al., 1996).

GFP based sensors can be expressed in the organism of interest and therefore do not require extensive pre-treatment of the cells. A further advantage of these probes is that they can be specifically targeted to different locations within the cells, allowing the study of the role of different organelles in pH homeostasis by the ability to monitor rapid localised changes in pH.

Wild-type GFP has a bimodal excitation spectrum (Ward, 1981; Ward et al., 1982) with peaks at 395 and 475 nm. Underlying the two maxima are protonated and deprotonated states of Tyr66, which forms part of the chromophore (Ward, 1981; Ward et al., 1982; Heim et al.,1991; Chattorai et al., 1996; Ormö et al., 1996; Yang et al., 1996 and Breje et al.,1997). Although critical residues exchange protons with the environment (Chattorai et al., 1996), the excitation spectrum of GFP is essentially unaltered between pH 5.5 and 10 (Ward, 1981). This implies that protonation-deprotonation reactions are constrained; a given GFP is trapped in either of two alternative conformations: in one the chromophore is protonated and can be excited at 395 nm, and in the other it is deprotonated and can be excited at 475 nm (Miesenböck et al., 1998).

To convert GFP into a pH sensor (pHluorins), Miesenböck et al. focused on amino-acid substitutions in positions known from X-ray crystallography (Ormö et al., 1996; Yang et al., 1996 and Breje et al., 1997) to be part of the proton-relay network of Tyr66 or to alter the excitation spectrum when mutated (Heim et al., 1991; Ormö et al., 1996; Ehrig et al., 1996 and Heim and Tsien 1996).

Since the development of pHluorins, targeted pHluorin fusion proteins have been used in several studies to measure dynamically the pH of various intracellular compartments, such as the cytoplasm (Karagiannis and Young, 2000), peroxisomes (Jankowski et al. 2001), endosomes and the *trans*-Golgi network (Machen et al., 2003).

1.2.2 Measuring pH in the filamentous fungus *Aspergillus niger*.

The probe used for pH-measurement in *A. niger* in this study, RaVC, is based on pHluorins and was developed by Tanja Bagar and Mojca Benčina at the National Institute of Chemistry, Ljubljana, Slovenia.

The gene encoding pHluorin (Miesenböck et al., 1998) was partially codon optimized to improve its level of expression with the result that RaVC produced a strong fluorescent signal within the fungal cells.
Parts of the original pHluorin cDNA were substituted by fragments of the fluorescent proteins Citrin (to improve expression, increase photostability and remove sensitivity to chloride) and Venus (to increase brightness of the probe and shorten maturation time of the chromophore). A detailed description of the design of RaVC can be found in Bagar et al., 2009.

The *in vitro* spectral characteristics of RaVC (Figure 1.1) are very similar to the original pHluorin (Miesenböck et al., 1998) from which it was derived, indicating that the modifications that were made did not alter its spectral properties or pH sensitivity (Bagar et al., 2009). Figure 1.1 a) shows the excitation spectra of partially purified RaVC in buffers of defined pH as determined on a spectrophotometer (Perkin Elmer LS 55). Excitation ranged from 350 nm to 500 nm (with a bandwidth of 5 nm) and emission was collected at the emission maximum of 508 nm (with a bandwidth of 5 nm). The spectra show excitation maxima at 395 nm and 475 nm and an isosbestic point at 428 nm. With increasing pH the ratio of fluorescence emission at the excitation maxima (395 nm/475 nm) increases (Fig. 1.1 a) and b)). The linear response of RaVC to pH is between pH 5.5 and 8.0 (Fig. 1.1 b). Minimum and maximum ratio values were therefore determined in buffers of pH 5.0 and pH 8.5. The pKa of RaVC as determined from the logarithmic plot of the fluorescence excitation ratio versus pH (Fig. 1.1 c) is 6.7.

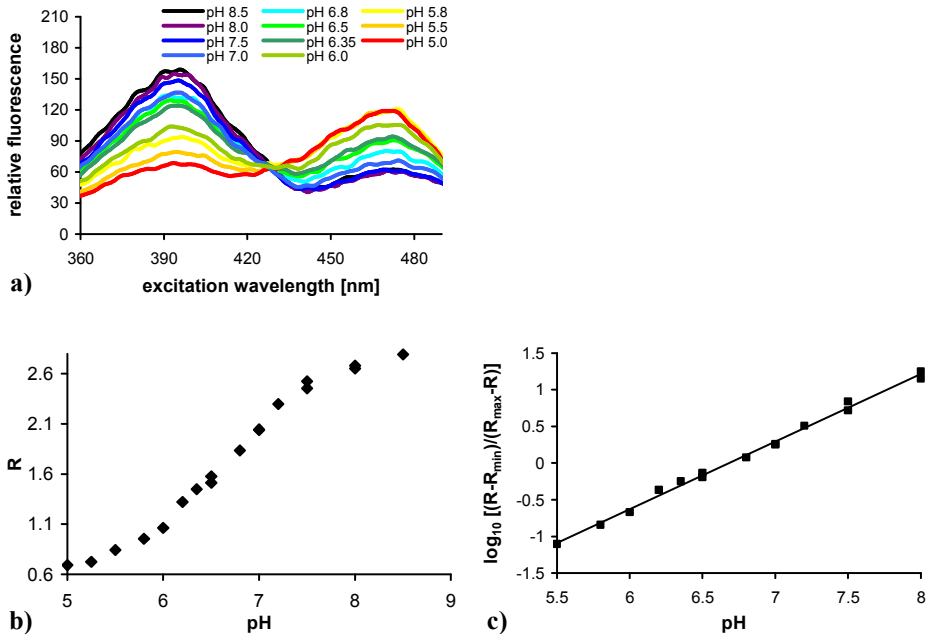

Figure 1.1: Fluorescent properties of the genetically encoded ratiometric probe RaVC. a) Fluorescence excitation spectra of RaVC in various pH-adjusted buffers b) *In vitro* calibration curve of RaVC presented as a plot of the fluorescence excitation ratio (395nm/475nm) versus pH. c) *In vitro* calibration curve of RaVC presented as a logarithmic plot of the fluorescence excitation ratio versus pH. (Bagar et al., 2009)

1.3 Calcium Signalling

1.3.1 Overview

Cells are highly responsive to signals from their environment. The signalling networks that have evolved to generate appropriate cellular responses by detection, amplification and integration of external signals vary and are generally composed of receptors, non-protein messengers, enzymes and transcription factors. Calcium stands out as a ubiquitous intracellular non-protein messenger, employed in all organisms, from prokaryotes to higher animals (Michiels et al., 2002; Gadd, 1994; Berridge et al., 2000; Carafoli, 2002; Sanders et al., 2002; Berridge et al., 2003). In eukaryotes calcium is involved in many signal-transduction pathways such as vision, the phosphoinositide cascade and the regulation of muscle contraction (Stryer, 1997).

The spectrum of stimuli evoking rapid changes in [Ca^{2+}] include abiotic stimuli like light, low and high temperature, touch and hyperosmotic as well as oxidative stress; biotic stimuli include the hormones abscisic acid (ABA) and gibberellin, fungal elicitors and nodulation (Nod) factors (Sanders et al., 2002).

Most Ca^{2+} systems function by generating brief pulses of Ca^{2+}. These Ca^{2+} transients are created by variations of basic on and off reactions (Berridge et al., 2003). During the on reactions, stimuli induce both the entry of external Ca^{2+} (driven by the presence of a large electrochemical gradient across the plasma membrane) and the formation of second messengers that release Ca^{2+} from the endoplasmic/sarcoplasmic reticulum (ER/SR). The release of Ca^{2+} from internal stores is controlled by Ca^{2+} itself, or by an expanding group of messengers (Bootman et al., 2002), such as inositol-1,4,5-trisphosphate (Ins(1,4,5)P_3), cyclic ADP ribose (cADPR), nicotinic acid adenine dinucleotide phosphate (NAADP) and sphingosine-1-phosphate (S1P), that either stimulate or modulate the release channels of the internal stores. Most of the Ca^{2+} is bound to buffers, whereas a small proportion binds to the effectors that activate various cellular processes operating over a wide temporal spectrum. During the off reactions, Ca^{2+} leaves the effectors and buffers and is removed from the cell by various exchangers and pumps.

The Na^+/Ca^{2+} (NCX) exchanger and the plasma-membrane Ca^{2+}-ATPase (PMCA) extrude Ca^{2+} to the outside, whereas the sarco(endo)plasmic reticulum Ca^{2+}-ATPase (SERCA) pumps Ca^{2+} back into the ER. Mitochondria also have an active function during the recovery process in that they sequester Ca^{2+} rapidly through a uniporter, and this is then released more slowly back into the cytosol. Cell survival is dependent on Ca^{2+} homeostasis, where the Ca^{2+} fluxes during on and off reactions exactly match each other.

The initial perception of a calcium signal occurs through the binding of calcium to many different calcium sensors which can be divided into two types, sensor relays and sensor responders (Sanders et al., 2002). Sensor relays, such as calmodulin and calcineurin B-like proteins, undergo a calcium-induced conformational change that is relayed to an interacting partner. The interacting partner then responds with a change in its conformation or enzymatic activity (bimolecular interaction, for example, calmodulin stimulation of an ACA calcium pump activity). In contrast, sensor responders undergo a calcium-induced conformational change (sensing) that alters the protein's own activity or structure (intramolecular interaction, e.g., activation of a Ca^{2+}-dependent protein kinase [CDPK]). Different CDPKs can be used to sense different calcium signals, and the specific activity of a given CDPK will depend on multiple factors, including its modification by other signalling pathways and its interaction with different downstream targets (Sanders et al., 2002).

Ca^{2+} is a potent activator of gene transcription (Carafoli et al., 2001; Crabtree 1999; Mellström et al., 2001; West et al., 2001; McKinsey et al., 2002), either functioning indirectly through protein kinases (CaMKII and CaMKIV) or protein phosphatases, such as calcineurin, to alter the phosphorylation state of various transcription factors. Alternatively, Ca^{2+} can promote gene transcription by recruiting either the Ras/mitogen-activated protein kinase (MAPK)- or cAMP-signalling pathways (Berridge et al., 2003). Furthermore, evidence that Ca^{2+} can alter the expression level of Ca^{2+}-signalling components such as pumps and channels is increasing (Carafoli et al., 1999; Guerini et al., 2000; Li et al., 2000; Genazzani et al., 1999; Graef et al., 1999).

1.3.2 Calcium signalling in fungi

Although little is known about Ca^{2+} signalling in fungi, particularly in filamentous fungi, the evidence for Ca^{2+} playing a crucial role in fungal signal transduction is growing constantly. Ca^{2+} concentration was demonstrated to have an important influence on establishing the correct cell polarity in *Schizosaccharomyces pombe* by regulating microtubule dynamics (Okorova et al., 2002). Furthermore several components of Ca^{2+}-mediated signalling of animal cells could be identified and characterised in this organism (Moser et al., 1997; Li et al., 1999). Isolation of the gene encoding the catalytic subunit of calcineurin in fission yeast allowed characterisation of calcineurin deficient cells (Yoshida et al., 1994). In these cells mating, microtubule distribution, chromosome segregation, spindle pole body and nuclear positioning were impaired indicating that Ca^{2+} homeostasis can have profound effects on cytoskeletal functions in fission yeast.

Calcium-mediated processes in *Saccharomyces cerevisiae* include the transcriptional response to alkaline pH (Serrano et al., 2002) and the defence response to antifungal treatment (Edlind et al., 2002). Not only does Ca^{2+} play an important role in signalling mechanisms of yeast, pharmacological studies indicate that in filamentous fungi Ca^{2+} signalling is involved in regulation of various processes such as secretion cytoskeletal organisation, hyphal tip growth, hyphal branching, sporulation, infection structure differentiation and circadian clocks (Gadd, 1994; Shaw and Hoch 2001).

Advances in genomic research provide further evidence for the presence of a Ca^{2+} signalling machinery in filamentous fungi. Analysis of Ca^{2+}-signalling proteins encoded in *Neurospora crassa*, *Aspergillus fumigatus* and *Magnaporthe grisea* led to the identification of fundamental Ca^{2+}-signalling proteins present in filamentous fungi, including previously unknown Ca^{2+}-permeable channels, Ca^{2+}-pumps and Ca^{2+}-transporters (Zelter et al, 2004).

1.3.3 Calcium sensitive probes

The different Ca^{2+} indicators available for measurement of intracellular calcium concentrations can be separated into the following 3 main groups: photoproteins; fluorescent dyes; fluorescent protein Ca^{2+} indicators.

1.3.3.1 Aequorin photoprotein

Photoproteins bioluminesce upon intramolecular reaction with Ca^{2+}. Aequorin, originally isolated from the jellyfish *Aequorea forskålea* (Shimomura et al., 1963) is the most commonly used photoprotein. The aequorin complex consists of apoaequorin, the luminophore coelenterazine and molecular oxygen (Inouye et al., 1985; Shimomura et al., 1988). When Ca^{2+} binds to aequorin, the molecular oxygen in aequorin is released, and the coelenterazine is oxidised to coelenteramide, resulting in the emission of blue light (465nm) (Takahashi et al., 1999). The mechanism of this reaction is shown in figure 1.2.

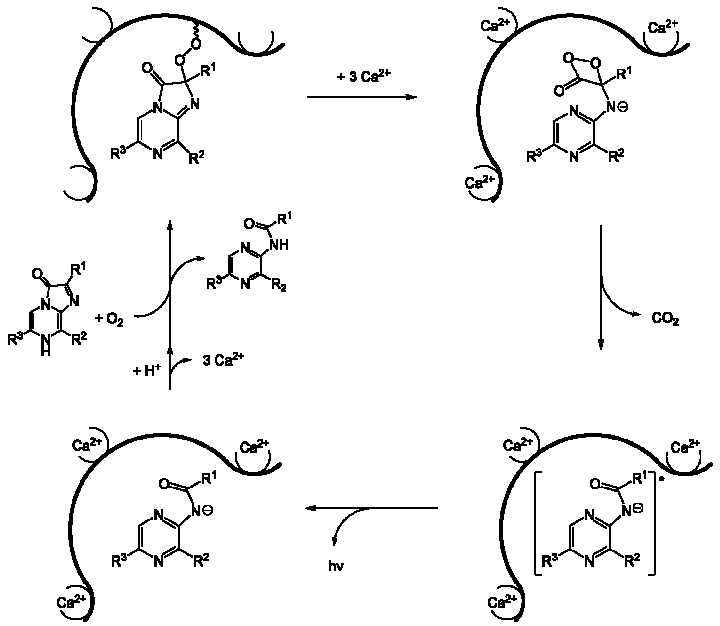

Figure 1.2: Mechanism of aequorin bioluminescence (light reaction of coelenterazine in aequorin)

1.3.3.2 Calcium sensitive dyes

Some fluorescent dyes show altered excitation or emission properties upon binding Ca^{2+}. The majority of these indicators are based on the Ca^{2+} chelator bis-(*o*-amino-phenoxy)-ethane-*N, N, N', N'*-tetra acetic acid (BAPTA, see figure 1.3)) .

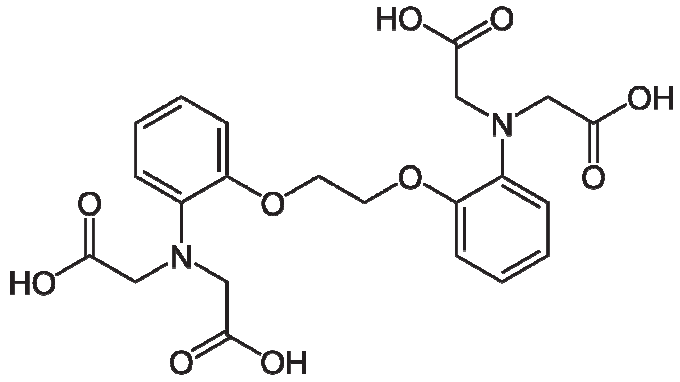

Figure 1.3: Chemical structure of BAPTA

Fluorescent dyes can be separated into single (non-ratiometric) and dual wavelength (ratiometric) dyes, the latter offering the possibility to correct for uneven dye distribution.

1.3.3.3 Fluorescent protein Ca^{2+} indicators

Fluorescent protein Ca^{2+} indicators are based on conjugates between calmodulin and fluorescent proteins. Binding of Ca^{2+} induces conformational changes that subsequently alter the probe's fluorescence properties.

The development of Cameleons, new fluorescent indicators for Ca^{2+} that are genetically encoded without cofactors and are targetable to specific intracellular locations (Miyawaki et al;, 1997), allows measurement of highly localized Ca^{2+} signals in the cytosol and organelles.

Advantages and limitations of different Ca^{2+} indicators are summarised in the following table:

Table 1.1: Characterisation of various Ca^{2+}-sensitive indicators as adapted from Brownlee, 2000.

Indicator	Usual loading methods	Advantages	Limitations
Aequorin	Injection	Low Ca^{2+} buffering	Low signal, integration normally required
	Transfection	Wide dynamic range	Single wavelength, non-ratiometric
		Low background	Potential calibration problems
		Targeting to subcellular components	Incubation with coelentrazine required to reconstitute functional aequorin
		Transfection is non-disruptive	
Fluorescent dyes		High spatiotemporal resolution	Unwanted compartmentalization of non-dextran conjugates
		Use with lifetime imaging and confocal microscopy	
	AM- ester loading	Simple loading method	Buffering at high loading concentrations
		Range of affinities for different applications	Not applicable to all cells
		Combination with electrophysiology	
	Patch loading	Co-injection with other reporters/factors/dye combinations	
	Microinjection	Dextran conjugates available for some dyes	Invasive
Single wavelength		Longer wavelength for use with most confocal applications	Calibration uncertainties
		Use with UV-Photolysis of caged compounds	Uneven dye distribution
Dual wavelength		Ratio calibration more reliable	Need for UV excitation
		Cell thickness and dye distribution artefacts reduced	
Fluorescent proteins	Transfection	Targeting to organelles or cell types	Potential buffering problems at high expression levels
		Use with confocal, multiphoton or CCDs	
		Range of affinities	

1.4 *Aspergillus niger* as the experimental system

The organism studied in this project is the filamentous fungus *Aspergillus niger* (Figure 1.4). It grows aerobically on organic matter and (in nature), can be found in the soil, on decaying plant material and in compost (Schuster et al., 2002).This fungus is industrially important for large-scale production of organic acids, especially citric acid and enzymes such as starch degrading and plant cell wall degrading enzymes like pectinases, (hemi) cellulases and xylanases.

Gene technology has been employed to improve production processes and to use *A. niger* as an expression system for foreign proteins (Schuster et al., 2002).

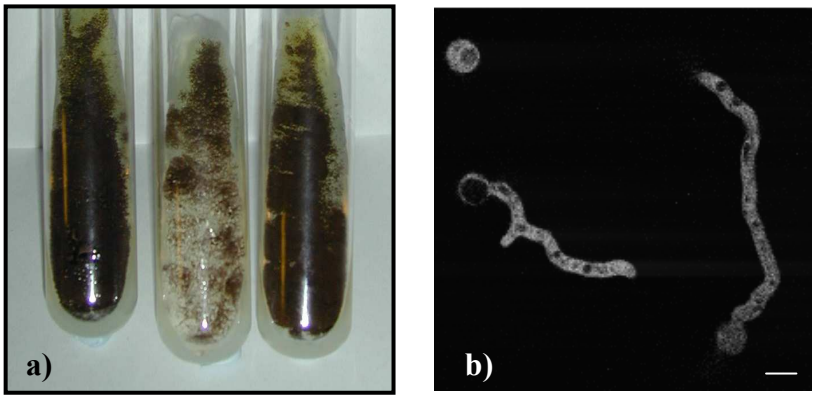

Figure 1.4: Images of *Aspergillus niger* as used in this study. a) Photograph of 7 day old cultures grown on agar slants. b) confocal image of 18 h old hyphae of *A. niger* expressing mCerulean. mCerulean was excited at 405 nm and emission collected between 470 nm to 490 nm. Bar = 10 µm.

The ability of *A. niger* to acidify its medium to pH values below 2.0 during production of organic acids (Ruijter et al. 1997) implies that a very efficient pH-homeostatic system exists in these cells.

Hesse et al. reported in 2002 that *A. niger* maintained constant cytoplasmic pH and vacuolar pH values of 7.6 and 6.2, respectively, when the extracellular pH was varied between 1.5 and 7.0.

This is not surprising considering how well adapted microorganisms are to their environment, nevertheless it poses the question as to the way in which the acid gets excreted into the medium and if localized changes in pH occur during this process. To study this aspect a pH sensor that enables monitoring of localised changes in pH within cells is essential.

The recent sequencing of the genome of *A. niger* by Pel et al. in 2007 allowed for the first time the identification of proteins regulating the intracellular concentration of calcium ions and protons in this fungus by comparative genomic analysis (Benčina et al. 2009). Figure 1.5 shows some of the proteins as identified by Benčina et al. to be part of the Ca^{2+}- and pH homeostatic systems in *Aspergillus niger.*

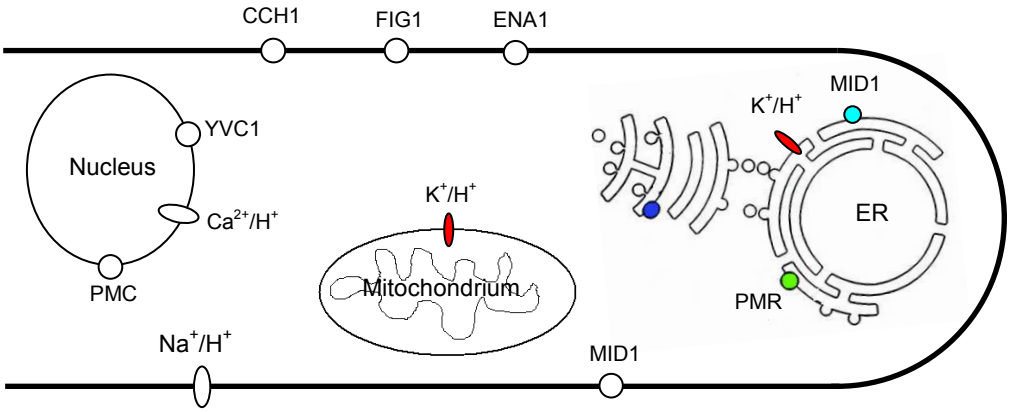

Figure 1.5: Model of fungal hypha showing different components of calcium signalling and pH-homeostasis in *A. niger* as identified by Benčina et al (2009), adapted from Bagar, 2009. MID1, CCH1, YVC1 and FIG1 are Ca^{2+}-channels; ENA1, PMR and PMC ATPases and $Ca2^{+}/H^{+}$, Na^{+}/H^{+} and K^{+}/H^{+} are cation/proton antiporters.

The ATPases ENA1, PMR and PMC hydrolyze ATP to drive the active transport of Ca^{2+} and H^{+} across biological membranes. The identified Ca2+-channels fall into different categories according to their working mechanism. MID1 is stretch activated, CCH1 voltage gated, FIG1 a low affinity and YVC1 a transient receptor potential Ca^{2+} channel. The final group of proteins shown to be involved in the regulation of calcium and proton concentration in Aspergillus are the cation/proton antiporters. These reduce the level of cations in the cytoplasm to resting level and transport Ca^{2+} and H^{+} across membranes.

1.5 FRET

FRET (Fluorescence Resonance Energy Transfer) is a quantum mechanical phenomenon based on the ability of a higher energy donor fluorophore to transfer energy directly and without radiation to a lower energy acceptor molecule, causing sensitised fluorescence of the acceptor molecule and simultaneous quenching of the donor fluorescence. FRET as a physical phenomenon was first described by Förster in 1948.

If a molecule in the energetic ground state S_0 absorbs a photon an electron is excited to a higher energy level,the excited state S_1 (Figure 1.6). In general, the vibronic levels of the singlet state S_1 and those above overlap and hence, regardless of the level reached initially, internal conversion relaxes the molecule to the lowest vibronic level of S_1.

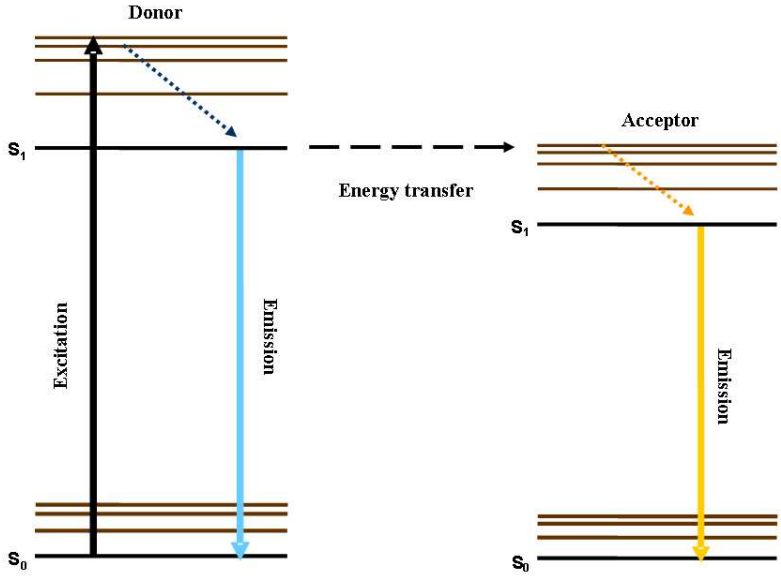

Figure 1.6: Modified Jablonski diagram for FRET. S_0 = electronic ground state, S_1 = excited singlet state; the vibronic energy states are shown in brown.

The return to the ground state can occur radiatively as fluorescence or via non-radiative quenching processes such as FRET (Webb, 2003).

In the case of fluorescence, the emitted photon has a lower energy than the absorbed photon and has a longer wavelength than the excitation light (Stokes' shift).

Prerequisites for FRET as reviewed by Gadella et al., 1999 are:

- The donor must be fluorescent
- There must be a spectral overlap between donor fluorescence and acceptor absorbance (Figure 1.7)
- The distance between donor and acceptor must be < 2 x R_0 (R_0 = Förster radius)
- The donor and acceptor transition moments should not be perpendicular

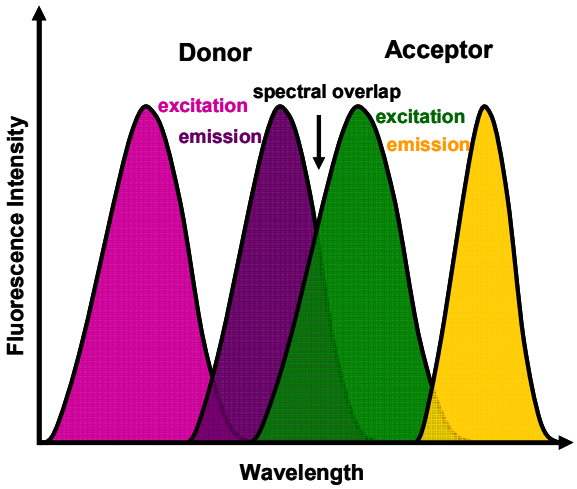

Figure 1.7: Schematic representation of the FRET spectral overlap integral

The efficiency of FRET is given by the expression $R_0^6/(R_0^6+r^6)$, where r is the actual distance between the donor and acceptor chromophores and R_0 is the Förster radius, the donor-acceptor distance at which FRET is 50% efficient. R_0 depends on the quantum yield of the donor, the extinction coefficient of the acceptor, the overlap of the donor emission and acceptor excitation spectra and the mutual orientation of the chromophores. Combinations of cyan donors and yellow acceptors have R_0 values of 49-52 Å (Tsien, 1998).

Experimental quantification of FRET as reviewed by Gadella et al. (1999) can be obtained by measuring the following parameters:

- Reduction of donor fluorescence intensity (or quantum yield):

$$E = 1 - \frac{I_{D+A}}{I_{D-A}}$$

(I_{D+A} = donor fluorescence in the presence of the acceptor, $I_{D\text{-}A}$ = donor fluorescence in the absence of the acceptor)

- Decrease in donor fluorescence lifetime (τ):

$$E = 1 - \frac{\tau_{D+A}}{\tau_{D-A}}$$

(τ_{D+A} = donor fluorescence lifetime in the presence of the acceptor, $\tau_{D\text{-}A}$ = donor fluorescence lifetime in the absence of the acceptor)

- Increase in acceptor fluorescence (so-called sensitised emission):

$$E = \frac{\varepsilon_A}{\varepsilon_D}\left[\frac{I_{D+A}}{I_{D-A}} - 1\right]$$

1.5.1 FRET probes

FRET indicators find application in 3 main areas of scientific interest, namely, protein-protein interaction, investigation of conformational changes on a molecular basis and the exploration of proteolytic processing of proteins *in vivo* (Figure 1.8).

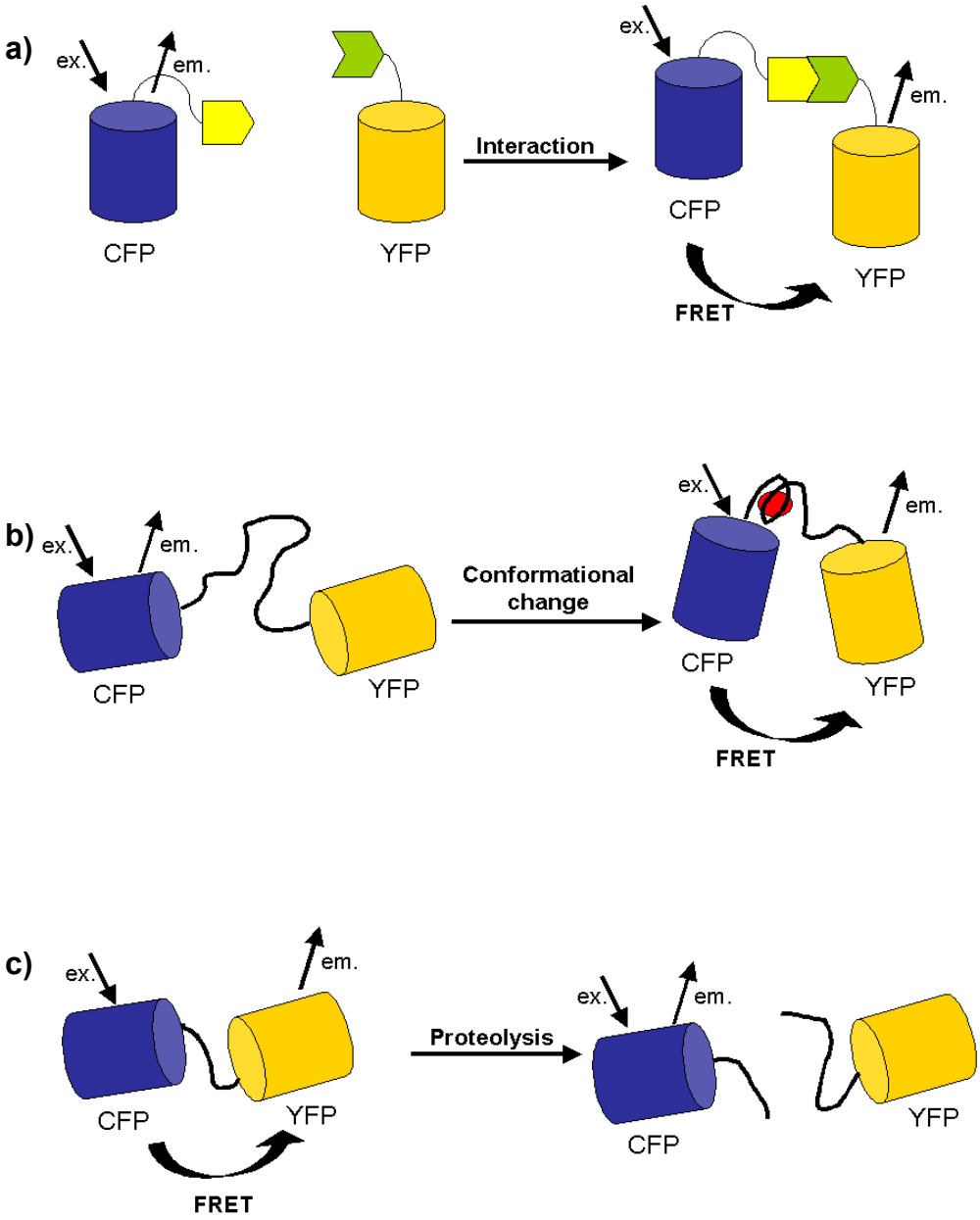

Figure 1.8: Possible uses of GFP-based FRET indicators, adapted from Gadella et al. (1997). a) protein-protein interaction, b) molecular conformational changes, c) proteolytic processing of proteins

To monitor protein-protein interactions via FRET (Figure 1.8 (a)), two separate fusion proteins consisting of the first protein fused to the donor fluorophore and the putative interacting partner fused to the acceptor fluorophore respectively are co-expressed in the cell type of choice. As donor and acceptor fluorophores need to be in close proximity for FRET to occur, detection of FRET in the sample cells provides direct evidence of protein-protein interaction.

The second area of application is the study of molecular conformational changes (Miyawaki et al., 1997, 1999) using sandwich-like fusion-proteins of a donor fluorophore, a protein of interest and an acceptor fluorophore (Figure 1.8 (b)). It is crucial that the protein of interest can be induced to undergo a conformational change that alters the proximity and/or relative orientation of the fluorophores, thereby changing the intramolecular FRET efficiency. In this way monitoring FRET efficiency can be used to investigate phosphorylation events as well as ligand- and ion-binding.

Finally, FRET indicators offer the possibility of investigating the proteolytic processing of proteins *in vivo*. Again, a tandem fusion of a donor-acceptor fluorophore pair and a protein of interest (or part thereof) is constructed (Pollok and Heim, 1999) (Figure 1.8 (c)). When the protein of interest is intact, FRET can be observed. As soon as the protein becomes cleaved the parts dissociate, the distance between the fluorophores increases and the FRET efficiency decreases.

Over the past years the number of available FRET probes has vastly increased. Although a large number of suitable fluorophores exist, it was the molecular cloning (Prasher et al., 1992) and subsequent engineering (Tsien, 1998) of the green fluorescent protein (GFP) from *Aequorea victoria* that took FRET imaging to a new level. Mutations of GFP (Heim et al, 1994; Tsien, 1998) and the discovery of coral derived proteins (Matz et al. 1999) resulted in a variety of donor and acceptor pairs becoming available for FRET imaging.

CFP and YFP pairs, as initially used by Miyawaki et al in 1997, and their improved variants such as mCerulean (Rizzo et al., 2004) and mVenus (Nagai et al. 2002) and mCitrine (Griesbeck et al., 2001) remain the most widely used.

The ideal FRET pair would be defined as a combination of fluorophores which allow selective excitation of each fluorophore and collection of their distinct fluorescence emission while at the same time displaying a maximum FRET efficiency.
Such a pair does not exist, but by considering the following parameters when choosing two fluorophores for a FRET sensor one can influence the ease of data collection and analysis as well as the possible FRET efficiency:

- Maximal overlap of donor emission and acceptor excitation
- Minimal direct excitation of the acceptor at the excitation wavelength used for the donor
- Well separated emission spectra of donor and acceptor

Since the spectra of fluorescent proteins are usually broad, an overlap of donor and acceptor excitation and emission spectra can generally not be completely avoided. Therefore it is important to design the experiments carefully and keep potential spectral bleedthrough in mind when analysing the data.

Bearing in mind the difficulties of FRET analysis when designing the probes can be a major advantage. A smaller overlap of donor emission and acceptor excitation of originally chosen fluorophores may, for example, be improved by selecting a donor variant with a higher quantum yield and an acceptor variant with a higher extinction coefficient as compared to the original fluorophores, to maximise the FRET signal (Piston and Kremers, 2007).

The fluorophore pairs used in this project are mCeruelan -Venus and mCerulean-mCitrin. The excitation and emission spectra of mCerulean and Venus are shown in Figure 1.9 (mCitrin spectra are essentially identical to Venus ones and have therefore been omitted).

As can be seen in Figure 1.9 a) and b), the clear separation of the two excitation spectra and overlap of Cerulean emission with the Venus excitation spectrum make these two fluorophores a good FRET pair. However, when looking at the emission spectra (Figure 1.9 c), it is apparent that the extensive overlap of the two spectra may cause difficulties.

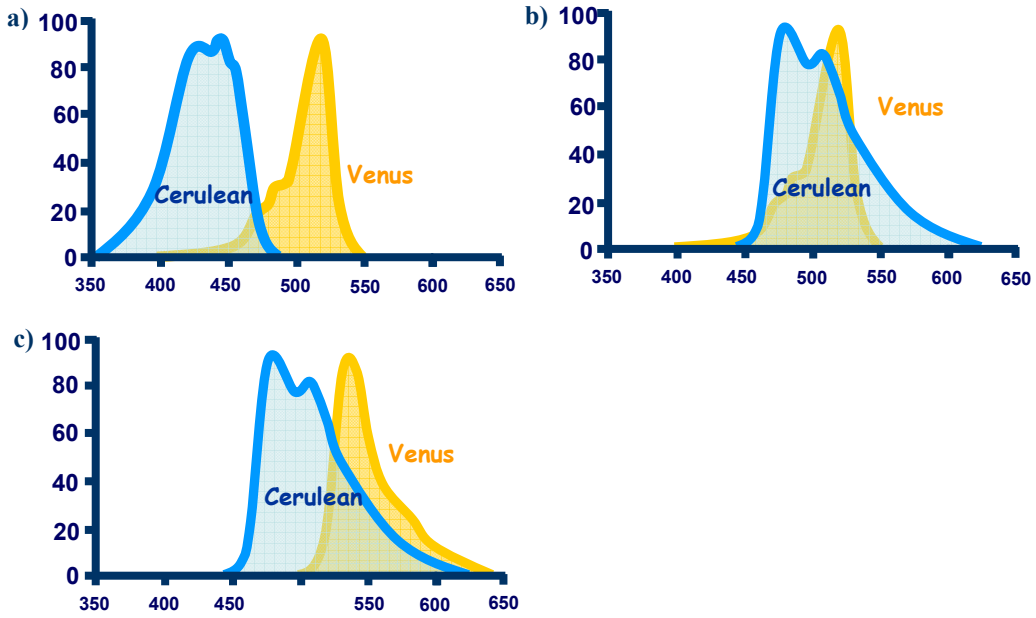

Figure 1.9: Excitation and emission spectra of mCerulean (donor) and Venus (acceptor).
a) Cerulean and Venus excitation spectra, b) overlap of mCerulean emission and Venus excitation spectra, c) overlap of mCerulean and Venus emission spectra

Venus and mCitrin are optimized versions of YFP, due to different mutations in each of these fluorophores when compared with the original YFP, they show minor variations in their emission and excitation spectra as well as differences as far as their fluorescence properties are concerned (see Table 1.2).

Table 1.2: Fluorescence properties of mCitrin and Venus, adapted from Shaner at al., 2005

Protein	mCitrin	Venus
Exc. max (nm)	516	515
Em. max (nm)	529	528
Extinction coefficient ($M^{-1}cm^{-1}$)	77000	92200
Fluorescence quantum yield	0.76	0.57
Brightness (EC*QY) $(mM*cm)^{-1}$	59	53
$t_{½}$ for bleaching (sec)	49	15
pKa	5.7	6

1.5.2 Cameleon Ca^{2+}-sensors and their improvements

The development of Cameleons, new fluorescent indicators for Ca^{2+} that are genetically encoded without cofactors and are targetable to specific intracellular locations (Miyawaki et al., 1997), allows measurement of highly localized Ca^{2+} signals in the cytosol and organelles. Cameleon-indicators consist of tandem fusions of a blue- or cyan-emitting mutant of the green fluorescent protein (GFP), calmodulin (CaM), the calmodulin-binding peptide M13, and an enhanced green- or yellow- emitting GFP (Fig. 1.10).

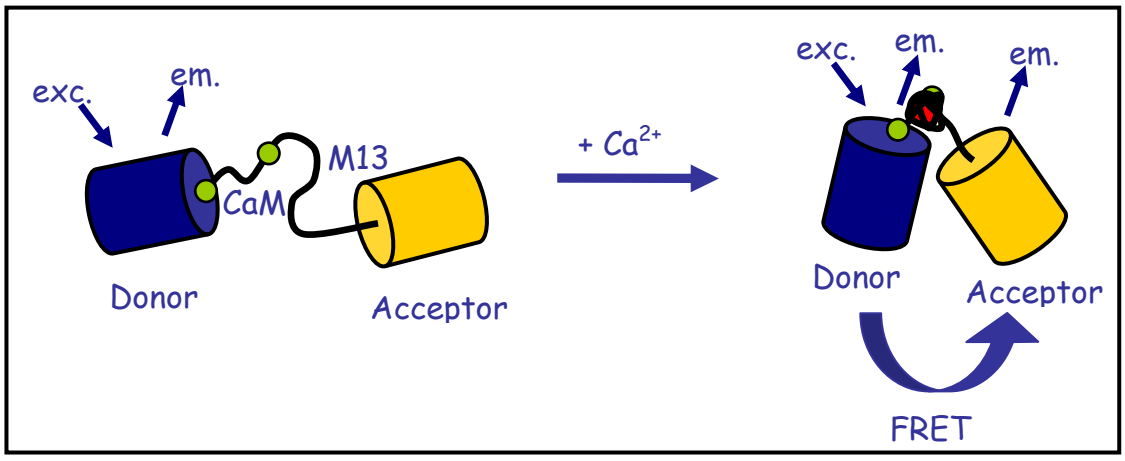

Figure 1.10: Schematic structures and sequences of cameleons, adapted from Miyawaki et al., 1997

Binding of Ca^{2+} results in calmodulin wrapping around the M13 domain thereby increasing the fluorescence resonance energy transfer (FRET) between the flanking GFPs (Heim and Tsien, 1994). Miyawaki et al. (1997) describe visualisation of free Ca^{2+} dynamics in the cytosol, nucleus and endoplasmic reticulum of single He La cells transfected with complementary DNAs encoding chimaeras bearing appropriate localization signals. Calmodulin mutations offer the ability to measure free Ca^{2+} concentrations in the range of 10^{-8} to 10^{-2} M.

Initial advances were made by introducing enhanced BFP and GFP [cameleon-2 (Miyawaki et al., 1997)], thereby improving expression and folding of the fluorophores in mammalian cells and resulting in higher fluorescence levels. By replacing EBFP and EGFP with ECFP and EYFP, respectively, fluorescence could be even further increased [yellow cameleon-2 (YC2)]; nonetheless the modifications resulted in minor disadvantages of these probes when compared to the first generation of cameleons. Shortcomings displayed by these probes are a decrease in the maximal ratio change of donor fluorescence emission to accepter fluorescence emission (1.5 fold) as compared to the original cameleon (1.8 fold) and that they are perturbed by acidification below pH 7.0, which mimics a fall in Ca^{2+} (Miyawaki et al., 1997).

Two of the probes analysed in this project are based on the 2.1 and 6.1 versions of the original YC indicators. YC 2.1 displays a biphasic Ca^{2+} binding curve with two apparent dissociation constants (100 nM and 4.3 μM). This property has been considered to be one of the desired characteristics of YC 2.1 since it can respond to free Ca^{2+}- concentrations over a range from 0.01 to 100 μM (Miyawaki et al., 1997).

The 2.1 version of the Yellow Cameleon has previously been improved by exchanging EYFP for the faster maturing and less pH-sensitive Venus (Nagai et al., 2002), leading to YC 2.12.

Following on from this progress the cameleon-type probes developed for this project contain Venus as acceptor fluorophore and mCerulean, an improved variant of ECFP (Rizzo et al., 2004) as donor fluorophore. Due to its increased extinction coefficient and quantum yield as compared to ECFP, Cerulean is 2.5 fold brighter than ECFP, resulting in an improved signal to noise ratio (Rizzo et al., 2004).

In an unstimulated eukaryotic cell, the concentration of free Ca^{2+} in the cytoplasm is approximately 0.1 μM, often rising to 1 μM following stimulation (Berridge et al., 2000). Hence it is advantageous to have an indicator with enhanced coverage in this physiologically relevant range. Based on the NMR structure of CaM in complex with the CaM-dependent kinase kinase (CKKp), Truong et al. (2001) designed a new cameleon probe (YC 6.1) that exhibits twofold increase in the FRET dynamic range within the physiologically significant range of cytoplasmic Ca^{2+} concentrations. Instead of being linearly combined with CaM like the M13 protein in previous cameleon probes, the CaM binding protein in YC 6.1 is fused at the linker region between the N- and C-terminal domains of CaM.

.

YC6.1 displays a monophasic Ca^{2+} binding curve with a single apparent dissociation constant of 110 nM, thus responding to free Ca^{2+} concentrations ranging from 0.05 to 1 μM (Truong et al., 2001). Although YC2.1 covers a larger range of free Ca^{2+} concentration than YC6.1, the emission ratio change of YC2.1 is distributed across this entire Ca^{2+} range, hence a smaller dynamic range is available for applications focused on specific Ca^{2+} concentrations. In contrast, the dynamic range of YC6.1 applies to the cytoplasmic free Ca^{2+} concentrations thus expanding the ability of cameleons to visualize Ca^{2+} mobilization in living cells where a high sensitivity is required for detection.

A new generation of calcium sensors was developed by Heim and Griesbeck in 2004. They developed different linkers based on chicken skeletal muscle Troponin C, a specialized Ca^{2+} binding protein regulating muscle contraction.

Since this is the only known function of TnC, and no additional binding peptide is included in these sensors, it is expected these sensors will only interfere minimally with biochemical processes within the host cell, thus overcoming calmodulin-related difficulties of cameleons.

One of the sensors used in this study is based on TN-L15, where truncated chicken skeletal muscle TroponinC (in which the N-terminal amino acid residues 1-14 are deleted) is inserted between CFP and mCitrine. With a K_d of 1.2 μm this probe responds well to changes in Ca^{2+} concentration between 0.1 and 10 μm (Heim and Griesbeck, 2004).
ECFP in the original TN-L15 plasmid kindly provided by O. Griesbeck was replaced with mCerulean, an approach that has subsequently been adopted and published by Heim et al in 2007. We named the probe obtained in this way TN-L15mCer.

In addition to the donor-only (mCerulean) and acceptor-only (Venus or mCitrin) constructs, positive FRET controls (CeVe and CeCi) were developed and expressed in *Aspergillus niger*. In these probes a short, 8 amino acid long linker (MHGGSGGTE) separates the donor and acceptor fluorophores. This linker should keep the chromophores of the two fluorophores at a short enough distance to allow them to continuously exhibit FRET and permit determination of the maximum FRET efficiency for the probes expressed in *A. niger*.

1.6 FRET-Imaging Techniques

1.6.1 Spectral Imaging

Spectral imaging offers a greater insight into the fluorescence spectra of fluorophores expressed in living cells than simple comparison of fluorescence intensities in one or two emission channels. Most modern confocal systems already allow performance of spectral scans to simultaneously collect fluorescence spectra and images of fluorescent proteins expressed in the organism of interest. For ratiometric probes like cameleons this is especially useful to set up and optimize protocols for image acquisition. Despite fluorescence spectra being widely available for most of the commonly used fluorophores, expressing these in different organisms can result in slight changes in the spectral properties. Knowing the true spectra of one's probe is particularly useful when choosing an emission bandwidth for collecting distinct signals of two or more fluorophores expressed together.

1.6.1.1 IRIS – Spectral imaging in a shapshot (adapted from Harvey et al. 2005)

A novel spectral imager, developed at Heriot-Watt University, Edinburgh was assessed as new approach to imaging fluorescent probes in living cells.
The new filter, named IRIS (Image Replicating Imaging Spectrometer) achieves spectral filtering and image replication at the same time, yielding a two-dimensional snapshot spectral imager. The principle of operation can be considered as a generalisation of the Lyot filter to achieve multiple bandpasses. The Lyot filter (Lyot, 1933 and 1944; Ohman, 1938 and 1958) employs polarising interferometry within multiple waveplates to yield a narrow-band filter suitable for recording monochromatic images. Light not transmitted by the Lyot filter is absorbed by film polarisers. In IRIS, the film polarisers are replaced with Wollaston prism polarising beam splitters as shown in Figure 1.11.

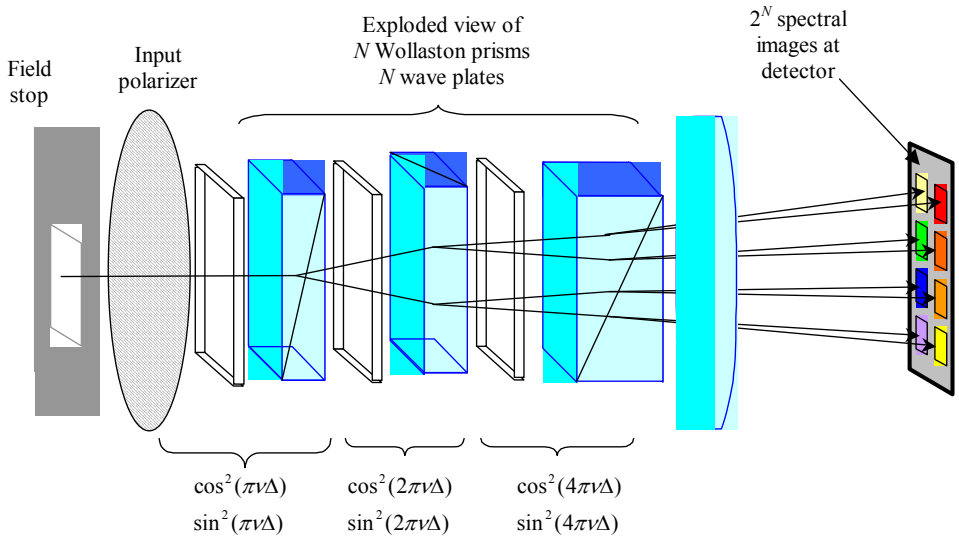

Figure 1.11: Illustration of the principle of operation of IRIS

The use of a polarising beam splitter means that after transmission through each waveplate the light is resolved into polarisations, both aligned with and orthogonal to, the input polarisation state. After transmission through n Wollaston prism polariser pairs 2^n replicated images are formed. The eight pass bands for the original IRIS employing three Wollaston Prisms are shown in Figure 1.12:

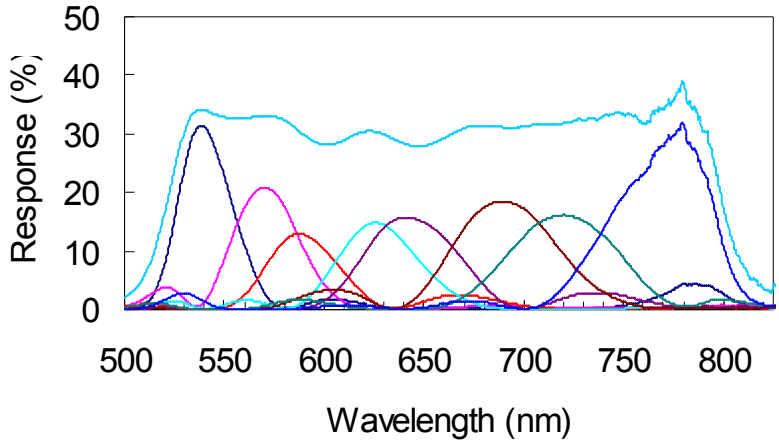

Figure 1.12: Band passes of the original IRIS 8 channel system.

A schematic view of an assembled 8-channel IRIS system is shown in Figure 1.13. It consists of an image relay system with an intermediate image plane. The IRIS components are located close to the pupil plane of the image relay system, replicating the image formed at the field stop onto the detector array. The field stop, or intermediate focal plane, is required to prevent overlapping of the replicated images at the detector plane.

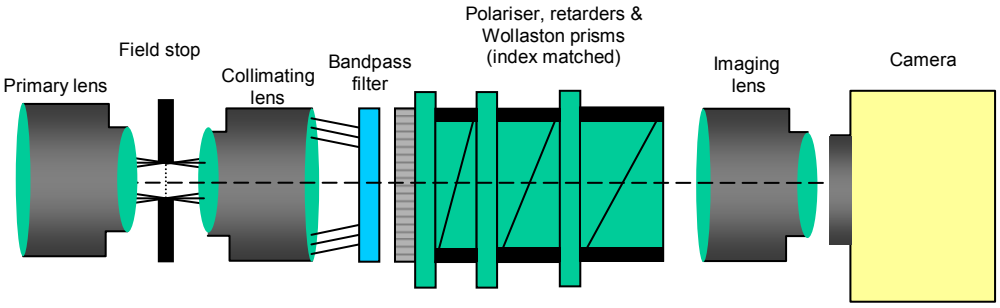

Figure 1.13: Representation of the 8-channel IRIS concept within a spectral imager

A major advantage of IRIS is that it can be readily added to imaging systems like conventional multi-port microscopes.

1.6.1.2 Spectral Imaging on Leica TSC SP5 confocal microscope
(adapted from: Leica Microsystems, 2006)

The new Leica TCS SP5 spectral confocal and multiphoton microscope system is based on the widely used SP® spectral detection module. This module allows selection of any spectral emission band in the visible range. The principal of the SP5 detection module is shown in figure 1.14. The emission is spread spectrally by a prism and then guided to a spectrometer slit that allows any emission band to be selected.

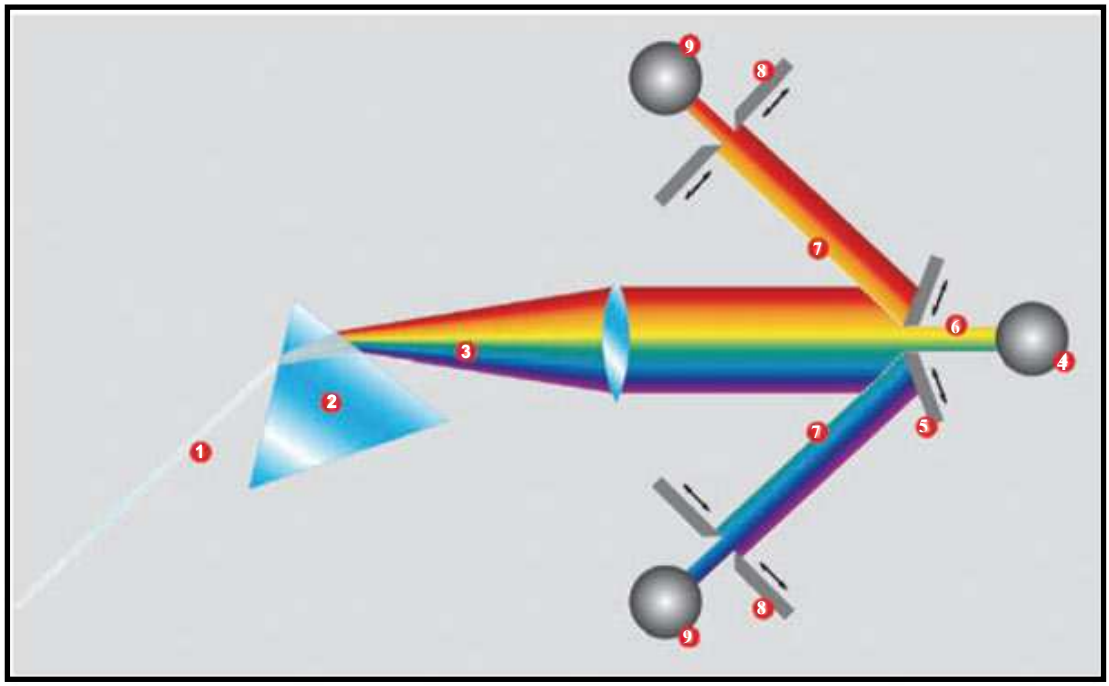

Figure 1.14. The SP principle. The emission from fluorochromes in the sample (1) is dispersed by a prism (2) into a spectrum (3). Detectors (4, 9) receive sections of the spectrum (6, 7) defined by movable mirrors (5, 8), which form spectrometer slits (Leica Microscystems, 2006).

1.6.2 Confocal laser scanning microscopy

Although conventional light and fluorescence microscopy allow the examination of both living and fixed specimens, certain problems do occur using these techniques. A major limitation is that emission signals originating from above and below the focal plane contribute to out-of-focus-signal that reduces the contrast and decreases resolution (Sekar & Periasamy, 2003). Confocal laser scanning microscopy can overcome this limitation as out-of-focus-signal is rejected by a pinhole. With this technique defocusing does not create blurring but gradually cuts out information from this part of the object, making it become darker until it completely disappears (optical sectioning).
Following collection of optical stacks from successive focal planes the information can be reconstructed to create a 3-D image of the specimen, thus allowing observation of structural features in three dimensions. Nevertheless, it needs to be considered that confocal live cell imaging is restricted by problems associated with photobleaching and photodamage. A further drawback is the limitation to standard laser lines for excitation.

For FRET experiments it is of major importance to prevent cross excitation of the acceptor fluorophore therefore the selection of the wavelength used for excitation and of appropriate filter sets to reduce spectral bleed through from the donor into the acceptor channel and vice versa needs to be carefully assessed. However, neither of these can be completely avoided, which makes it essential to account for them when determining FRET efficiencies.

Intensity-based FRET measurements are mainly complicated by factors such as differences in the concentration or brightness of the two fluorophores and bleedthrough between them.

The two components contributing to bleedthrough are first, overlap of the excitation spectra of the two fluorophores resulting in excitation of the acceptor at the excitation wavelength of the donor; and second, extensive overlap of the emission spectra causing donor emission to leak through into the acceptor detection channel.

Due to the broad spectra of fluorescent proteins commonly used in FRET assays, it is necessary to perform confocal FRET measurements with caution and correct the resulting datasets for spectral bleedthrough as first described by Youvan et al. in 1997. Since then several corrective approaches for sensitized emission FRET imaging have been reported (Periasamy and Day, 1999; Hoppe et al., 2002; Erickson et al., 2003). A general approach to FRET analysis as used in this project is described below.

Apart from the actual FRET probe, one additionally needs samples expressing each fluorophore alone (Donor only and Acceptor only constructs) to acquire images to correct for spectral bleedthrough, and ideally a positive FRET control, e.g. a construct where the two fluorophores are separated by a short linker keeping them close enough together to continuously exhibit FRET.

For FRET analysis images are collected in the following three different channels:

- Donor channel (donor excitation, donor emission)
- Acceptor channel (acceptor excitation, acceptor emission)
- FRET channel (donor excitation, acceptor emission)

The following figure summarizes the images necessary to perform FRET analysis using intensity based microscopy techniques.

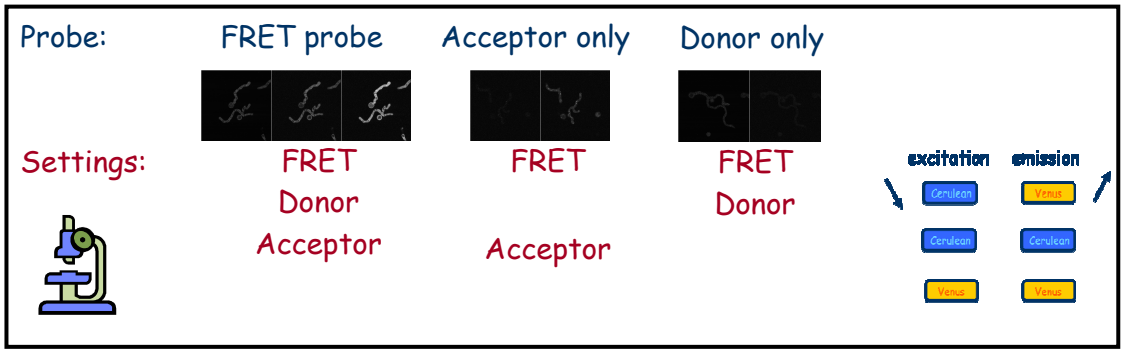

Figure 1.15: Images necessary to collect for analysis of intensity based FRET measurements

The FRET efficiency is calculated from the intensity values of the images after subtraction of the background noise. Correction for spectral bleedthrough is performed by determining the following two correction factors based on intensity ratios of acceptor and donor only samples in the channels specified above:

- Factor A
  (correction for excitation of the acceptor at the donor excitation wavelength)
  A = Intensity ($Acceptor_{FRETchannel}$) / Intensity ($Acceptor_{Acceptorchannel}$)

- Factor D
  (correction for donor emission leaking into the acceptor emission channel)
  D = Intensity ($Donor_{FRETchannel}$) / Intensity ($Donor_{Donorchannel}$)

The intensity of the FRET probe is then corrected by subtracting the bleedthrough contribution as shown in equation 1:

Equation 1:

$$I_{FRETcorr} = I\ FRET_{FRETchannel} - (A * I\ FRET_{Acceptorchannel}) - (D * I\ FRET_{Donorchannel})$$

The corrected fluorescence intensity values of the FRET sample can then be converted into relative FRET efficiencies by dividing them by the maximum intensity value possible for the collected images (ie 255 for an 8 bit image) and then multiplying the resulting value by 100.

This approach is necessary to compare results between different samples, especially when the fluorescence intensity varies more than just slightly between them.

Despite this being a reasonable approach to FRET analysis, the amount of image processing involved further increases the initial noise present in the images and thus might make it impossible to detect small FRET signals (Piston and Kremers, 2007).

1.6.3 Fluorescence lifetime imaging microscopy

In intensity-based imaging, changes in quantum efficiency cannot be distinguished from variations in concentration, which causes difficulties when working with ratiometric probes (and for the analysis of FRET data). Fluorescence Lifetime Imaging Microscopy (FLIM), however, is based on the analysis of the decay kinetics of electronically excited molecules. Unlike intensity-based imaging, FLIM presents the advantage of producing image contrast that is independent of excitation intensity as well as fluorophore concentration and is not affected by (moderate levels of) photobleaching. These are significant advantages for imaging dynamic events within living cells. By enabling spatial changes in probe fluorescence lifetime to be monitored (Gerritsen and de Grauw, 2001), FLIM offers a new approach to FRET analysis. Additionally FLIM enables the discrimination between fluorescence of different dyes, including autofluorescent materials that exhibit similar absorption and emission properties but show a difference in fluorescence lifetime. In general the lifetime of autofluorescence is very short and can therefore be easily distinguished from the one of the sample material.

The fluorescence lifetime of a molecule is the mean duration of time the fluorophore remains in the excited state. Following pulsed excitation, the intensity of a single emitting species decays according to:

$$I(t) = I_0 \exp(-t/\tau)$$

where I_0 is the intensity at t = 0 and τ is the lifetime. A variety of molecular interactions such as FRET can influence the decay time (Lakowicz and Szmacinski 1996).

The fluorescence lifetime (τ) is dependent on both the radiative and the nonradiative decay rates (Elson et al. 2002, Fig. 1.16). In the event of FRET, the quenching of the donor results in a decrease of the donor lifetime.

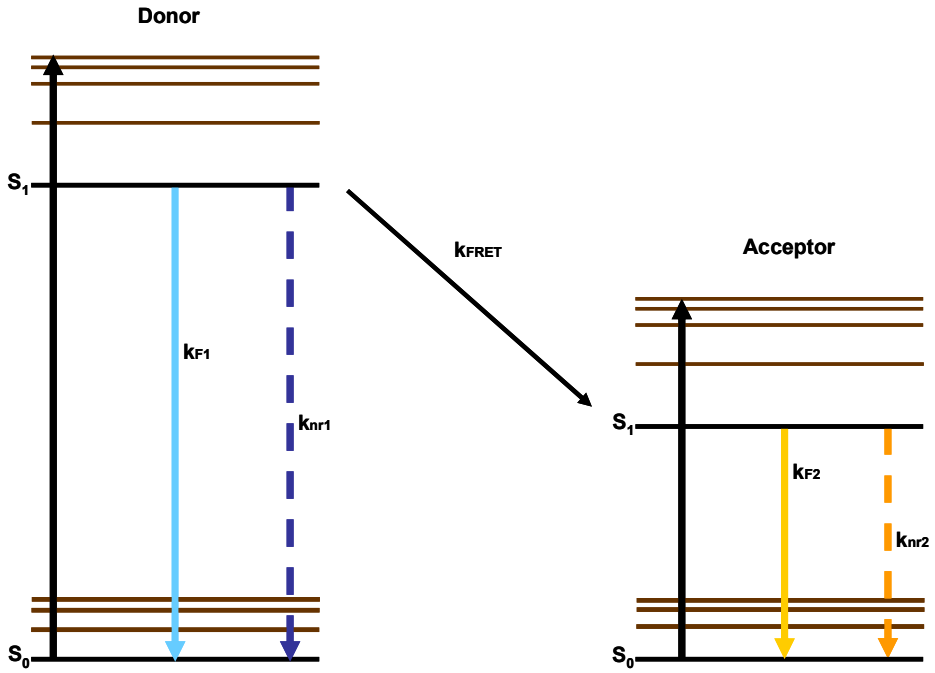

Figure 1.16: Jablonski diagram modified for FLIM with k_F=radiative decay rate, k_{nr} = nonradiative decay rate, k_{FRET} = FRET decay rate, S_0 = electronic ground state, S_1 = excited singlet state; the vibrational energy levels are shown in brown.

If donor and acceptor fluorophore do not exhibit FRET, their lifetimes are represented by the following equations:

$$\tau_D = \frac{1}{k_{f1} + k_{nr1}}$$

$$\tau_A = \frac{1}{k_{f2} + k_{nr2}}$$

Where τ_D is the lifetime of the donor fluorophore and τ_A the lifetime of the acceptor

In the event of FRET the donor lifetime changes as characterised in the equation below, whereas the lifetime of the acceptor remains the same as under no FRET conditions:

$$\tau_D = \frac{1}{k_{f1} + k_{nr1} + k_{FRET}}$$

To obtain quantitative results the decay of the molecules undergoing FRET and those which are not must be distinguished.

The technique used for FLIM measurement during this project is Time and Space Correlated Single Photon Counting (TSCSPC) using a quadrant anode detector (Europhoton GmbH, Berlin). The principle of TCSPC is the detection of single photons and the measurement of their arrival times with respect to a reference signal, usually the excitation light pulse. A schematic representation of a typical system is shown in Figure 1.17.

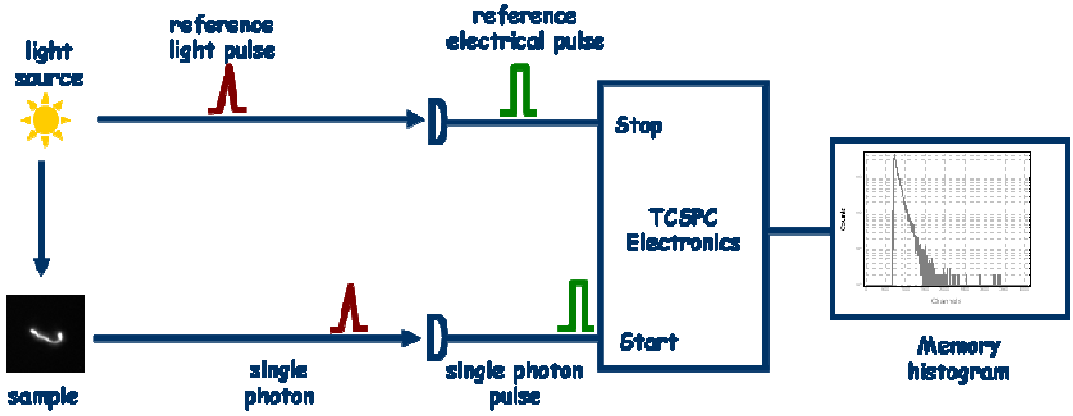

Figure 1.17: Principal components of a TCSPC system. A single photon pulse from the sample provides the start signal for the electronics, a reference pulse from the light source the stop signal (reverse mode). The times measured between the two pulses are collected in form of a histogram of fluorescence intensity versus time.

The TCSPC electronics can be compared to a fast stopwatch with two inputs. The clock is started by the START signal pulse and stopped with the stop signal pulse. The time measured for one START-STOP sequence will be accumulated in a histogram of photon counts versus time. With a high repetition rate light source many START-STOP sequences can be measured in a short time. The resulting histogram of counts versus channels will represent the fluorescence intensity versus time.

The data acquisition was in reverse mode, with the detected photon being used as a start pulse for the Time to Amplitude Converter (TAC) and the next laser pulse, triggered by the photodiode, the stop signal (see Figure 6.1). This ensured that the TAC only ran when a photon had been detected, and not after each laser pulse, when a photon may not arrive.

The detector used in this study was a quadrant anode microchannel-plate photomultiplier tube (QA-MCP-PMT) detector as depicted in figure 1.18. This detector allows simultaneous acquisition of time- and space information on the picosecond timescale (Kemnitz et al., 1997). For (nearly) every absorbed photon the photocathode emits an electron (photoelectric effect).

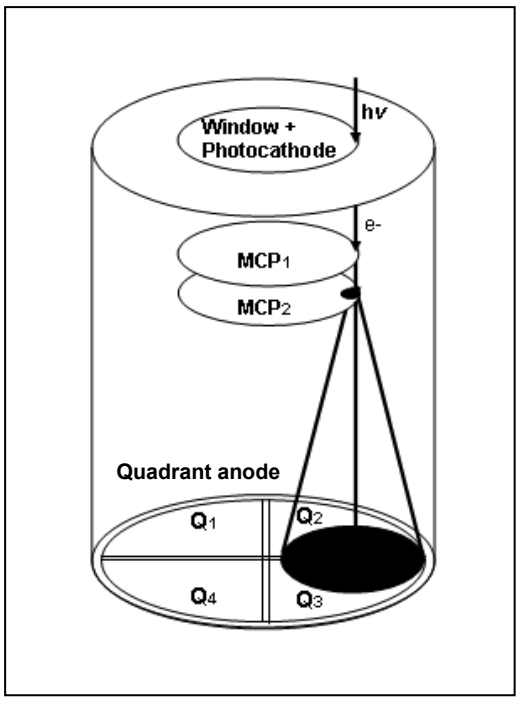

Figure 1.18: Schematic view of a QA-MCP-PMT detector, adapted from Kemnitz et al., 1997. The photocathode emits electrons upon absorbing photons, which are then directed towards the quadrant anode. Collisions of electrons with the microchannel wall result in release of secondary electrons. The so released electron cloud spreads out until it hits the quadrant anode.

The electric field within the detector directs the electrons from the cathode towards the anode. Due to the bias between the cathode and the MCPs the electrons are accelerated during this process. When an electron inside the microchannel collides with the microchannel wall, secondary electrons are released. The electron cloud leaving the MCP expands until it reaches the quadrant anode. The spatial position where the electron cloud hits the anode is identical to that of the original photon.

Chapter 2

Materials and Methods

2.1 Transformation of *E.coli*

Amplification of plasmid DNA was performed by chemical transformation of competent *E. coli* DH5α with appropriate plasmid DNA as described in Sambrook *et al.* (2001).

2.2 Culturing *E.coli*

E. coli was grown on solid or in liquid LB medium (Appendix A) containing 50 mg/ml ampicillin.

Solid LB plates were spread with 100 µl of bacterial cell suspension using a sterile glass spreader. Liquid medium was inoculated with single colonies grown on solid medium using a sterile toothpick.

2.3 Ligating into plasmid vectors

The plasmids used in this project are summarized in Table 2.1. For expression in bacteria the inserts coding the different probes were ligated into pRSET (Invitrogen), for fungal expression into pMoj009 (described in Millington et al. 2007). Unless otherwise stated the plasmids have been designed during this project.

Table 2.1: Plasmids used in this project

Protein	Genes provided by	based on	Reference
mCer	DW Piston		Rizzo et al
CeVe			
CeVe 2.12		Yellow Cameleon 2.12	Nagai et al
CeVe 6.1		Yellow Camleon 6.1	Truong et al
mCit	O Griesbeck		Griesbeck et al 2001
CeCi			
TNL15Cer		TN-L15	Heim et al 2004

2.3.1 Cameleon-type probes

Previously designed plasmids of cameleon type probes employing Sapphire (Zapata-Hommer and Griesbeck, 2003) as donor and Venus as acceptor fluorophore were used as the starting point for constructing pRSET containing mCerulean and Venus. Sapphire in the original probes was substituted by mCerulean using the NcoI and SpHI restriction sites. The inserts were then cut out with NcoI and EcoRI and ligated into pMoj009.

2.3.2 Modification of TN-L15 and corresponding controls

Plasmids containing mCitrin in pRSET and pMoj009 had previously been constructed. The BamHI and SpHI restriction sites were used to introduce the TN-L15 fragment minus CFP into pRSET_mCerulean, resulting in pRSET_TN-L15mCer.

TN-L15mCer was then ligated into pMoj009 via the NcoI and EcoRI restriction sites. Sequencing of the different plasmids confirmed the expected DNA sequences.

2.4 Transformation of *A. niger*

100 ml of liquid CM medium (see Appendix A), supplemented with final concentrations of leucin (1.5 mM), nicotinamide (0.08 mM) and uridine (5mM) were inoculated with a conidial suspension (approximately 5×10^7 conidia per ml) of the *Aspergillus niger* strain A455 [*cspA1*, *pyrA6*, *leuA1*, *nicA1*] from the Microbial Culture Collection of the National Institute of Chemistry, Ljubljana, Slovenia (MZKI) and incubated for 16h at 30 ºC and 150 rpm in a shaking incubator. Protoplasts were prepared after harvesting the mycelium by treatment with 10µg/ml Caylase C4 (Cayla, Toulouse, France) and transformed as described by Kusters-van-Someren et al.. pGW635 containing the *A. niger* orotidine-5-phosphate decarboxylase (*pyrA*) gene was used as a selection marker for the fungal transformation. Transformants were selected and purified by re-plating at low conidial densities on selective medium (MM^{++}, Appendix A).

2.5 Culturing of *A. niger*

For transformation A455 was grown on CM^{+++} agar slants (appendix A) for 4 days at 30ºC. A conidial suspension was then used to inoculate 100 ml of liquid CM^{+++} for overnight cultures as described above.After purification positive transformants were kept on MM^{++} agar slants.

For confocal microscopy, 100 µl drops of Vogel's medium (supplemented with nicotinamide and leucin) containing *A. niger* conidia (10^5 conidia per ml) were incubated on a coverslip in a humidity chamber for 18 h at 30ºC prior to imaging.

2.6 Protein extraction from fungal cells

100 ml samples of liquid CM medium (see Appendix A), supplemented with final concentrations of leucin (1.5 mM), nicotinamide (0.08 mM) and uridine (5mM) were each inoculated with conidial suspension (approximately 5×10^7 ml^{-1}) of the *A. niger* strains expressing the different FRET probes and control contstructs and incubated for 16h at 30 ºC and 150 rpm in a shaking incubator. The mycelium was harvested by vacuum filtration, washed with dH_2O and then ground up under liquid nitrogen with pestle and mortar before being transferred into 2 ml Eppendorf tubes. 500 µl extraction buffer was added on ice, the samples vortexed and kept for a further 15 minutes on ice before being centrifuged at 4 ºC for 10 mins at 10000 rpm. The resulting supernatant was used for further analysis.

2.7 Western Blot

Protein extracts were obtained as described above and the amount of total protein quantified using BCA Protein Assay (Pierce). For each sample 20 µg of protein were added to 5 µl prestained sample buffer (SDS with 2-mercaptoethanol), boiled for 10 minutes and then loaded onto a 10% SDS-PAGE gel. After electrophoresis, proteins were transferred onto a nitrocellulose membrane (Hybond-ECL, Amersham) and detected with the following antibodies:

- Primary antibody: rabbit polyclonal anti-GFP (Invitrogen)
- Secondary antibody: goat anti-rabbit IgG-HRP (Abcam)

The blots were developed using ECL reagent (Amersham Biosciences).

2.8 Sample preparation for microscopy assays

For the microscopy assays 100 µl drops of Vogel's medium(supplemented with nicotinamide and leucin) containing 10^5 *A. niger* conidia per ml were incubated on a coverslip in a humidity chamber for 18 h at 30ºC prior to imaging.

2.9 Confocal microscopy of *A. niger* transformants

Initial screening of transformants was performed on a Bio-Rad Radiance 2100 Rainbow system (Bio Rad Microscience, Hemel Hempstead, UK) equipped with a 5 mW 514 argon-ion laser line and a 4 mW Blue Diode (405 nm) mounted to a Nikon Eclipse TE 2000-U inverted microscope.

A water immersion plan apochromatic x60 objective (N.A. 1.2) was used throughout. Images were captured with the Bio-Rad Lasersharp 2000 software; the settings used to capture the different images are listed in Table 2.2.

Table 2.2: Settings used to acquire FRET images on a Biorad Radiance 2100 Rainbow system

	FRET	Donor	Acceptor
Excitation	405 nm	405 nm	514 nm
Laserpower	40 % (of 4 mW)	40 % (of 4 mW)	16 % (of 5 mW)
Emission filter	530 – 550 nm	470 – 490 nm	530 – 550 nm

Images were processed and converted into montages using Image J software.

2.10 Protein expression in bacteria and protein extraction

E. coli BL21 (DE3) (Novagen) was used for protein expression. *E. coli* cells were grown using standard LB broth supplemented with 50 mg/ml ampicillin in a shaking incubator at 37°C for 16 h. Induction of protein was initiated with the addition of 0.4 mM IPTG. Cultures were centrifuged at 4ºC, 9000 rpm for 25 minutes, after which the supernatant was discarded. The cells were resuspended in 1ml lysis buffer, incubated for 20 min at -20ºC and left to melt on ice before being sonicated. Sonication was performed for 9 min on ice, with a repeated 1 s ultrasound pulse followed by a 2 s pause (Tekmar Sonic Disruptor). The cell lysate was centrifuged for 15 min at 12000 rpm and 4ºC. The supernatant was used for *in vitro* analysis.

2.11 Protein purification (Peterka et al., 2005)

Protein purification was performed using CIM IDA Cu^{2+} disks [immobilized metal-ion affinity columns preloaded with Cu^{2+} (BIA Separations d.o.o., Ljubljana, Slovenia)]. The disks were equilibrated with loading buffer (0 mM imidazole) before 200 µl protein extract were applied. The disks were then washed with buffers of 0, 20 and 50 mM imidazole, elution was started with 100 mM imidazole buffer and finished with 250 mM. The disk was finally stripped of His-tags by washing it with a buffer of 500 mM imidazole, then washed with loading buffer before being stored in EtOH after a final wash step with dH_2O.

To remove salt, purified protein was dialysed overnight against PBS, pH 7.4 at 4ºC, with continuous stirring.

2.12 Concentration of protein

Protein extracts were concentrated in Vivaspin 6 columns (Sartorius AG, Goettingen, Germany). The membrane of the columns were wet by washing with 2ml MilliQ water and centrifuging with a fixed rotor for 2 minutes at 5000 rpm. 2 ml samples were added and centrifuged for 5 minutes at 4ºC at 5000 rpm.

2.13 Tagging protein extracts to beads

Bacterial protein extracts were tagged to Chemicell SiMAG-Cyanuric beads (chemicell GmbH, Berlin, Germany) according to the manufacturer's protocol (chemicell, protocol A8), using either 25 µl of concentrated protein or 500 µl of unconcentrated protein.

2.14 Sample preparation for imaging beads tagged with fluorescent proteins

Beads were imaged on coverslips in either dH_2O, 0.5 M $CaCl_2$ buffer (pH 7.0) or 50 mM EGTA buffer (pH 7.0).

2.15 Sample preparation for spectral imaging

For the microscopy assays 100 µl drops of Vogel's medium(supplemented with nicotinamide and leucin) containing 10^5 *A. niger* conidia per ml were incubated on a coverslip in a humidity chamber for 18 h at 30ºC prior to imaging.

Sample preparation and initial imaging of *Cochliobolus heterostrophus* and *Neurospora crassa* on IRIS was performed as described in Harvey et al, 2005.

2.16 Spectral Imaging with IRIS

For spectral snapshot imaging of fluorescently labelled fungal cells, IRIS was mounted onto a Nikon TE2000U inverted epi-fluorescence microscope. The samples were excited at 433 nm or 511 nm using a Hamamatsu Monochromator lightsource. To minimise bleedthrough of the excitation light into the detector channel the following dichroic mirrors were used:

- CFP: 455 DCLP (blocking light of wavelengths below 455 nm)
- YFP: 515 DCLP (blocking light of wavelengths below 515 nm)

2.17 Spectral Imaging on a Leica TSC SP5 confocal system

Confocal spectral imaging was perfomed on a Leica TCS SP5 laser scanning microscope mounted onto a Leica DMI 6000 CS inverted microscope (Leica Microsystems, Germany) with an HCX plan apo 63 × oil immersion objectives (NA 1.4). Images were captured with Leica ASF software at the settings listed in Table 2.3.

Table 2.3: Settings used for acquisition of emission spectra on a Leica TSC SP5 confocal system

	Donor only and FRET constructs	Acceptor only constructs
Excitation	405 nm	488 nm
Laserpower	25 % (of 4 mW)	15 % (of 5 mW)
Emission range	450 – 552 nm	501 – 552 nm
Bandwidth	10 nm	10 nm
Stepsize	3 nm	3 nm
Scanspeed	700 lines per second	700 lines per second

2.18 Imaging of Calcium sensors and FRET controls:

100 µl drops of Vogel's medium containing *A. niger* 10^5 conidia per ml were incubated on a coverslip in a humidity chamber at 30º C for 18h prior to imaging. During this period, the conidia germinated and a mycelium was formed.

Initial imaging was performed on a Bio-Rad Radiance 2100 Rainbow system (Bio Rad Microscience, Hemel Hempstead, UK) equipped with a 5 mW argon-ion laser and a 4 mW Blue Diode mounted onto a Nikon Eclipse TE 2000-U inverted microscope. A water immersion plan apochromatic x60 (N.A. 1.2) objective was used throughout. Images were captured with the Bio-Rad Lasersharp 2000 software, the settings used to capture the different images are listed in Table 2.4.

Table 2.4: Settings used to acquire FRET images on Biorad Radiance 2100 Rainbow system

	FRET	Donor	Acceptor
Excitation	405 nm	405 nm	514 nm
Laserpower	40 %	40 %	16 %
Emission filter	530 – 550 nm	470 – 490 nm	530 – 550 nm

Due to software limitations the images had to be collected sequentially, acquisition of a set of 3 images took 20s.

Further analysis was performed on a Leica TCS SP5 confocal system (settings as described in table 2.5) mounted on a Leica DMI 6000 inverted microscope (Leica Microsystems, Germany) and equipped with a 25 mW argon laser. A HCX plan apo x63 oil immersion objective (NA 1.4) was used throughout. Images were captured using Leica LAS AF Software. A combined simultaneous (FRET and donor channel) and sequential (acceptor channel) method allowed capturing a complete set of 3 images within 1.2 seconds.

Table 2.5: Settings used to acquire FRET images on Leica TSC SP5 confocal microscope

	FRET	Donor	Acceptor
Excitation	458 nm	458 nm	514 nm
Laserpower	19 %	15 %	5 %
Emission filter	520 – 550 nm	470 – 500 nm	520 – 550 nm

All images were processed and converted into montages using Image J software.

2.19 pH imaging and analysis of the genetically encoded pH sensor RaVC in *Aspergillus niger* (adapted from Bagar et al., 2009)

For the confocal assays 100 µl drops of Vogel's medium (supplemented with nicotinamid and leucin) containing *A. niger* conidia at a concentration of 10^5 conidia per ml were incubated on a coverslip in a humidity chamber for 18 h at 30ºC prior to imaging.

Initially imaging was performed on a Bio-Rad Radiance 2100 Rainbow system (Bio Rad Microscience, Hemel Hempstead, UK) equipped with a 5 mW Argon-ion laser and a 4 mW Blue Diode mounted to a Nikon Eclipse TE 2000-U inverted microscope. A water immersion plan apochromatic x60 (N.A. 1.2) objective was used throughout. Images were captured with the Bio-Rad Lasersharp 2000 software. The probe was sequentially excited at 405 nm and 476 nm; the settings used to capture the different images are listed in Table 2.6. Using this method images were acquired within 25 seconds of each other.

Table 2.6: Settings used to acquire Ratio images on Biorad Radiance 2100 Rainbow system

	Channel 1	Channel 2
Excitation	405 nm	476 nm
Laserpower	37 %	18 %
Emission filter	500 – 530 nm	500 – 530 nm

Ratio images were then obtained in the following way:

1. subtraction of average background fluorescence from both images
2. 3x3 binning
3. division of corresponding pixels in the two images (405 nm/476 nm)

Further imaging was perfomed on a Leica TCS SP5 laser scanning microscope mounted on a Leica DMI 6000 CS inverted microscope (Leica Microsystems, Germany) with an HCX plan apo 63× oil (NA 1.4) oil immersion objective. For sequential excitation, a 50 mW 405 nm diode laser and the 476 nm line of a 25 mW argon laser were used. Laser powers of 6% for the diode laser and 12% for the argon laser were employed. Successive images excited at 405 and 476 nm were captured within 1.2 sec of each other. Fluorescence emission was detected at 500-530 nm.

A calibration curve for measurements of intracellular pH was obtained as described in Bagar et al., 2009. Images were analyzed using either the ImageJ plugin PixFret (Feige et al., 2005) or a software program custom written for this application incorporating equations 1 and 2 below. Ratio images were obtained by first subtracting the background from each fluorescence image pair followed by division of corresponding pixels in the 2 images (equation 1):

$$R_i = (F(405nm)_i - F(405nm)_{background}) / (F(475nm)_i - F(475nm)_{background}) \quad \text{(Equ. 1)}$$

$F(405nm)_i$ and $F(475nm)_i$ are the average fluorescence intensities, $F(405nm)_{background}$ and $F(405nm)_{background}$ the average background fluorescence intensities of a given pixel or region of interest.

The ratio of fluorescence signals emitted at each excitation wavelength was converted into pH values as described in equation 2 (Grynkiewicz et al., 1985; Cobbolt and Rink, 1987):

$$pH = pK_a - \log_{10} [(R_i - R_{min}) / (R_{max} - R_i)] \quad \text{(Equ. 2)}$$

Value R_i is the emission ratio at a given pH, and R_{max} and R_{min} are the limiting values for the ratio at the extreme acid (pH 5.0) and alkaline (pH 9.0) pH values, respectively, and were determined individually for each set of experiments. The constant, pK_a, was determined from the *in situ* calibration curve.

Visually, the pH profile along the hyphae was expressed by displaying the ratio image in pseudocolors. All data are shown as the mean with standard deviation of at least three independent experiments and a minimum of three images were taken for each experiment. To reduce noise, 3x3 binning was performed on the initial images before ratio calculation.

Mean pH values were calculated from cytoplasmic areas that excluded detectable organelles or cytoplasmic regions in which the RaVC reporter was concentrated.

2.19.1 *In situ* calibration of RaVC

To obtain a calibration curve, conidia of *A. niger* were prepared as stated above before being incubated in buffer solutions with pH values ranging from 5.0-9.0.
The following buffers were used at a concentration of 50 mM with 150 mM KCl added:

- acetate (pH 5.0-5.5)
- MES (pH 6.0-6.75)
- MOPS (pH 7.0-7.8)
- Tris (pH 8.0-9.0)

To equilibrate the intracellular pH with the extracellular pH the ionophore nigericin was added to a final concentration of 5 µM and incubated for at least 30 minutes (Jankowski et al., 2001; Jernejc and Legisa, 2004)).
After mycelia had been treated in this way, images were recorded in 5 minute intervals until the mean ratio value reached a steady state. Final images were collected 10 minutes after reaching the steady state and their ratio converted into pH values as described above using equation 1.

2.19.2 Chemical treatments applied to living hyphae

All chemicals were prepared as 10× stock solutions in appropriate solvents. The solvents did not have an effect on intracellular pH (data not shown). The extracellular pH was changed by addition of 5 mM KOH or 50 mM HCl to Vogel's medium and the responses of intracellular pH were monitored over 20 min. Oxidative phosphorylation was inhibited using 10 μM carbonyl cyanide m-chlorophenylhydrazone (CCCP, Fluka) or 40 μM cyanide p-(trifluoromethoxy) phenylhydrazone (FCCP, Sigma). For each chemical treatment, images were captured before and for 10 min following chemical addition.

2.20 Sample preparation for FLIM

For the microscopy assays 100 μl drops of Vogel's medium (supplemented with nicotinamide and leucin) containing *A. niger* conidia at a concentration of 10^5 conidia per ml were incubated on a coverslip in a humidity chamber for 18 h at 30ºC prior to imaging.

Protein extracts of *A. niger* expressing mCerulean or CeVe were obtained as described above (section 2.7). Prior to analysis the extracts were diluted 1:500 in fungal extraction buffer (Appendix A).

2.21 Fluorescence Lifetime Imaging Microscopy

The excitation source was a Ti-Sapphire femtosecond laser system from Coherent (10W Verdi and Mira Ti-Sapphire laser). FLIM experiments were performed using excitation at 429 nm.

To analyse protein extracts the beam was directed into the cuvette sample chamber of a TCSPC F900 spectrometer (Edinburgh Instruments, Livingston, UK), data was acquired using F900 software.

For microscopy assays the laser was mounted on a Nikon Eclipse TE 300 inverted microscope equipped with a water immersion plan apochromatic 60x (N.A. 1.2) objective, a DM455 dichroic mirror (Nikon) and a 480/30 nm bandpass filter for emission of mCerulean. Data and images were obtained with QA capture software (Europhoton GmbH, Berlin). Fluorescence emission from the sample was imaged using the technique of time and space correlated single photon counting (TSCSPC) using a quadrant anode detector as described above. Each detected photon was assigned to one of 4080 channels, each of 27ps. Data were typically recorded for about 20 minutes.

Data were imported into QAAnalysis software supplied by Europhoton GmbH. The software was used to select regions of interest in the different images, extract the lifetime decay data and generate lifetime maps (Figure 2.1).

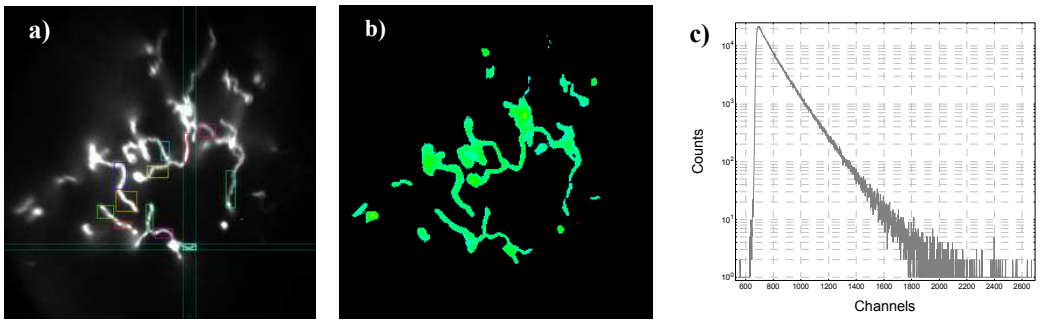

Figure 2.1: The different FLIM datasets. After importing the TSCSP data into QAAnalysis, different regions of interest were selected from the fluorescence intensity image (a) and fluorescence decay data of those regions extracted. A lifetime map (b) was produced as described below. The average lifetime displayed in the map offers fast initial results, indicating if there is a difference in lifetime between different samples and whether the fluorescence lifetime is evenly distributed throughout the cells. Quantitative analysis resolving multiple decay components was performed by importing the extracted decay data into F900 and fitting the decay curves (c) as described below.

Lifetime maps were produced after background subtraction by fitting data from each point in the field of view to a single exponential decay and assigning a colour on a 16-bit pseudocolour scale to the lifetimes. These lifetime maps only represent the approximate average lifetime of the sample and were used to confirm the uniform lifetime distribution of the probes expressed in *Aspergillus niger*.

Analysis of the extracted fluorescence decay data was performed with F900 software (Edinburgh Instruments), via a tail-fitting procedure from the peak of the decay. The decay data was fitted to the following multiexponential decay function (Equ. 3):

Equation 3: $$I(t) = \sum_{i=1}^{n} A_i \exp^{(-t/\tau_i)} + B$$

where A_i is the fractional amplitude of the i^{th} decay component, τ_i is the i^{th} fluorescence lifetime component and B is the background.

The quality of fit was judged on the basis of the reduced chi-square statistic, χ^2, and the randomness of residuals.

Chapter 3

Results and Discussion

3.1 Development of new calcium sensitive probes

The *Aspergillus niger* strains analysed during this project are summarised in Table 3.1, the relevant plasmid maps are shown in Appendix B. Sequences of the different plasmids have been verified by sequence analysis and can be found in appendix C. All plasmids and transformants were produced during this project, unless otherwise stated.

Table 3.1: Plasmids and *A.niger* strains developed in this study. pMoj009_Venus and _Citrin were constructed by Tanja Bagar, who also transformed *A. niger* with the Venus plasmid.

Plasmid	Protein	Function	Strain
pMoj009_mCer	mCeruelen	Donor only control	KI_A752
pMoj009_Venus	Venus	Acceptor only control	KI_A691
pMoj009_CeVe	CeVe	positive FRET control	KI_A756
pMoj009_CeVe2.12	CeVe2.12	Cameleon-FRET-probe	KI_A767
pMoj009_CeVe6.1	CeVe6.1	Cameleon-FRET-probe	KI_A771
pMoj009_Cit	mCitrin	Acceptor only control	KI_A818
pMoj009_CeCi	CeCi	positive FRET control	KI_A813
pMoj009_TN-L15mCer	TN-L15mCer	TroponinC FRET-probe	KI_A765

Positive transformants as determined from fluorescence measurements of protein extracts (data not shown), were screened for expression of the fluorescent probes on a BioRad Radiance 2100 Rainbow confocal system.

The figures below (Figures 3.1 and 3.2) show confocal images of the *A. niger* strains chosen for FRET analysis. The settings to acquire the images of the different strains were kept constant as required for intensity based FRET-Imaging. Confocal images of *A. niger* strains expressing single fluorophores (either Donor or Acceptor) are shown in Figure 3.1.

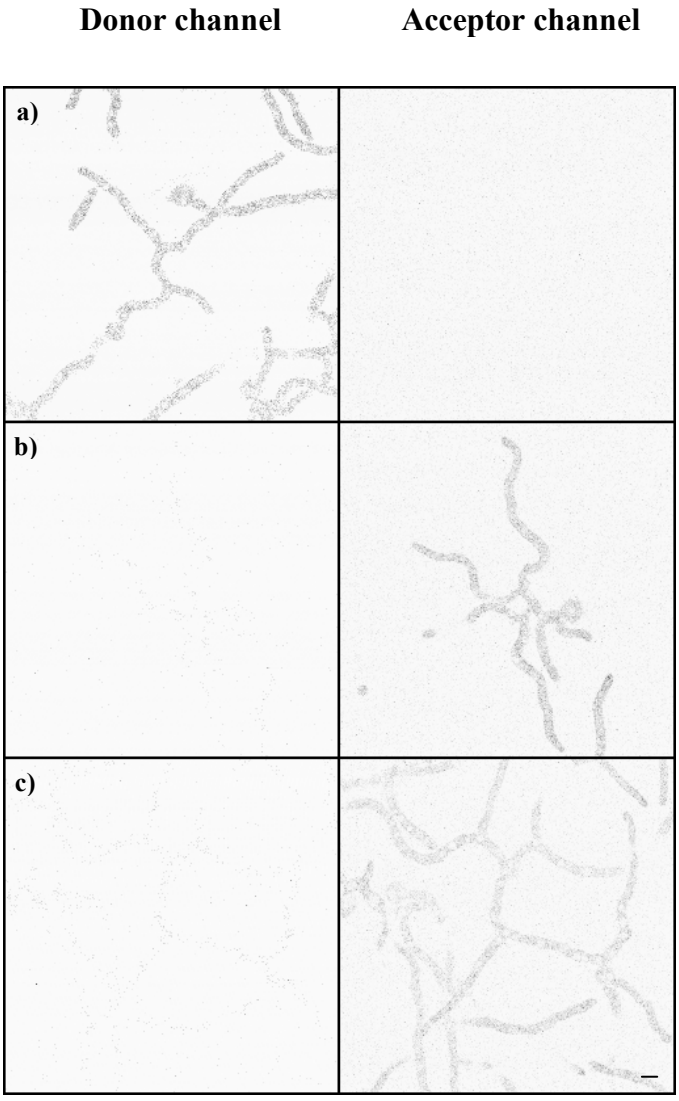

Figure 3.1:Confocal images of *A. niger* expressing single Fluorophores: a) mCerulean, b) Venus, c) Citrin. In the donor channel the samples were excited at 405 nm, in the acceptor channel at 514 nm. Emission was collected between 470 nm to 490 nm for the donor channel and 530 nm to 550 nm in the acceptor channel. Bar = 5 µm

As expected, the donor only construct mCerulean (Fig. 3.1a) shows emission between 470 nm to 490 nm after excitation at 405 nm (donor channel) whereas the emission for the two acceptor only constructs Venus (Fig. 3.1b) and Citrin (Fig. 3.1c) is collected between 530 nm to 550 nm after excitation at 514 nm (acceptor channel). The collected images show clearly that fluorescence for the donor only (Fig 3.1 a) and acceptor only (Fig 3.1 b and c) controls could be collected in separate emission channels as necessary for intensity based FRET analysis.

Images of strains expressing both fluorophores (positive controls or Ca^{2+}-sensitive probes) are displayed in Figure 3.2. Both positive controls, where the donor mCerulean is separated from the acceptor Venus (CeVe, Fig 3.2a) or Citrin (CeCi, Fig. 3.2b) by a short linker, display emission in the donor as well as the acceptor channel, as do the actual Ca^{2+}-sensors CeVe 2.12 (Fig. 3.2 c), CeVe 6.1 (Fig. 3.2 d) and TNL15mCer (Fig. 3.2 e). The presence of both donor and acceptor fluorescence emission signal in these constructs is expected and a good indicator that the probes are successfully expressed in *A. niger*.

As can be seen when comparing the fluorescence of the different strains, the control strains (donor only mCerulen, acceptor only mVenus or mCitrine as shown in Figure 3.1) and positive FRET controls (CeVe and CeCi, as shown in Figure 3.2 a and b) display particularly weak fluorescence signals when compared to the actual Ca^{2+} sensors. This difference is due to the varying level of expression of the different constructs in *A. niger*. Ideally the expression level and therefore fluorescence output of the different strains would be more similar, but from the transformants available the ones shown were the ones most comparable in terms of intensity of the fluorescence emission signal.

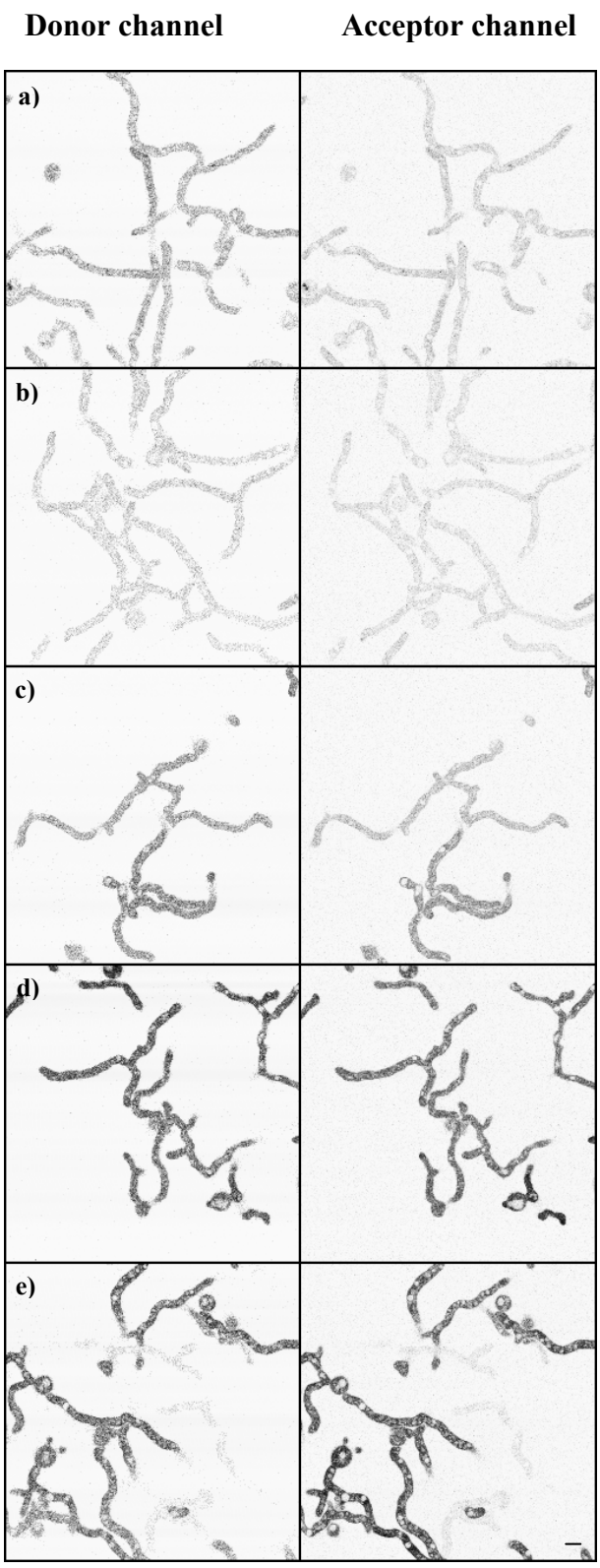

Figure 3.2: Confocal images of *A. niger* expressing positive controls and probes: a) CeVe, b) CeCi, c) CeVe 2.12, d) CeVe 6.1 and e) TN-L15mCer. Settings in the donor and acceptor channels were the same as described for Figure 3.1. Bar = 5 µm

In addition to the confocal screen a Western Blot was performed to analyse the fluorescent proteins and probes expressed in *A. niger* (Figure 3.3).

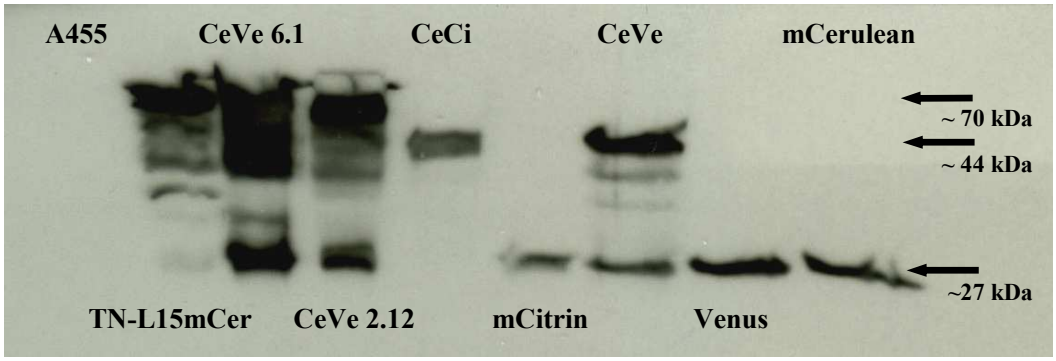

Figure 3.3: Western Blot of fungal protein extracts. Single GFPs run at about 27 kDa, the positive controls CeCi and CeVe at 44 kDa and the Ca^{2+}-sensitive probes at 70 kDa. As expected no signal is detected for the Wildtype A455 (first lane).

The Western Blot reveals that apart from the single GFPs (Donor only mCerulean and Acceptors only Venus and mCitrine) and the positive FRET control CeCi all other proteins show degradation. The smallest bands visible are the ones for single GFPs, showing that no partially degraded GFPs were detected on the Western Blot. As expected no signal is detected for the Wildtype A455.

The lack of bands smaller than single GFPs indicates that no partially degraded GFPs were detected, either due to them being stable in the cell or completely degraded and therefore not detected. The β-barrel structur of GFP itself renders it extremely resistant to protease activity, making it more likely that the linker of the probes is degraded rather than the GFPs. Although it is possible that some of the probes expressed in *A. niger* degrade, this process is more likely to occur during extraction of the protein when mechanical disruption of the fungal cells leads to the release of proteases from organelles.

3.2: *In vitro* analysis of bacterial and fungal protein extracts

3.2.1 Expression of FRET constructs and controls in *E. coli* BL21 cells

E. coli BL21 cells were transformed with the 8 different constructs expressed and analysed in *A. niger* during this project. Only two constructs, CeCi (positive FRET control) and TN-L15mCer (Ca^{2+}-sensor) could be successfully expressed in bacteria and purified from bacterial cell extracts. These 2 proteins were then tagged to Chemicell SiMAG-Cyanuric beads as described above and analysed using FLIM and confocal imaging techniques as described previously (Chapter 2).

3.2 .2 Tagging fungal protein to beads

A second attempt at tagging the different protein extracts to beads was performed by incubating Dynabeads 450 Epoxy and Subcellular 500 (Invitrogen, UK) with fungal protein extracts. Confocal microscopy revealed that this attempt failed, autofluorescence from untagged beads equalled the fluorescence emission from the beads incubated with protein extracts and no distinct signal could be detected for the different constructs.

3.2.3 Confocal microscopy of fungal protein

To allow FRET analysis of the different constructs on the same slide imaging fungal protein extracts in capillaries was attempted. This attempt failed since the extracts bleached before the necessary 3 images could be collected.

3.2.4 Confocal imaging of beads tagged with bacterial protein extracts

Further analysis was performed by imaging beads tagged with the positive FRET control CeCi or the Ca^{2+}-sensor TN-L15mCer on a Leica TSC SP5 confocal system. Figures 3.5 (beads tagged with CeCi) and 3.6 (beads tagged with TN-L15mCer) reveal that the beads tend to aggregate (Figs. 3.5 b) and 3.6 a) and b) show clusters of beads, rather than single ones). Furthermore the difference in fluorescence intensity of the emission signals indicates that the $CaCl_2$ and EGTA buffer affect the emission signal of the beads, as explained below.

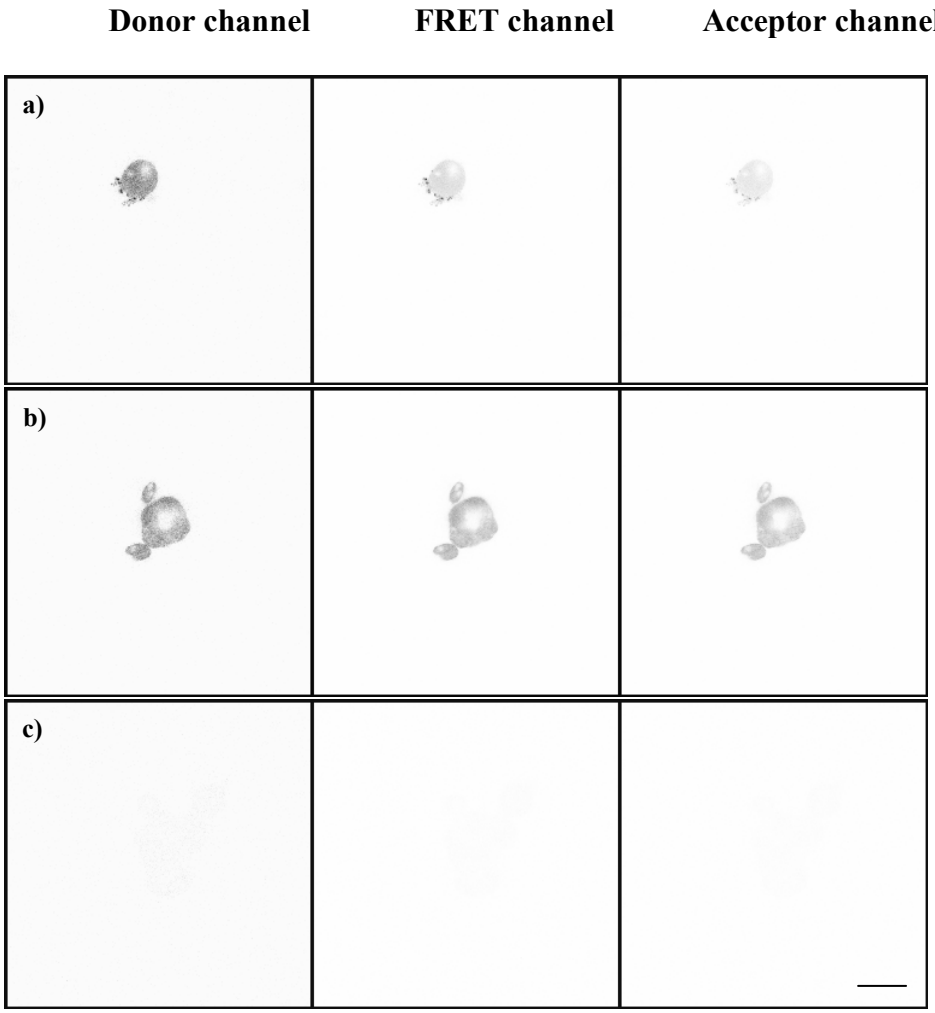

Figure 3.4: Confocal images of bacterial CeCi protein extract tagged to beads. Images were collected in a) $CaCl_2$ buffer, b) dH_2O, c) EGTA buffer. In the donor and FRET channel the samples were excited at 458 nm, in the acceptor channel at 514 nm. Emission was collected between 470 nm to 500 nm for the donor channel and 530 nm to 550 nm in the FRET and acceptor channels. Bar = 2 µm.

The signal for beads tagged with the positive control CeCi should remain constant when imaged in different Ca^{2+} concentrations, since the linker of this probe does not react to changes in Ca^{2+}-concentration. For both probes the highest emission signal can be detected when the beads are imaged in dH_2O (Fig. 3.4 and 3.5 b)), with a (minor) decrease in fluorescence intensity when imaged in $CaCl_2$ buffer (Figs. 3.4 and 3.5 a)) and no visible emission signal when imaged in EGTA buffer (Figs. 3.4 and 3.5 c)). A possible explanation could be that adding buffer solution to the beads resulted in stripping part of the proteins from the beads and thereby decreasing the fluorescence signal detected from the latter.

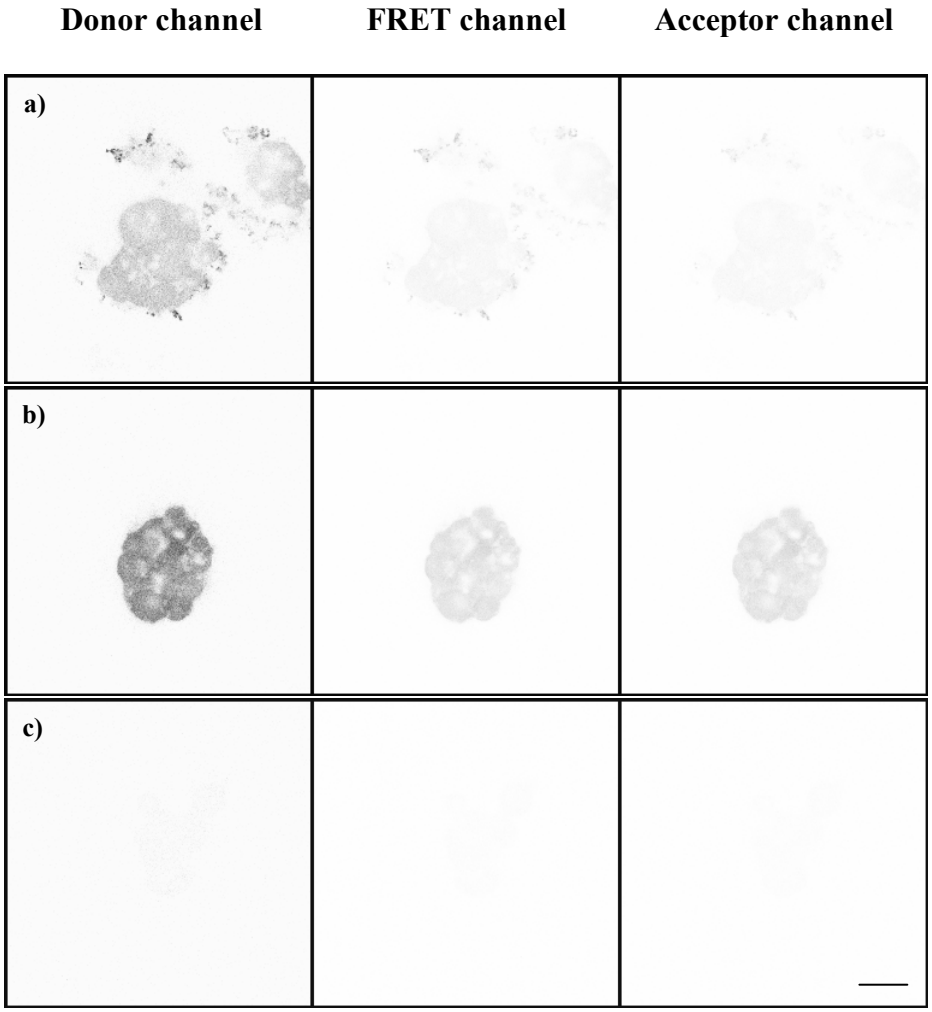

Figure 3.5: Confocal images of bacterial TN-L15mCer protein extract tagged to beads. a) $CaCl_2$ buffer, b) dH2O, c) EGTA buffer. In the donor and FRET channel the samples were excited at 458 nm, in the acceptor channel at 514 nm. Emission was collected between 470 nm to 500 nm for the donor channel and 530 nm to 550 nm in the FRET and acceptor channels. Bar = 2 µm.

Due to these results and the lack of FRET controls tagged to beads, further attempts at obtaining a Ca^{2+}- calibration curve by imaging beads in different Ca^{2+}-concentrations were abandoned.

3.2.4 TSCSPC FLIM analysis of beads tagged with TN-L15mCer

Beads were imaged in different solutions (dH_20, 0.5 M $CaCl_2$ buffer or 50 mM EGTA buffer at pH 7.0) and TSCSPC data treated as previously described for fungal cells in Chapter 2. Figure 3.6 displays the fluorescence intensity images as obtained after loading the data into QAAnalysis software.

The beads are evenly distributed throughout the field of view but seemed to have mostly aggregated in clusters. The low fluorescence intensity in image c) (beads in EGTA buffer) is due to the low signal to noise ratio for this dataset. Further increasing of the brightness in QAAnalysis resulted in an equal increase of background noise in this image rather than improving the image quality for selecting regions of interest for further analysis.

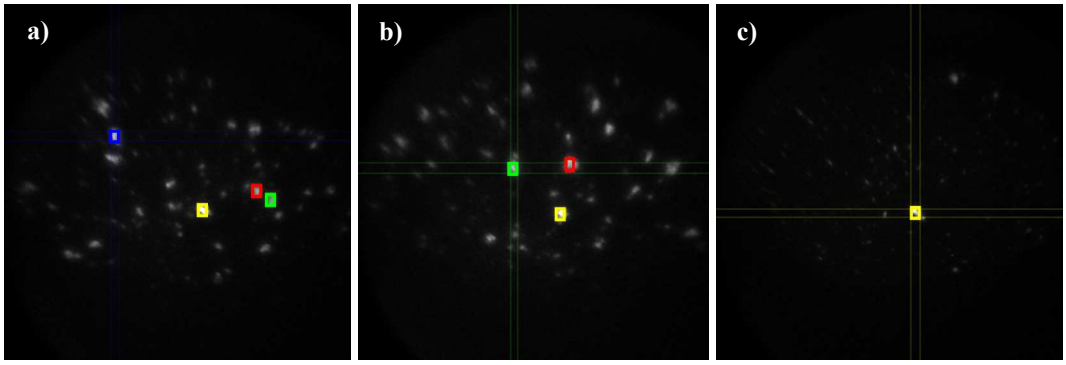

Figure 3.6: Fluorescence intensity images collected of beads tagged with TNL15mCer in different solutions. Images shown as displayed after import of acquired TSCSPC data into QAAnalysis. Highlighted are regions of interest chosen for further analysis of fluorescence decays. Beads were imaged in either a) dH_2O, b) 0.5 M $CaCaCl_2$ buffer (pH 7.0) or c) 50 mM EGTA buffer (pH 7.0).

The high background fluorescence for beads imaged in EGTA buffer (shown by low signal to noise ratio and low fluorescence intensity of the beads as compared to background fluorescence in Fig. 3.6 c) supports the theory that the buffer may strip the protein off the beads, leading to a lower fluorescence signal from the beads themselves and detection of higher levels of background fluorescence. Since the detector used for FLIM experiments enables detection of lower fluorescence levels than the confocal microscope, these results support the initial results obtained from confocal microscopy of the beads.

Analysis of decay data for beads imaged in dH_2O, $CaCl_2$ or EGTA buffers revealed no significant difference in lifetime parameters between the samples (Table 3.2).

Table 3.2: Results from analysis of fluorescence decay data obtained for beads tagged with TNL15mCer and imaged indifferent solutions and initial results for CeVe 2.12 and 6.1 expressed in *A. niger*

	Beads in H_20	**Beads in CaCl**	**Beads in EGTA**	**CeVe 2.12**	**CeVe 6.1**
τ_1 (ns)	0.86 ± 0.04	0.83 ± 0.08	0.90 ± 0.07	0.54 ± 0.06	0.50 ± 0.07
τ_2 (ns)	2.04 ± 0.11	2.03 ± 0.23	2.12 ± 0.17	1.68 ± 0.08	1.56 ± 0.10
τ_3 (ns)	-	-	-	3.49 ± 0.11	3.39 ± 0.06
A_1 (%)	67.56 ± 5.65	67.30 ± 6.14	68.75 ± 6.35	13.92 ± 2.46	24.37 ± 4..01
A_2 (%)	32.44 ± 5.65	32.70 ± 6.14	31.25 ± 6.35	54.58 ± 1.48	47.14 ± 3.24
A_3 (%)	-	-	-	31.50 ± 1.03	28.49 ± 0.80
χ^2	1.042 ± 0.056	1.060 ± 0.071	1.062 ± 0.070	1.022 ± 0.006	1.056 ± 0.076

Imaged in dH_2O two lifetime components of 0.86 ± 0.04 ns and 2.04 ± 0.11 ns with A-factors of 67.56 ± 5.65 % and 32.44 ± 5.65 % respectively and a value for χ^2 of 1.042 ± 0.056 were resolved. These values did not change significantly when the beads were imaged in $CaCl_2$ or EGTA buffer. In comparison initial results for the Ca^{2+}-sensitive probes CeVe 2.12 and 6.1 expressed in *A. niger* (as discussed in Chapter 3.5 and included in Table 3.2) revealed lifetimes and A-factors of 0.54 ± 0.06 ns (13.92 ± 2.46 %), 1.68 ± 0.08 ns (54.58 ± 1.48 %) and 3.49 ± 0.11 ns (31.50 ± 1.03 %) for CeVe 2.12 and 0.50 ± 0.07 ns (24.37 ± 4..01 %), 1.56 ± 0.10 ns (47.14 ± 3.24 %) and 3.39 ± 0.06 ns (28.49 ± 0.80 %) for CeVe 6.1. Further discussion of these results is included in Chapter 3.5.

The absence of a long lifetime component of about 3.4 ns in the protein extract on beads together with a predominant short component of about 0.86 ns in these samples suggests that either FRET occurs efficiently in these samples, or quenching occurs by other mechanisms (such as collisional energy transfer or excited state complex formation). It is possible that donor and acceptor fluorophores of different probes are in such close proximity on the beads that FRET occurs more efficiently than when the probes are expressed in fungal cells.

Further possibilities for the difference in lifetime parameters of the protein on beads as compared to the samples expressed in fungal cells are that the donor and acceptor part of the fusion protein, when tagged to beads, potentially affect each others lifetime due to their close proximity or that the lifetime parameters of the protein are affected by the His-tag that was used for purifying and tagging the protein to beads.

3.3 Spectral Imaging of recombinant Ca^{2+}- sensors and FRET controls expressed in the filamentous fungus *Aspergillus niger*

Spectral imaging was performed using either IRIS, a novel spectral imaging device developed at Heriot-Watt University, Edinburgh, or a Leica TSC SP5 confocal system.

3.3.1 IRIS – Spectral imaging in a snapshot

Initial proof of concept demonstrations were performed by imaging germinated spores of the maize pathogen *Cochliobolus heterostrophus* stained with the pH sensitive dye carboxy-SNARF-1 and *Neurospora crassa* germlings with GFP tagged nuclei stained with the membrane selective dye FM 4-64 (Harvey et al., 2005).

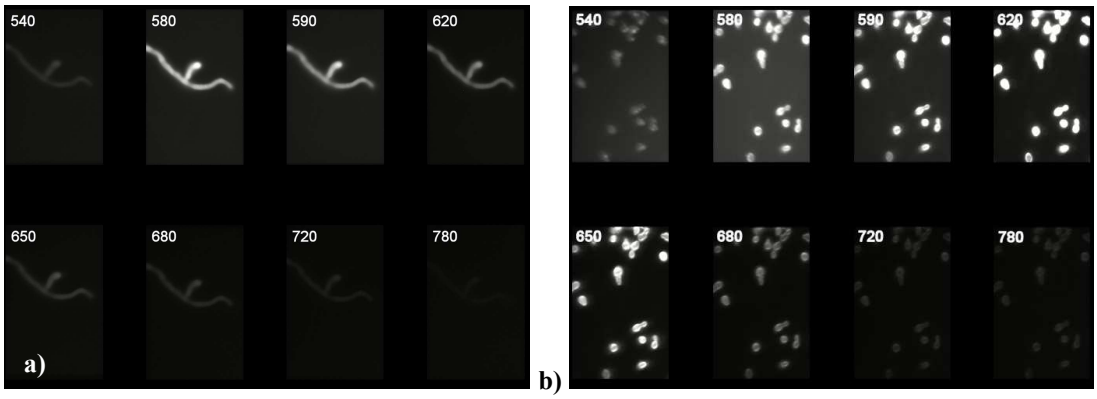

Figure 3.7: Narrow band images of a) *Cochliobolus heterostrophus* stained with carboxy-SNARF1 and b) *Neurospora crassa* labelled with GFP and FM4-64 (Harvey et al., 2005)

Figure 3.7 a) shows 8 narrow band images of the maize pathogen *Cochliobolus heterostrophus* stained with the pH-sensitive dye carboxy-SNARF-1. After excitation, carboxy-SNARF-1 fluorescence could be detected between 580 and 620 nm. The fluorescence spectrum of carboxy-SNARF-1 responds to changes in pH. Using IRIS, changes in the fluorescence emission spectrum of this dye could be monitored in real time and, after appropriate calibration, be used to measure intracellular pH. Figure 3.7 b) shows 8 narrow band images of germinating spores of *Neurospora crassa* labeled with GFP and the membrane selective dye FM4-64. After excitation the GFP tagged nuclei were detected at 540 nm whereas FM4-64 emission was detected between 580 and 680 nm.

These results highlight the potential of IRIS for live cell imaging. The ability to collect fluorescence emission signals in 8 narrow bandpasses simultaneously is not only ideal for imaging several different dyes (provided they can be excited at the same wavelengths), but also offers the opportunity to get spectral information (if restricted to 8 maxima) of fluorescence behaviour over a whole wavelength range in a snapshot, rather than compromising on the time factor to collect the information bandpass by bandpass.

For imaging of the probes designed during this project, the wavelength range covered by the original IRIS device (500 nm – 800 nm) is not well suited. Additionally, fluorescent proteins commonly used in live cell imaging show emission maxima from 475 nm (mCerulean) to 649 nm (mPlum), a range that is not optimally covered by the original IRIS. To allow more accurate spectral imaging in the range interesting for cell biologists, the IRIS system used in this project was adapted to cover a wavelength range from 450 nm to 600 nm. The resulting bandpasses and their location on the images are shown in figure 3.8.

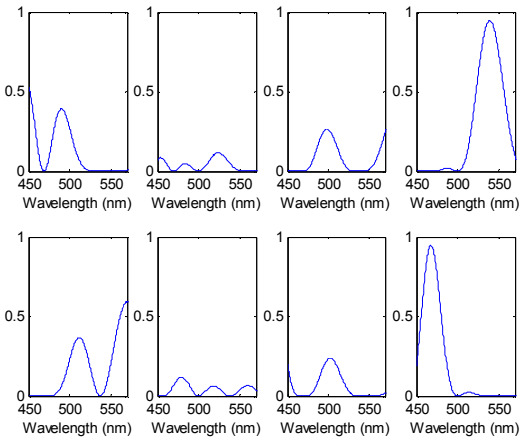

Figure 3.8: Bandpasses of wavelength range adjusted IRIS shown with their position on the final 8 channel image

When compared to the original IRIS it is obvious that the new version is not yet optimised. The peaks of the different passbands are rather broad, overlap extensively and vary significantly in their response (min of 10 % to max of ~90 % as compared to min of 15 % to max of 30 % for original IRIS). The wavelength range the system responds to has been adjusted though, and initial experiments were performed by imaging a donor only (mCerulean), an acceptor only (Venus) and a positive FRET control (CeVe) expressed in *A. niger* to assess the new IRIS imaging device.

For the donor only control, mCerulean, and the positive FRET control, CeVe, it was possible to detect a fluorescence signal using IRIS (Figures 3.9 and 3.10).

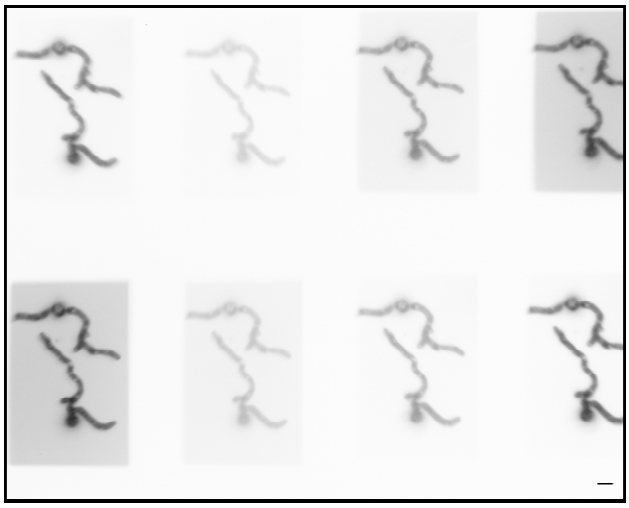

Figure 3.9: 8 bandpass image of mCerulean expressed in *A. niger* after excitation at 433 nm. Emission was collected between 450 nm and 600 nm in the different bandpasses as shown in Figure 3.8. Bar = 10 μm

The fluorescence emission signals for both probes were collected in all of the 8 available channels without revealing any significant difference in the spectral signature when comparing the two datasets.

Figure 3.10: 8-channel IRIS image collected for CeVe expressed in *A. niger* The emission signal was collected after excitation at 433 nm between 450 nm and 600 nm in the different bandpasses as shown in Figure 3.8. Bar = 10 μm

After excitation at 433 nm one would expect the biggest difference in fluorescence emission between mCerulean and CeVe to be detected above 510 nm, as seen in the spectra collected on the Leica TCSSP 5 confocal. The signal detected for mCerulean should be lower compared to the one from CeVe above this wavelength.

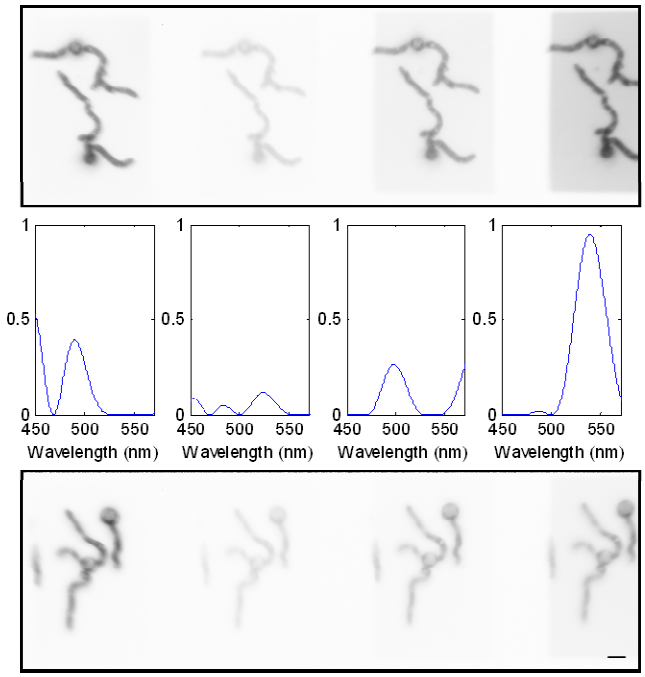

Figure 3.11: Comparison of 4 channels of the mCerulean (top) and CeVe (bottom) datasets including the relevant bandpasses (middle). Bar = 10 µm

A major difference between the images would therefore be expected in channel number 4 (far right). As figure 3.11 shows, it is not possible to conclude anything from the datasets as such.

The variation in background levels between the different channels and datasets already hints at the necessity of further image processing (eg background subtraction), before conclusions about any difference in the fluorescence emission signature can be made. As previously mentioned, the fact that the bandpasses in the different channels are broad and or multiple bandpasses are collected in one channel further complicates the analysis.

The main problem when trying to compare the datasets of all three probes (including the one for the acceptor only control Venus) with each other is the poor quality of the Venus data (Figure 3.12). The low signal to noise ratio makes it impossible to confirm a fluorescence signal at all for this probe.

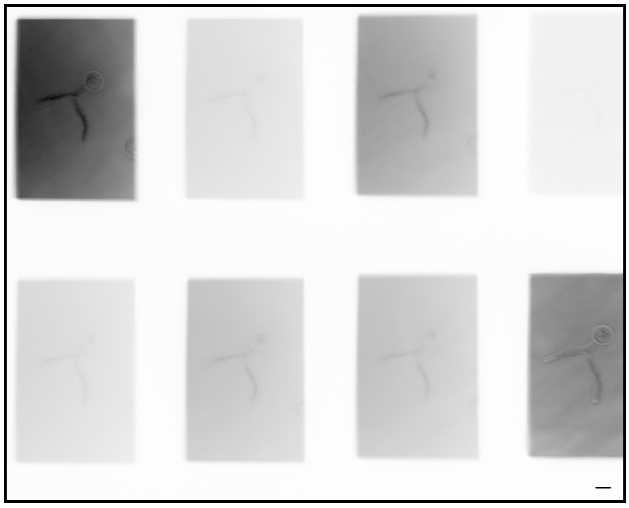

Figure 3.12: 8 channel image of Venus expressed in *A. niger*. The emission signal was collected between 450 nm and 600 nm in the different bandpasses as shown in Figure 3.8. The probe was excited at 511 nm. Bar = 10 µm

Imaging of the venus probe with a standard YFP filtercube, however, confirmed that the fluorescent protein was expressed in *A. niger* and excited at 515nm. With an emission maximum of Venus at 528 nm and emission usually collected between 530 and 550 nm without problems, one would expect the greatest signal in the 4th image (top left). This being the dimmest image of the 8, it seems unlikely that there was any fluorescence to detect. The probe might have been bleached during the image acquisition and the light used for excitation of the probe (despite the use of a 515 LP dichroic mirror) leaked through into the emission channel. Again definite conclusions are difficult to make due to the broad and multiple bandpasses in the 8 channels.

3.3.2 Spectral imaging on Leica TSC SP 5 confocal microscope

To demonstrate the differences in the fluorescence spectra of the different control contructs (donor mCerulean or acceptor only Venus or mCitrin and positive FRET controls CeVe and CeCi) and the 3 Ca^{2+}-sensitive probes (CeVe 2.12, CeVe 6.1 and TN-L15mCer) their spectra were collected on a Leica TSC SP5 confocal microscope. In contrast to IRIS, spectral information can not be obtained in a snapshot, data is acquired sequentially for each bandpass at a time. The comparatively long acquisition time makes this approach unsuitable for intensity based FRET analysis, where the relevant emission signals should be collected simultaneously.

Spectra were obtained from confocal images using Leica LAS AF software and shifted to display a maximum value of 1 for peak emission. The different fluorescence intensity values at the starting point of the spectra are due to the variation in fluorescence intensity of the strains. Lower fluorescence intensity (e.g. due to lower expression level of one probe as compared to another) resulted in a higher background level as compared to the peak emission signal when determining the spectra.

Figure 3.13 shows the spectra of the different control constructs. The donor only (mCerulean) was excited at 405 nm only, the acceptor fluorophores (Venus and mCitrine) at 488nm only and the two positive FRET controls (CeVe and CeCi) at both wavelengths. Prior to collection of spectral data it was confirmed that no distinct signal could be collected for the acceptor only constructs Venus and mCitrin when excited at 405 nm (data not shown).

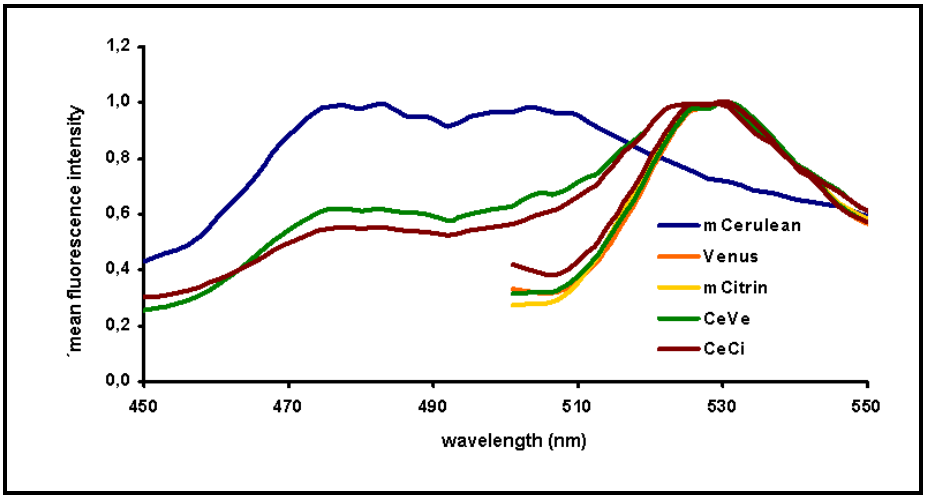

Figure 3.13: Fluorescence emission spectra as normalised by Leica LAS AF software of donor or acceptor only constructs and positive FRET controls expressed in *A. niger*. mCerulean was excited at 405 nm and emission collected between 450 nm and 552 nm. Venus and mCitrin were excited at 488 nm, emission collected between 501 nm and 552 nm. CeVe and CeCi were excited at both wavelengths and emission collected as stated above.

As shown in figure 3.13, both positive controls displayed the maxima of the donor as well as the acceptor fluorophore when excited at 405 nm. This is not only an indication that donor and acceptor fluorophore are successfully expressed in both strains, but as well that the positive controls do indeed exhibit FRET when expressed in *A. niger*.

A comparison of the emission spectra collected for mCerulean, Venus, mCitrin and the positive controls CeVe and CeCi showed that, when performing standard confocal microscopy with 2 emission channels, it should be possible to detect distinct donor and acceptor signals by choosing emission channels of 470 nm to 490 nm and 530 nm to 550 nm, respectively.

A comparison between the emission spectra of Venus and mCitrin alone expressed in *A. niger* (Figure 3.14) revealed that both spectra are essentially identical. No major differences could be detected when comparing the normalised spectra of both fluorophores. These results were expected and correlate with spectral properties published for protein extracts of both fluorophores (Shaner et al 2005, see Table 1.2).

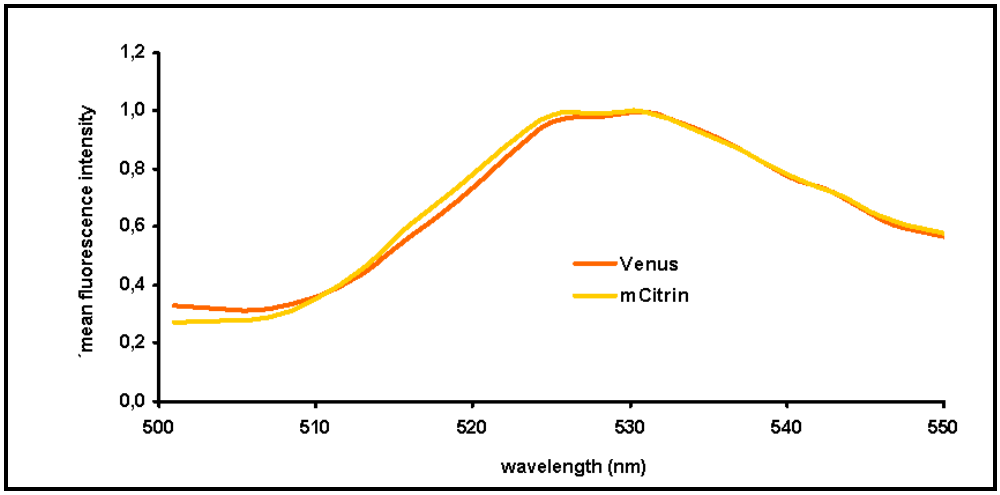

Figure 3.14: Normalised emission spectra of Venus and mCitrin expressed in *A. niger* at an excitation wavelength of 488nm. Spectra were collected between 501 nm and 552 nm.

The comparison of emission spectra of the different Ca^{2+}-sensitive probes and positive FRET controls CeVe and CeCi (Figure 3.15) showed that all 5 different probes display the maxima of the relevant donor and acceptors (mCerulean and either Venus or mCitrine).

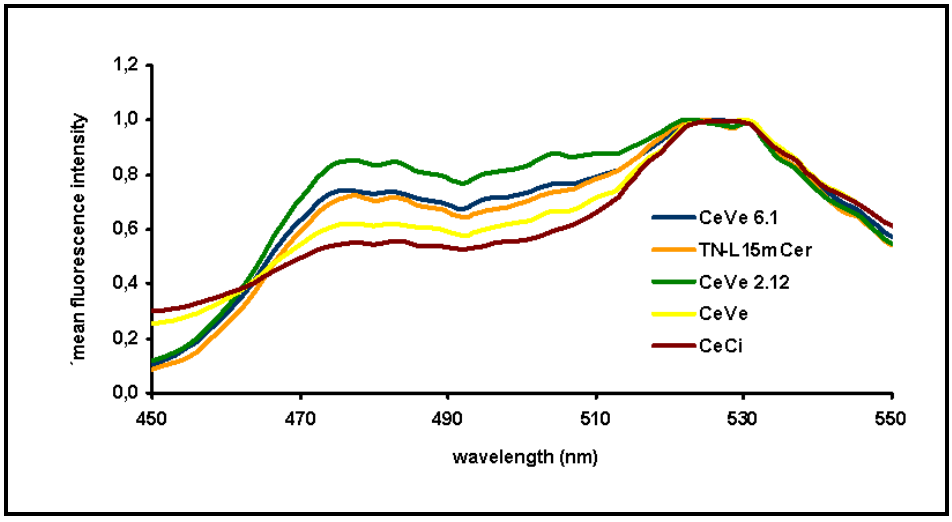

Figure 3.15: Normalised emission spectra of the different Ca^{2+}-sensors and positive FRET controls expressed in *A. niger*. Probes were excited at 405 nm and emission signals collected from 450 nm to 552 nm.

For better comparison of these results with data obtained by the spectral snapshot device IRIS, montages of a selection of Leica confocal images at different emission wavelengths were made using Image J software. Since IRIS covers a broader detection wavelength than the one chosen for spectral imaging on the Leica TSC SP5, only 6 images were selected for mCerulean and CeVe and 3 for Venus expressed in *A. niger* (Figure 3.16).

Despite the differences in fluorescence intensity between the 3 constructs, it is possible to detect a variation in the spectral signature when looking at the images. Maximum fluorescence intensity for mCerulean is detected in images 2-4 (471nm – 513 nm), whereas the maximum emission signal for CeVe is evident in image 5 (534 nm), displaying clearly the same peak as Venus.

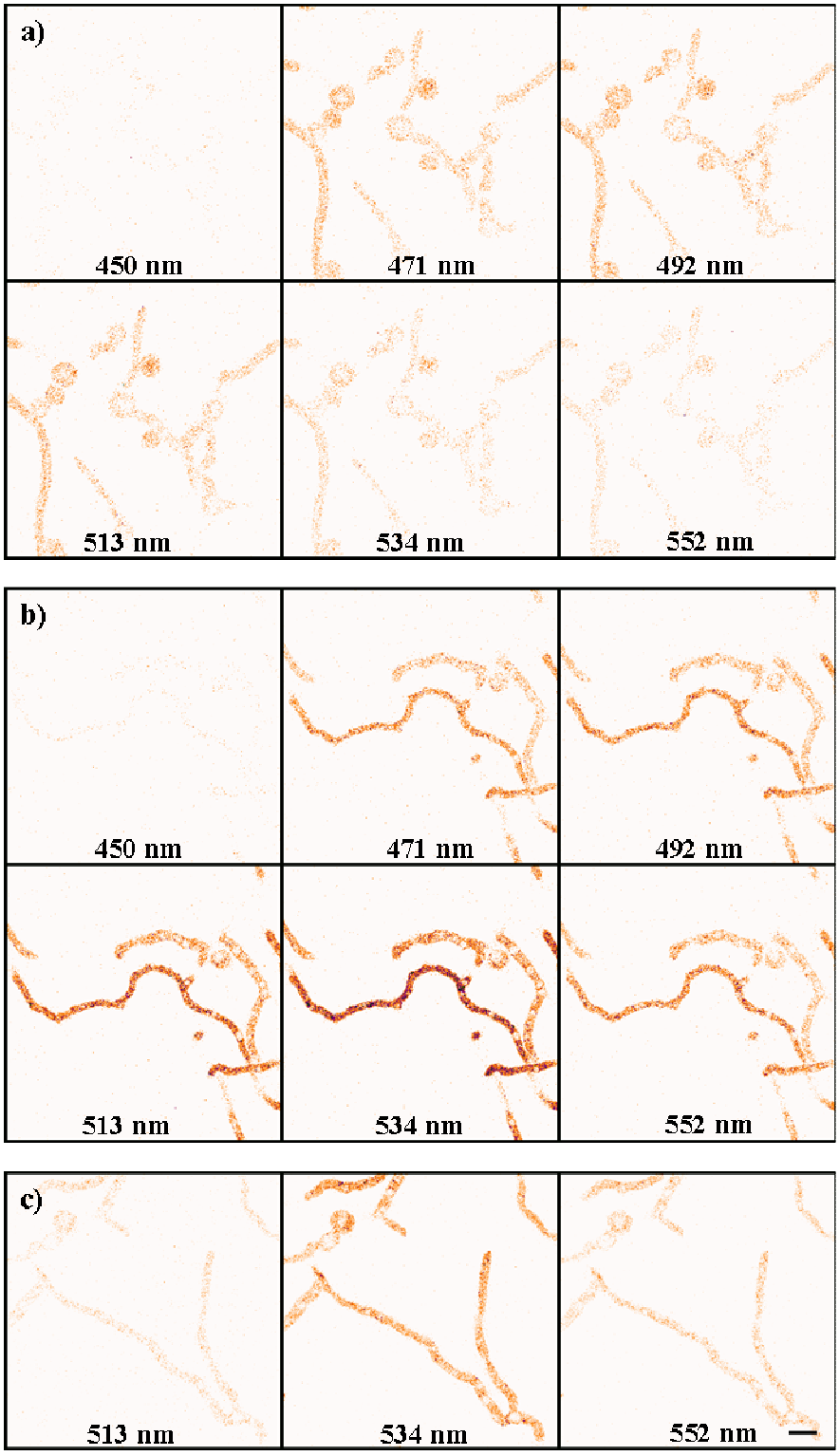

Figure 3.16: Images collected during spectral acquisition on Leica TSC SP5. a) mCerulean, b) CeVe both excited at 405 nm and c) Venus excited at 488 nm. Emission band maxima as labelled. Bar = 10 µm.

The main drawback of this method is the long acquisition time together with the repeated illumination of the sample necessary to obtain the spectral information. Although acceptable as long as no adverse effects on the fungus or fluorescent proteins are observed (such as changes in morphology or bleaching), this is not ideal for *in vivo* studies of calcium signatures, where images need to be collected at high speed.

3.4 Live Cell Imaging of recombinant proteins expressed in *Aspergillus niger* – Confocal analysis of Ca^{2+} and pH sensors

3.4.1 Intensity based FRET analysis of Ca^{2+} sensors and controls

Analysis of the different probes and controls expressed in *Aspergillus niger* was initially performed on a Bio Rad Radiance 2100 confocal system and later on a Leica TSC SP5 confocal microscope.

To be able to image probes and controls at the same settings the acquisition modes were adjusted to minimise saturation in the bright probes while at the same time allowing detection of emission signals from the weaker probes. This step was considered necessary to be able to compare the results for the different probes with each other and is commonly done in intensity based FRET analysis.

The different images necessary to perform FRET analysis as described in materials and methods are summarised in Table 3.3.

Table 3.3: Images collected for FRET analysis of positive controls and Ca^{2+} sensors expressed in *Aspergillus niger*

	Donor channel exc: 405 nm em: 470 nm - 490 nm	**FRET channel** exc: 405 nm em: 470 nm - 490 nm	**Acceptor Channel** exc: 488 nm em: 430 nm - 500m
mCerulean	x	x	
Venus		x	x
Citrin		x	x
CeVe	x	x	x
CeCi	x	x	x
CeVe 2.12	x	x	x
CeVe 6.1	x	x	x
TN-L15mCer	x	x	x

To accurately determine FRET, a set of 7 images was required for each probe, the donor in the donor and the FRET channel, the acceptor in the acceptor and the FRET channel, and the probe in the FRET, donor and acceptor channel. Correction factors can be determined from separate experiments and, provided the same donor and acceptor are present, do not need to be determined separately for every different probe.

A sample set of images used for FRET analysis of CeVe is shown in Figure 3.17. mCerulean as donor was excited at 458 nm and emission collected at either 520 nm to 550 nm (FRET channel) or at 470 to 500 nm (donor channel). Venus as acceptor fluorophore was excited at either 458 nm (FRET channel) or 514 nm (acceptor channel), in both cases emission signals were collected between 520 nm to 550 nm. The final set of images shows emission collected for the positive FRET control CeVe in all 3 different channels (FRET, donor and acceptor).

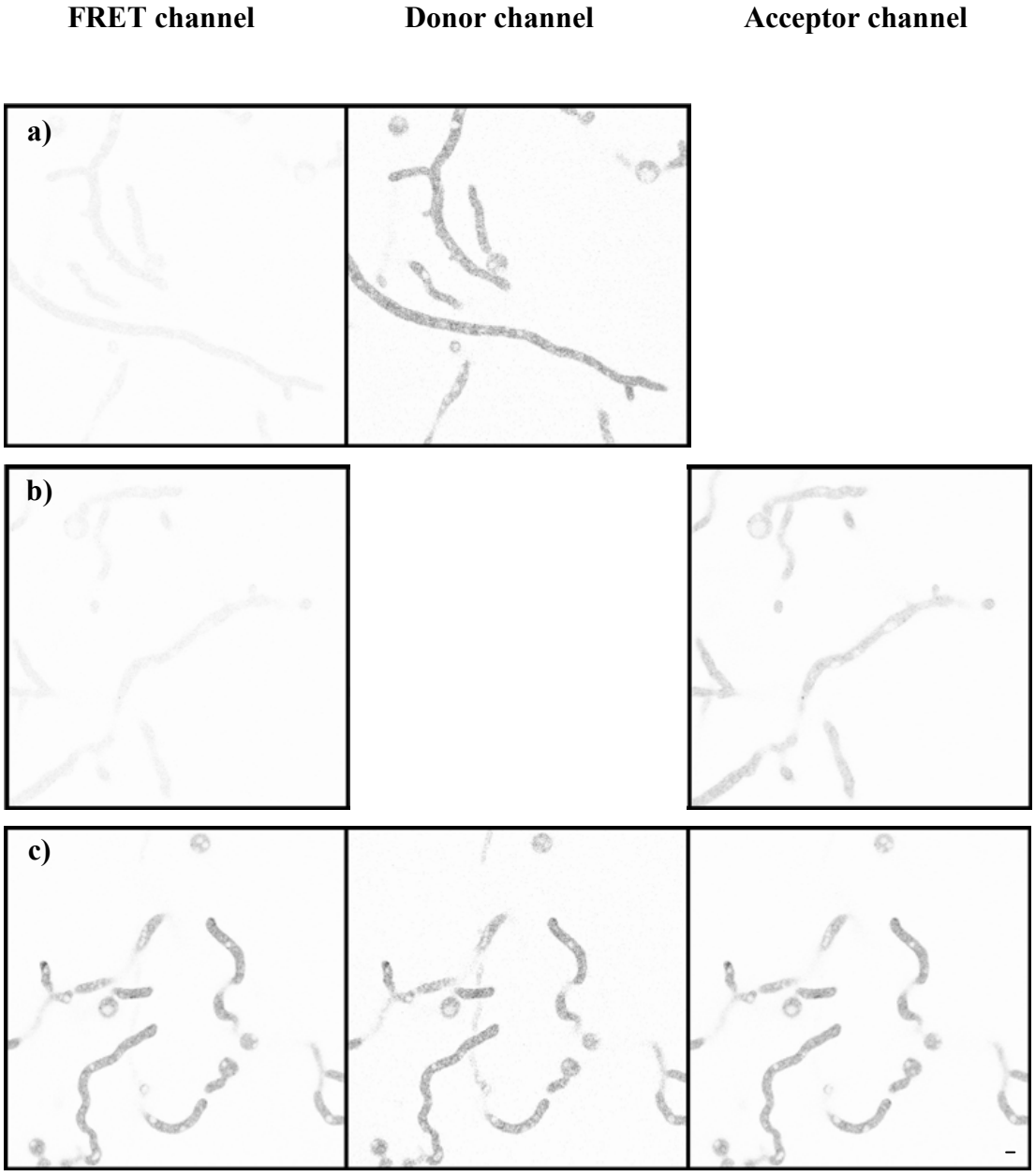

Figure 3.17: Sample set of images collected to determine correction factors D and A and perform FRET analysis of the positive FRET control CeVe. a) mCerulean imaged in FRET and donor channel, b) Venus imaged in FRET and acceptor channel and c) CeVe imaged in all 3 channels. Excitation was at 458 nm for the FRET and donor channel and at 514 nm for the acceptor channel. Emission in the donor channel was collected between 470 nm to 500 nm, in the FRET and acceptor channel between 520 and 550 nm. Images were collected on a Leica TSC SP5 confocal system. Bar = 5 μm.

Correction factors and FRET values for the different probes were obtained from a minimum of 5 different dataset and analysis of at least 3 hyphae within each of these per sample. Correction factors for mCerulean, Venus and mCitrin as determined from images collected on the Bio Rad Radiance 2100 and Leica TSC SP5 confocal systems are shown in table 3.4.

Table 3.4: Results of determination of correction factors D (mCerulean) and A (Venus and Citrin) Shown are the factors determined for correction of bleedthrough from donor emission signal into the acceptor channel (D) and cross excitation of the acceptor at the donor excitation wavelength (A) as determined on Bio Rad Radiance 2100 and Leica TSC SP5 confocal microscopes.

	Bio Rad Radiance 2100	Leica TSC SP5
D (mCerulean) Intensity (Donor $_{FRETchannel}$) Intensity (Donor $_{Donorchannel}$)	0.48 ± 0.04	0.17
A (Venus) Intensity (Acceptor $_{FRETchannel}$) Intensity (Acceptor $_{Acceptorrchannel}$)	0.44 ± 0.05	0.43 ± 0.02
A (Citrine) Intensity (Acceptor $_{FRETchannel}$) Intensity (Acceptor $_{Acceptorrchannel}$)	0.38 ± 0.04	0.38 ± 0.01

The values of the correction factors for the two acceptor fluorophores Venus and mCitrin do not vary significantly when determined from images collected on the Bio Rad Radiance 2100 or Leica TSC SP5 confocal.

A major difference, however, is detected for the donor correction factor as determined for mCerulean. The value obtained from images collected on the Bio Rad system is more than double that obtained from images taken on the Leica confocal system, indicating a larger amount of bleedthrough from mCerulean emission into the acceptor channel on the Bio Rad Radiance 2100 than on the Leica TSC SP5.

Since the acceptor fluorescence is collected over a broader bandwidth on the Leica confocal system (520 nm to 550 nm as compared to 530 nm to 550 nm on the Bio Rad system), this does not explain the significant difference in the two values. It is likely that the different laser lines used for excitation of mCerulean (405 nm on Bio Rad system, 458 nm on Leica TSC SP5) are the cause of this though. It seems that the settings chosen for the Bio Rad method (excitation at 40% of 405 nm) resulted in a more efficient excitation of mCerulean than the ones chosen for the Leica TSC SP5 (15 % of 458 nm). From the excitation spectrum of mCerulean as shown in figure 1.9 it is obvious that the 458 nm line only excites the fluorophore at the tail end of the spectrum.

FRET values for the two positive FRET controls CeVe and Ceci and the 3 Ca^{2+}-sensitive probes CeVe 2.12, CeVe 6.1 and TN-L15mCer as determined from images collected on either the Bio Rad Radiance 2100 or the Leica TSC SP5 confocal systems are listed in Table 3.5.

Table 3.5: FRET values determined for different FRET probes expressed in A. niger on the two different confocal systems.

	Bio Rad Radiance 2100		Leica TSC SP5	
	FRET	FRET %	FRET	FRET %
CeVe	- 11.13 ± 4.15	- 4.36 ± 1.63	17.17 ± 2.98	6.73 ± 1.05
CeCi	- 2.64 ± 1.91	- 1.04 ± 0.75	6.88 ± 1.00	2.70 ± 0.35
CeVe 2.12	_	_	7.20 ± 2.07	2.82 ± 0.73
CeVe 6.1	_	_	15.94 ± 4.85	6.25 ± 1.70
TN-L15mCer	_	_	20.71 ± 1.36	8.12 ± 6.48

Considering the FRET values determined for the two positive controls CeVe and CeCi from datasets obtained on the Bio Rad Radiance 2100 confocal system are negative, it is evident that it was impossible to detect FRET.

Taking into account previous results obtained from spectral data, it is unlikely that the probes do not exhibit FRET but more likely that the settings chosen for image acquisition were not optimal. Additionally, the relatively low fluorescence intensity of mCerulean, Venus and the two positive FRET controls CeVe and CeCi might have introduced errors when attempting to analyse the data. Furthermore the long acquisition time necessary to collect the relevant images does not help to improve the quality of the data.

The analysis of images collected on the Leica TSC SP5 confocal showed positive FRET values. Maximum amounts of FRET were expected for the two positive controls CeVe and CeCi, values of 6.73 ± 1.05 and 2.70 ± 0.35 respectively however are so low, that further discussion about the difference in FRET efficiencies between the various probes is unfeasible.

It is known that intensity based FRET imaging is very sensitive to minor changes in the microscopy setup as well as slight changes in the treatment of the images for analysis (one needs to be particularly careful about thresholding the images as it is easy to introduce errors at this stage). Bearing this in mind the difference in fluorescence intensity of the different probes might have caused more complications than initially assumed. If possible, donor-only and acceptor-only controls should show the same or at least very similar fluorescence intensities as the FRET probes. This would allow accurate determination of the correction factors necessary to further analyse the probes with respect to their FRET efficiencies. Considering the initial results obtained from spectral imaging on the Leica TSC SP5, it might have been beneficial to excite mCerulean and the FRET probes at 405 nm rather than at 458 nm.

3.4.2 Analysis of pH-sensor RaVC expressed in *A. niger*

The probes used for pH-measurement in *A. niger* in this study are based on pHluorins and were developed by Tanja Bagar and Mojca Benčina at the National Institute of Chemistry, Ljubljana, Slovenia.

Initial imaging of the probe and experiments on the Bio Rad Radiance 2100 were performed as part of this PhD. The additional experiments described in this chapter had been attempted on the Bio Rad system but did not reveal any change in intracellular pH of *A. niger* (ratio changes of the probe could not be determined or were so low, that they did not show any significant difference to the variation in fluorescence ratio of the controls imaged on different days).

To highlight the suitability of RaVC for determination of changes in intracellular pH and give an example of the potential of a working genetically encoded sensor, the experiments as successfully performed by Tanja Bagar using a Leica TSC SP5 confocal microscope and published in Bagar et al., 2009 are included in this chapter.

3.4.2.1 Initial imaging of RaVC on Bio Rad 2100 Radiance

Initial imaging of RaVC was perfomed using confocal microscopy to confirm RaVC expression in germinated spores of *A. niger*. In 18h old hyphae of *A. niger* the probe is expressed throughout the cytoplasm and as shown in Figure 3.18 excluded from organelles that seem to be vacuoles while being concentrated in small spherical structures.

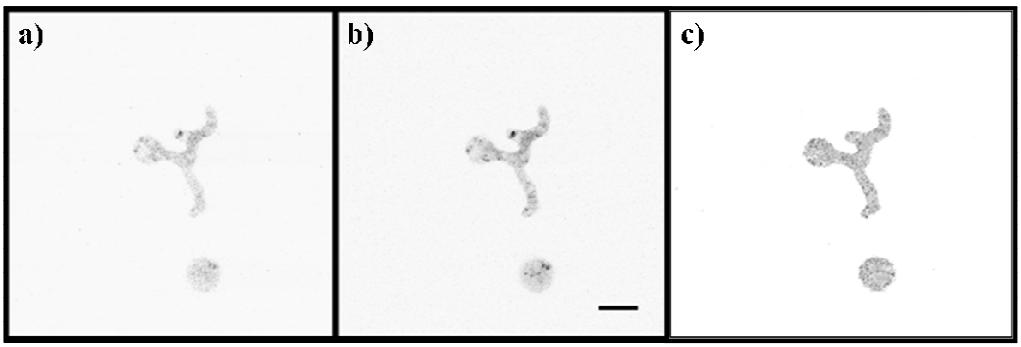

Figure 3.18: Confocal images of RaVC expressed in *A. niger*. The probe was sequentially excited at 405 nm (a) and 476 nm (b). Fluorescence emission was collected between 500 to 530 nm. A ratio image (c) was obtained by dividing the fluorescence value of the relevant pixels of image a) by the ones in image b) after 3x3 binning. Bar = 10 µm

The ratio image in Figure 3.18 reveals that by 3x3 binning the noise of the original two images (caused by the non uniform distribution of the probe) can be reduced; as a result the cytoplasm does appear inhomogeneous though.

3.4.2.2 A first attempt at calibrating RaVC in *A. niger*

Spore samples of *A. niger* have been prepared and treated to obtain a calibration curve as described in materials and methods. A significant difference in the ratios of the mean fluorescence intensities detected after excitation at 405 nm and 476 nm could only be detected in the range of ph 6.0 to pH 7.0 (Figure 3.19). With increasing pH the ratio (405/476) of the mean fluorescence intensity increased from 0.44 at pH 6.0 to 0.72 at pH 7.0. Although displaying a roughly 2 fold increase in ratio over the range from ph 6.0 to pH 7.0, comparable with the results obtained *in vitro*, the latter experiments allowed detecting changes in the ratio of fluorescence intensity (395/ 475) over the range from pH 5.0 to pH 9.0

On the plus side it has to be noted that a change in the ratio can be observed and that from looking at the ratio images in Figure 4.8 there seems to be no pH gradient within the hyphae (differences in pseudocolour are due to uneven distribution of the probe and artefacts caused by 3x3 binning), suggesting that nigericin has been successfully used to equilibrate the internal pH in *A. niger* with the external pH of the buffer.

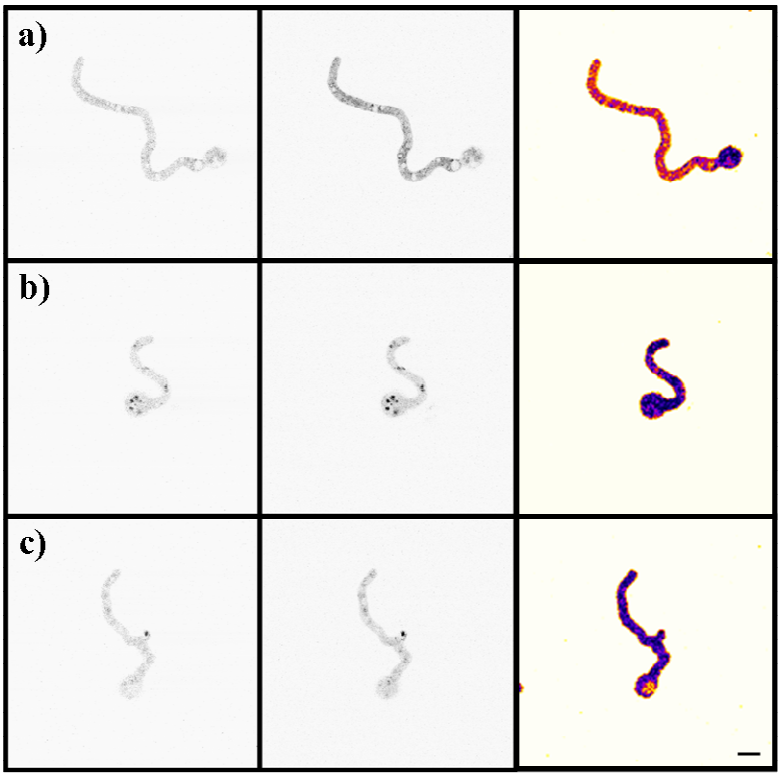

Fig 3.19: Confocal and ratio images of *A. niger* imaged in different pH buffers. 18h old hyphae of *A. niger* have been incubated in 5 µM nigericin and pH buffers of pH 6.0 (a) pH 6.5 (b) and pH 7.0 (c) 50 min prior to imaging . Images were collected after excitation at 405 nm and 476 nm, ratio images determined as described above. Bar = 10 µm

The main problem identified during imaging and analysis was the time delay between the collection of both images. Within the 35 seconds necessary to obtain the set of 2 images, organelles within the fungal hyphae as well as the hyphae themselves had moved. Even if the overall movement was usually small, this did affect the analysis significantly. Additionally it was in some cases possible to observe a shift of several pixels from one image to the other.

When imaging at high speed without shift between the images, pixels of high fluorescence intensities will be present at the same defined point in both images, whereas initial imaging showed that in our method the location of corresponding features within the hyphae had often moved by several pixels.

Due to these problems further analysis was performed by Tanja Bagar on a Leica TSC SP5 confocal microscope, allowing much faster acquisition times. Only experiments that had been previously (but unsuccessfully) performed on the Bio Rad system as part of this project have been included.

The following results are adapted from Bagar et al. as published 2009.

3.4.2.3. *In situ* calibration allows determination of intracellular pH

An *in situ* calibration was performed to accurately determine the cytoplasmic pH in living hyphae. Fungal hyphae were permeabilized with nigericin in the presence of buffers with different pH values. Images (Figure 3.20 a)) were collected and ratios (Figure 3.20 b)) of emission intensities after excitation at 405 nm and 476 nm were calculated based on Equation 1 (R_{min} and R_{max} were calculated from the emission intensities at pH 5.0 and 8.5). The *in situ* calibration clearly shows that RaVC displays pH sensitivity in the normal physiological range within living hyphae. A logarithmic plot of the standard curve is presented in 3.20 c). The pK_a determined *in situ* for RaVC is 6.9 (±0.1) and its optimal linear response to pH is between pH 5.5 and 8.0 (Figure 3.20 c). The K_a as well as R_{min} and R_{max}, as determined for each set of experiments separately, were used to calculate intracellular pH pixel-by-pixel within hyphae using Equation 2 (see 2.19).

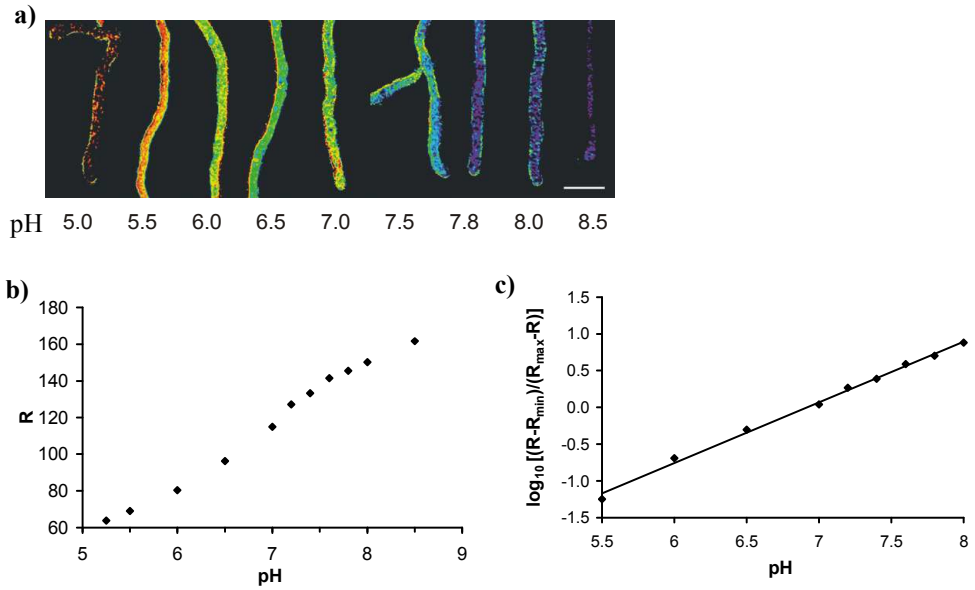

Figure 3.20. *In situ* calibration of RaVC. a) Pseudocolored images of *A. niger* expressing RaVC. Different colours have been assigned to defined pH values according to the *in situ* calibration curve shown below (b). Bar = 10 µm. b) plot of the fluorescence excitation ratio versus intracellular pH. The ratio (R) between the emission intensities collected after excitation at 405 nm and 476 nm was calculated using Equation 1. c) logarithmic plot of the fluorescence excitation ratio (b) versus intracellular pH. Adapted from Bagar et al., 2009.

The mean value for cytoplasmic pH in growing hyphae from 18-h-old colonies was 7.6 (±0.1) and varied between pH 7.4 and 7.7. Mean pH values were calculated from cytoplasmic areas that excluded detectable organelles or cytoplasmic regions in which the RaVC reporter was concentrated.

3.4.2.4 Cytoplasmic pH recovers in response to sudden changes in external pH

To assess the effects of sudden changes in extracellular pH on the cytoplasmic pH of *A. niger*, either a strong acid (50 mM HCl) or a strong base (5 mM NaOH) were added to growing hyphae. In response to this the cytoplasm was transiently acidified (after addition of HCl) or alkalinized (after addition of NaOH) as shown in Figure 4.21.

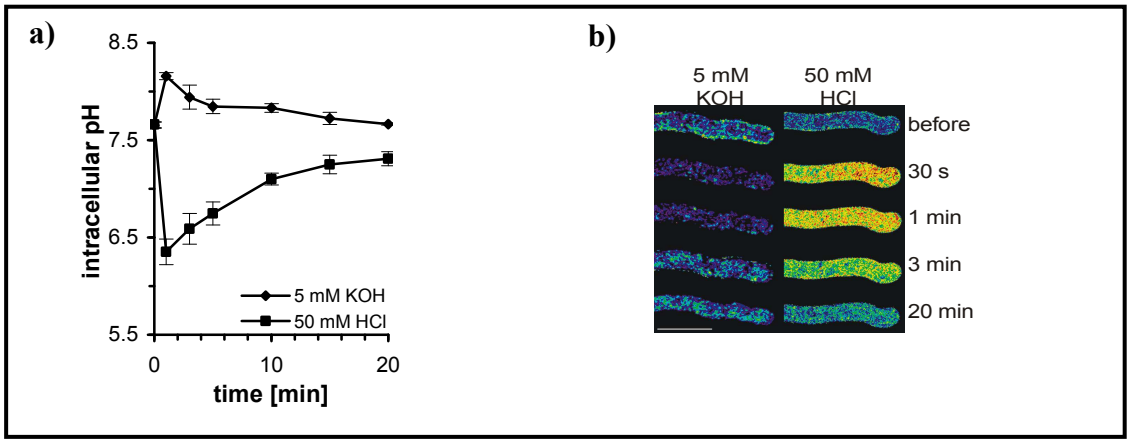

Figure 3.21. Response of cytoplasmic pH to a sudden change in extracellular pH. a) change in cytoplasmic pH of 18 h old hyphae of *A. niger* after addition of strong acid (50 mM HCl) or base (5 mM KOH). b) pseudocolored fluorescence ratio images of hyphae. The pseudocolors correspond to defined pH values calculated from the fluorescence ratios using the *in situ* calibration (blue = alkaline; red = acidic). Bar = 10 µm. Adapted from Bagar et al., 2009.

Thirty seconds after the addition of HCl, the cytoplasmic pH transiently dropped from 7.6 (± 0.1) to 6.3 (± 0.2). Similarly, the addition of NaOH transiently increased the cytoplasmic pH from 7.6 (±0.1) to 8.3 (±0.1). The cytoplasmic pH returned to its homeostatic pH value (7.4-7.7) within 20 min. The addition of 50 mM HCl or 5 mM NaOH resulted in the pH of the extracellular media changing by 3.5 or 0.5 pH units, respectively.

The spectral properties of RaVC determined *in situ* showed only small differences with those measured *in vitro*. The *in situ* calibration showed that RaVC expressed inside fungal cells could be used to measure intracellular pH over the physiological range of pH 5.5 and 8.0. The pK_a of RaVC inside fungal cells was shown to be 6.9 compared with a pK_a of 6.7 measured *in vitro*. This slight shift in pKa is probably due to differences between the intracellular environment and the *in vitro* calibration solutions. Ionic strength, viscosity and hydrophobicity of the medium have all been identified as potential factors that influence the response of ion-sensitive dyes (Fricker et al., 1999).

RaVC was localized in the cytoplasm in young hyphae from 18-h-old colonies of *A.niger*. Its cytoplasmic distribution, however, was non-uniform and concentrated in certain regions (organelles or cytoplasmic domains) which could not be identified.
After addition of a strong acid or base, the intracellular pH was found to recover within 20 minutes. This demonstrates the presence of strong pH buffering in the cytoplasm and also strong proton pumping that expels excess protons in a short period of time and maintains homeostatic pH while the external pH is several units higher or lower.

3.5 FLIM analysis of mCerulean and different FRET probes expressed in *A. niger*

The only probes where a statistically significant number of samples could be analysed were mCerulean and CeVe, results for CeVe 2.12 and CeVe 6.1 are still included to show the initial results we obtained. A detailed discussion of the difference between these FRET probes however is excluded due to the small amount of data collected for them.

18 h old hyphae of *Aspergillus niger* expressing mCerulean (donor only), the positive FRET control CeVe or the Ca^{2+}-sensors CeVe 2.12 or CeVe 6.1 were studied using TSCSPC. Typical fluorescence intensity images as used to extract decay data and generate lifetime maps in QAAnalysis software are shown in Figure 3.22.

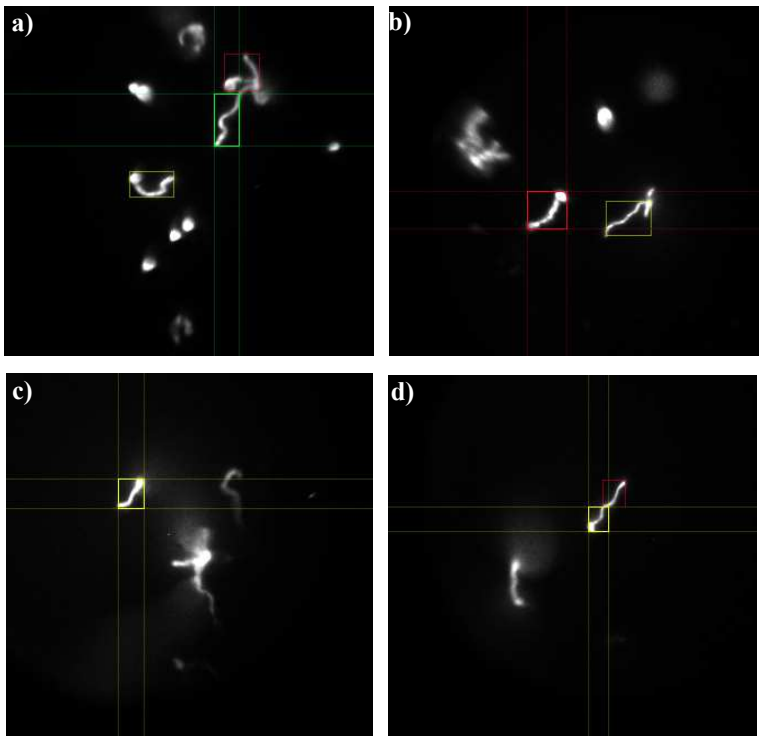

Figure 3.22: Fluorescence intensity images as displayed by QAAnalysis software. Shown are images of the donor only mCerulean (a), the positive FRET control CeVe (b) and the two Ca^{2+}-sensitive probes CeVe 2.12 (c) and 6.1 (d) expressed in *A. niger*. Fluorescence decay data was extracted from regions of interest (ROIs) highlighted in the images.

The fluorescence intensity images reveal that the fluorescence signal within the hyphae was evenly distributed. The brightness of the different images was adjusted to facilitate choosing ROIs, therefore the signal between the different probes cannot be compared from these images. The size of the ROIs however was selected to include approximately the same amount of counts; decays extracted from the ROIs were as a result comparable in the amount of counts in the peak channel (generally about 10^4).

From the intensity images a decision was made whether to further analyse the data or not. In cases where the cells had moved out of focus completely by the end of the experiment, the number of counts for selected regions of interest was far below 10^4, or when the amount of counts per pixel in the background was similar in magnitude as the ones for the samples, further analysis was precluded.

The above mentioned difficulties were usually due to problems such as the detector heating up (which prolonged the acquisition time and resulted in poor signal to noise ratio) or the system not being properly aligned. Heating up of the detector was later prevented by cooling the system with liquid nitrogen when the temperature of the detector rose above 28ºC.

An initial comparison of the probes was made using the fluorescence lifetime maps created in QAAnalysis. Average lifetime values as determined visually from liftetime maps (Figure 3.23) are presented in Table 3.6.

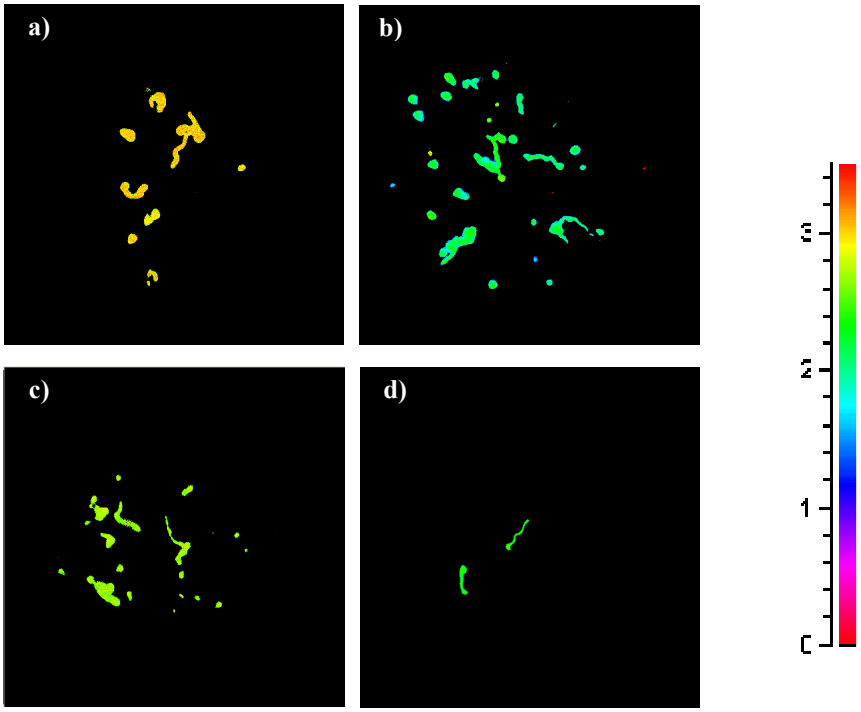

Figure 3.23: Lifetime maps created in QAAnalysis. Maps shown are typical lifetime maps obtained for the donor only construct mCerulean (a), the positive FRET control CeVe (b) and the two Ca^{2+}-sensitive probes CeVe 2.12 (c) and CeVe 6.1 (d). The calibration bar shows the colours assigned to the different lifetime values (e).

Table 3.6: Average lifetime values as determined visually from liftetime maps for the donor only (mCerulean) and different FRET probes expressed in *A. niger*

probe	mCerulean	CeVe	CeVe 2.12	CeVe 6.1
lifetime (ns)	3.2	2.2	2.7	2.5

Although the maps only represent approximate average lifetime values it is evident that mCerulean shows the highest value whereas CeVe displays the lowest, with values for CeVe 2.12 and 6.1 ranging between these two.

It is evident from the lifetime maps that it is possible to distinguish between FRET and no FRET situations. The donor only mCerulean displays the highest lifetime value, and as expected in the event of FRET, the value for the positive FRET control CeVe appears significantly lower. The lifetime maps reveal as well that FRET seems to occur in the Ca^{2+}-sensors CeVe 2.12 and CeVe 6.1. From the lifetime map it seems that the amount of FRET in the Ca^{2+}- probes is lower as compared to the amount in the positive FRET control; due to the approximate nature of these values this has to be regarded as a strong possibility rather than a certainty though.

Further data analysis was performed in F900 software as described above. Figure 3.24 shows a comparison between 3 different fits for mCerulean. mCerulean has been described to be an improvement over ECFP in that it shows simpler decay kinetics, namely a monoexponential decay (Rizzo et al., 2006). For this reason it was initially tried to fit a monoexponential decay to the TSCSPC data collected for mCerulean in this project. Figure 3.24 reveals clearly that a better fit is obtained assuming a bi exponential decay for this protein. Not only does the structure in the residuals disappear upon adding an additional decay component, the value for the reduced χ^2 also decreases significantly from 6.519 to 1.102, showing a better fit is obtained assuming 2 lifetime components for mCerulean.

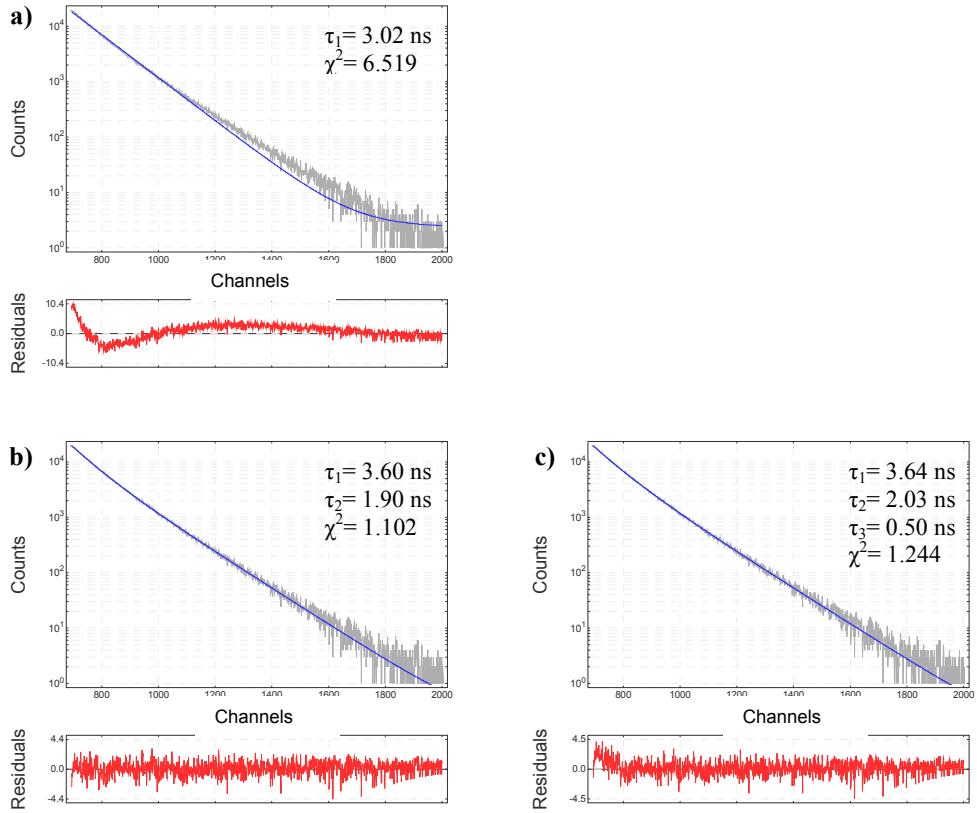

Figure 3.24: Different fits for mCerulean decay data Displayed are a sample monoexponential (a), biexponential (b) and triple exponential (c) fit for TSCSPC data collected for mCerulean expressed in A. niger. The actual decay is shown in grey, the fit in blue.

In contrast, adding a further decay component (Fig. 3.24 c)) does not improve the goodness of the fit, and the reduced χ^2 parameter increases again, confirming the best fit for mCerulean is obtained with 2 lifetime components.

A comparison of 2- and 3-exponential fits for the positive FRET control CeVe expressed in *A. niger* (Fig. 3.25) revealed, that the best fit for the decay data was obtained by fitting 3 lifetime components. The structure in the residuals disappeared and the value for χ^2 decreased from 1.364 to 1.067 upon addition of a third lifetime component. From these results it appears that a difference between FRET and no FRET situations can be determined by the appearance of an additional lifetime component in case of FRET as compared to the no FRET situation.

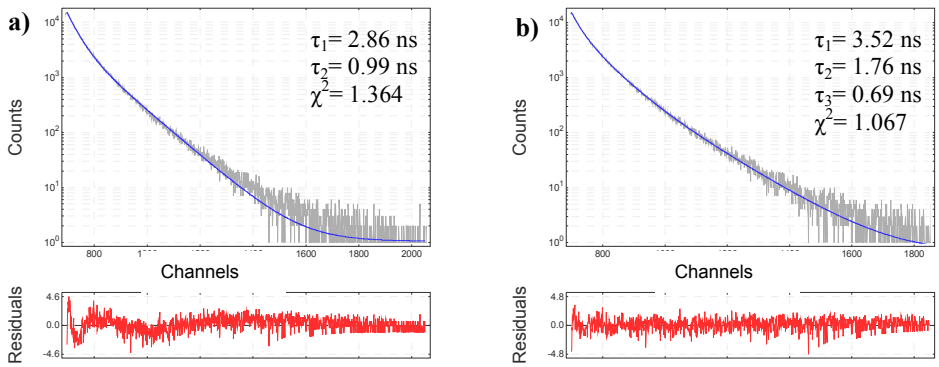

Figure 3.25: Comparison of 2- and 3-exponential fit for TSCSPC data of CeVe expressed in *A. niger*. Displayed are a sample monoexponential (a) and biexponential (b) fit for the collected TSCSPC data. The actual decay is shown in grey, the fit in blue.

Further data analysis of decay data for mCerulean and CeVe confirmed the initial results (Table 3.6). For mCerulean two lifetime components of 3.75 ± 0.21 ns and 1.89 ± 0.09 ns and A-factors of 48.83 ± 5.83 % and 51.17 ± 5.83 % respectively were resolved. The three lifetimes determined for CeVe were 3.70 ± 0.42 ns (18.34 ± 9.91 %), 1.92 ± 0.22 ns (45.95 ± 4.67 %) and 0.80 ± 0.12 ns (35.71 ± 11.69 %). While the amount of the short mCerulean lifetime component stays essentially unchanged in CeVe, the amount of the long one decreases to about 20 % and is balanced by the appearance of the third, shortest lifetime component in CeVe. Initial results for CeVe 2.12 and CeVe 6.1 reveal 3 lifetime components for each of them, since it was not possible to analyse a significant number of samples for the two Ca^{2+}-sensors, the actual values as displayed in Table 3.7 should be regarded with caution and cannot be used for further discussion and comparison between the different FRET probes.

Using conventional photon-counting FLIM, FRET between CFP and YFP (Tramier et al., 2002; Duncan et al., 2004; Becker et al., 2004) and for a Cerulean-mCitrin fusion protein (Rizzo et al., 2004) has previously been described by biexponential decays, although Becker at al. already suggested the possibility of a third lifetime component for CFP-YFP FRET.

More complex kinetics were first described by Millington et al. (2007) using TSCSPC, where the acquisition of higher photon counts as compared to conventional photon-counting FLIM allows to resolve more complex decay kinetics.

Table 3.7: Results of fluorescence decay data analysis for donor only mCerulean and different FRET probes expressed in *A. niger*

probe	mCer	CeVe	CeVe 2.12	CeVe 6.1
τ_1 (ns)	3.75 ± 0.21	3.70 ± 0.42	3.49 ± 0.11	3.39 ± 0.06
τ_2 (ns)	1.89 ± 0.09	1.92 ± 0.22	1.68 ± 0.08	1.56 ± 0.10
τ_3 (ns)	-	0.80 ± 0.12	0.54 ± 0.06	0.50 ± 0.07
A_1 (%)	48.83 ± 5.83	18.34 ± 9.91	31.50 ± 1.03	28.49 ± 0.80
A_2 (%)	51.17 ± 5.83	45.95 ± 4.67	54.58 ± 1.48	47.14 ± 3.24
A_3 (%)	-	35.71 ± 11.69	13.92 ± 2.46	24.37 ± 4.01
χ^2	1.046 ± 0.046	1.070 ± 0.056	1.022 ± 0.006	1.056 ± 0.076

To confirm the complex decay behaviour for mCerulean, protein extracts of mCerulean and CeVe were analysed as described in Millington et al. (2007), see Table 3.8. Since only one sample per protein was analysed, the actual values need to be treated with caution.

Table 3.8: Results of fluorescence decay data analysis for donor only mCerulean and positive FRET-control CeVe expressed in *A. niger* or obtained from protein extracts

probe	mCer (*A. niger*)	CeVe (*A. niger*)	mCer (extract)	CeVe (extract)
τ_1 (ns)	3.75 ± 0.21	3.70 ± 0.42	3.33	3.42
τ_2 (ns)	1.89 ± 0.09	1.92 ± 0.22	1.42	1.50
τ_3 (ns)	-	0.80 ± 0.12	-	0.35
A_1 (%)	48.83 ± 5.83	18.34 ± 9.91	45	26
A_2 (%)	51.17 ± 5.83	45.95 ± 4.67	55	33
A_3 (%)	-	35.71 ± 11.69	-	31
χ^2	1.046 ± 0.046	1.070 ± 0.056	1.007	1.040

These lifetime values not only confirm the complex decay kinetics of mCerulean as measured in living cells of *A. niger*, but are furthermore in good agreement with the results found in living cells. The fact that the decay times are shorter in the protein extracts can be explained as an effect of the different environment of the probes (buffer medium as compared to living cell).

The complex decay behaviour for mCerulean as determined in this study stands in contrast to the originally reported monoexponential decay of mCerulean in solution (Rizzo et al., 2004), but has recently been supported by TSCSPC measurements of mCerulean lifetime in living COS-7 cells (Jose et al., 2008). In the latter paper the two lifetime components of mCerulean were resolved to be 3.37 ± 0.03 ns (τ_1) and 1.32 ± 0.05 ns (τ_2), values that are in good agreement with the results obtained in this study, especially considering the lifetimes were collected from proteins expressed in different cell types and under different conditions (fixed COS-7 mammalian cells - living hyphae of *Aspergillus niger*).

In terms of FRET analysis the data can be interpreted with two models, as described by Millington et al. 2007. The discussion below is adapted from this paper.
Two of the three donor decay times measured for the positive FRET control CeVe (τ1 and τ2) were very similar to those measured for the donor mCerulean (Table 3.7). The long-lifetime and short-lifetime conformations of mCerulean were labelled as D1 and D2, and assigned the lifetimes as τD1 and τD2, respectively. The value of A2 (the contribution of D2 to the emission) was essentially unchanged in CeVe, compared to mCerulen, whereas the decrease in value of A1 was balanced by the new contribution (A3) from the third decay component.
Since it has been demonstrated that the protonated chromophore of Venus cannot act as a FRET acceptor (Elslinger et al. (1999)), it was assumed that the Venus protein in CeVe can exist in two different forms; one can participate in energy transfer by acting as an acceptor (AC1), whilst the other cannot (AC2). When the donor mCerulen undergoes energy transfer to the acceptor Venus (AC1), the new donor protein lifetime is labelled τDA1 when D1 is the donor and τDA2 when D2 is the donor. When mCerulean is fused to the protonated form of Venus, AC2, the donor lifetimes are unchanged.

The first model used to interpret the data is labelled "3τ" (Fig. 3.26). This is the simplest interpretation of the data and assumes that only one of the two donor conformations (D1) participates in energy transfer. Thus, both the lifetime and A-factor of D2 are essentially unchanged in the fusion protein CeVe because none of the D2 population undergoes FRET. The persistence of τD1 in CeVe, with a reduced A-factor, shows that only a fraction of the population of D1 undergoes FRET to give the new short decay time τDA1. The A-factor of τDA1 (A3 in Table 3.7)) thus corresponds to the decrease in the A-factor of τD1. This model requires an absence of FRET for one conformation.

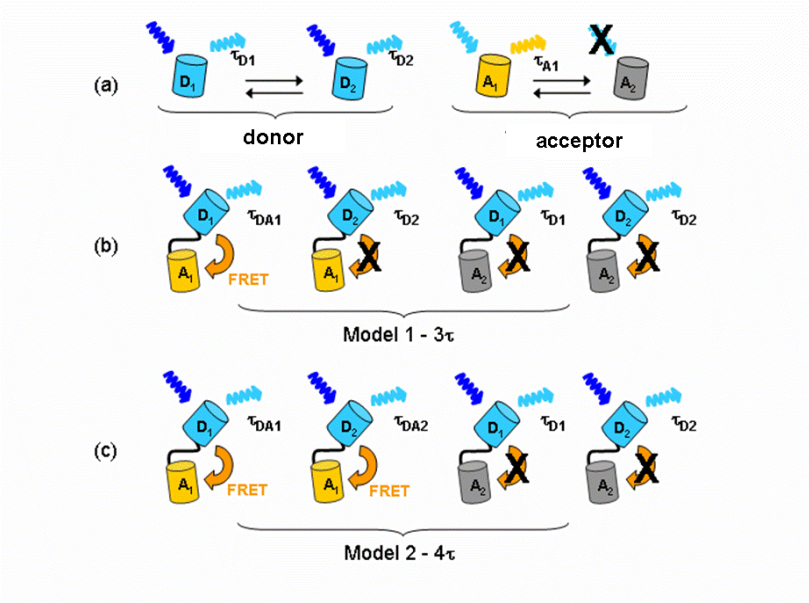

Fig. 3.26: Schematic model of photophysical processes involved in FRET for cells expressing donor or donor-acceptor fusion proteins. (a) The donor is in equilibrium between two conformations (D1 and D2). The acceptor protein is in equilibrium between non-protonated (AC1) and protonated states (AC2). Only AC1 acts as a FRET acceptor with the lifetime τA1. (b) In the 3τ model, FRET only occurs between one of the donor conformations and the acceptor, giving three unique lifetimes. (c) In the 4τ model, both donor conformations participate in FRET, resulting in four unique lifetimes. Adapted from Millington et al. (2007).

In the second model, labelled "4τ", it is assumed that both conformations participate in FRET, but that one of the unquenched donor lifetimes, τD2, is so similar to one of the donor–acceptor lifetimes, τDA1, that they cannot be resolved and appear as a single lifetime, τ2, in the fitted decay function. In other words, there are actually four decay components, but only three can be resolved.

Thus, the A-factor (A2) of τ2 (Table 3.7) remains essentially unchanged in CeVe because the increase in A-factor of τDA1, as result of FRET from D1 to AC1, is exactly balanced by the decrease in A-factor of τD2, as a result of FRET from D2 to AC1.

In both models, the fraction of unquenched donor fluorescence in the fusion, due to donor bound to AC2, is the same and is given by the value of A1, the A-factor of τD1, in the fusion.

The amount of unquenched donor in the positive FRET control can either be explained with the possibility that a certain amount of mCerulean is not bound to Venus at all (i.e. due to the linker being degraded, the Venus protein not having matured or a certain amount of the Venus proteins themselves being degraded by the cell due to misfolding), or mCerulean being bound to a form of Venus that cannot take part in FRET. As previously reported by Elslinger et al. (1999) only the deprotonated form of Venus can participate in FRET. The intracellular pH in 18h old hyphae of *A. niger*, as used in these experiments, has been determined to be 7.6 (Bagar et al., 2009), the same value as previously reported by Hesse et al. (2002).

With a pKa of Venus at 6.0 (Nagai et al., 2002), 2.5 % of Venus as expressed in *A. niger* exist in the protonated form which does not take part in FRET. Since the amount of unquenched donor in the positive FRET control lies at about 20% though, this only contributes minimally to the overall amount of unquenched donor. Since the Western Blot did not show any partially degraded GFPs, the remaining amount of unquenched donor is most likely due to probes being split in the linker region.

Chapter 4

Conclusions

4.1 Development of new calcium sensitive probes

The successful change of fluorescent proteins in existing probes and positive as well as negative controls was confirmed by sequencing the plasmids designed during this project. As a first positive result this meant that in a following step *Aspergillus niger*, the filamentous fungus chosen as experimental system in this study, could be transformed with these plasmids. Successful transformation was confirmed by microscopy assays. The collected images showed clearly that fluorescence for the donor and acceptor only controls could be collected in separate emission channels whereas positive controls and the actual Ca^{2+}-sensors displayed emission in both the donor as well as the acceptor channel.

The Western Blot of fungal protein extracts revealed degradation products for all fusion proteins apart from the positive FRET control CeCi, due to the lack of bands smaller than single GFPs and the resistance of it to protease activity the degradation occurred most likely in the linker region of the probes.

4.2 *In vitro* analysis of bacterial and fungal protein extracts

Confocal imaging revealed that the beads tend to aggregate to an extensive amount. Additionally confocal microscopy of beads tagged with CeCi and TN-L15mCer revealed a slight decrease in fluorescence emission signal of beads imaged in $CaCl_2$ buffer as compared to ones imaged in dH_2O. For beads imaged in EGTA buffer a fluorescence signal was barely detectable, most likely due to the buffer stripping the protein from the beads.

TSCSPC analysis of beads tagged with TN-L15mCer revealed no difference in fluorescence lifetime parameters when imaging the beads in solutions of different Ca^{2+}-concentration. The high levels of background fluorescence detected for beads imaged in EGTA buffer support the theory that the buffers may strip the protein from the beads.

When imaged in dH_2O beads tagged with TNL15mCer revealed two lifetime components of about 0.86 ns and 2.04 ns with A-factors of 68 % and 32 % respectively. The absence of a long lifetime component of about 3.4 ns in the protein extract on beads as compared to proteins expressed in fungal cells, together with a predominant short component of about 0.86 ns in these samples suggests that either FRET occurs efficiently in these samples, or that the lifetime parameters are affected by other factors such as additional quenching mechanisms, the close proximity of donor and acceptor fluorophores of different probes on the beads, or the His-tag that was used for purifying and tagging the protein to beads.

4.3 Spectral Imaging of recombinant Ca^{2+}- sensors and FRET controls expressed in the filamentous fungus *Aspergillus niger*

4.3.1 IRIS – Spectral imaging in a snapshot

The initial proof of concept experiments highlight the great potential of IRIS for live cell imaging. The data acquired with the different FRET controls expressed in *A. niger* however mainly points at the necessity of further improvement of the system before the "spectrum in a snapshot" function of IRIS can be fully explored. Once optimised to show the same bandpass distribution as the original over the new range of 450 to 600 nm, this imaging device will be an extremely useful tool for live cell imaging, combining 8-point spectral information with high speed acquisition. IRIS could prove a great improvement over existing methods for FRET analysis. High speed acquisition of spectral information would allow observing fast changes in FRET efficiency *in vivo*, at the same time one would gain more information that could be used for normalising the data (e.g. with respect to expression levels of the different probes) and correcting for spectral bleedthrough than currently available from intensity based measurements.

4.3.2 Spectral imaging on Leica TSC SP 5 confocal microscope

Acquiring spectral information for the different FRET probes and controls on the Leica TSC SP5 confocal system was straightforward and the collected datasets showed a significant difference between the donor or acceptor only constructs and the various FRET probes and positive controls expressed in *A. niger*. Both positive FRET controls and Ca^{2+}-sensitive probes exhibit the emission peaks of donor and acceptor fluorophores after excitation of the donor fluorophore alone, a clear sign that FRET occurs in these probes.

Furthermore the spectral information obtained helps to select initial emission channels for confocal FRET imaging of the different mCeruelan and Venus/Citrin constructs. Due to the long acquisition time of this method it is not suitable for imaging cellular processes in real time, the results clearly highlight the potential of high speed spectral imaging for FRET sensors though.

4.4 Live Cell Imaging of recombinant proteins expressed in *Aspergillus niger*

Genetically encoded sensors in general allow monitoring of cellular processes without the necessity for physical perturbation or manipulation (necessary if a probe first needs to be introduced into the cell) and additionally offer the opportunity to measure changes in ion concentration in different organelles since they can be easily targeted to these.

The different types of sensors studied in this project highlight the difficulties of intensity based analysis of fluorescent probes and reveal that it is necessary to carefully optimize the microscopy methods as well as the experimental procedures.

Considering the pH sensor was already available expressed in *A. niger* at the beginning of the study, whereas the Ca^{2+}-sensors still needed to be cloned, it is not surprising that problems with the latter could not be resolved in time to allow actual imaging of Ca^{2+} in *A. niger* during this project. Optimisation of the microscopy method may well reveal that these probes are suitable for visualising changes in Ca^{2+}- levels inside filamentous fungi.

The successful determination of intracellular pH and imaging of changes in internal pH using RaVC already show the great potential of genetically encoded sensors for imaging dynamic processes in *A. niger* and filamentous fungi in general.

4.5 FLIM analysis of mCerulean and different FRET probes expressed in *A. niger*

FLIM revealed a difference in decay behaviour between the donor only mCerulean (no FRET) and the positive FRET control CeVe as expressed in *A. niger*. mCerulean alone (without Venus acting as acceptor) displayed a biexponential decay with lifetimes of about 3.7 ns and 1.9 ns. In the event of FRET a third, subnanosecond lifetime component was measured, with the other two decay times remaining essentially the same as the donor ones. Furthermore initial results revealed that the additional lifetime component resolved for CeVe was equally present in both CeVe 2.12 and CeVe 6.1, a first indication that the probes do exhibit FRET when expressed in *A. niger* and should be further investigated with regard to their potential as Ca^{2+}-sensors for filamentous fungi. The results of the Western Blot confirmed that the major amount of unquenched donor in the positive FRET control CeVe and the Ca^{2+}-sensors CeVe 2.12 and 6.1 was most likely due to degradation of the probes in the linker region.

While TSCSCP-FLIM was shown to be the most consistent of the methods used in this project to detect FRET, the long measurement time to acquire sufficient data meant this method was not ideal for imaging dynamic molecular interactions occurring *in vivo*. With development of new photon counting detectors and associated electronics underway though, it is anticipated that this method can in future be used for real time analysis of complex decay kinetics in living cells.

Appendix A: Media and solutions

Minimal medium:
71 mM $NaNO_3$
11 mM KH_2PO_4
6.7 mM KCl,
2 mM $MgSO_4 * 7H_2O$
pH 6.0
0.2 ml trace metal solution /l

Trace metal solution:
34.3 mM EDTA,
15.3 mM $ZnSO_4 * 7H_2O$
8 mM $MnCl_2 * 4H_2O$
1.6 mM $CoCl_2 * 6H_2O$
1.3 mM $CuSO_4.5H_2O$
0.2 mM $(NH_4)_6Mo_7O_{24} * 4H_20$
10 mM $CaCl_2 * 2H_2O$
3.6 mM $FeSO_4 * 7H_2O$
pH 6.5

Complete medium:
minimal medium +
0.1% (w/v) yeast extract
0.1% (w/v) casamino acids
2% (w/v) glucose.

Vogel's medium:
8.5 mM $Na_3(C_6H_5O_7)$
36.8 mM KH_2PO_4
25.0 mM NH_4NO_3
0.7 mM $CaCl_2 * 2H_2O$
0.8 mM $MgSO_4 * 7H_2O$
pH 6.0
0.2 ml trace metal solution/l
20 µM D-biotin
2% (w/v) glucose.

Plates:
1.5 % agar

Fungal transformation:

KMC buffer:
1 M KCl
25 mM $CaCl_2$
10 mM Tris
pH 5.8

STC buffer:
1.33 M sorbitol
50 mM $CaCl_2$
10 mM Tris
pH 7.5

PEG buffer:
25% PEG 600
50 mM $CaCl_2$
10 mM Tris
pH 7.5

MMS top agar:
71 mM $NaNO_3$,
11 mM KH_2PO_4,
6.7 mM KCl,
2 mM $MgSO_4.7H_2O$,
pH 6.0,
0.2 ml trace metal solution,
2% (w/v) glucose and
0.95 M sucrose
0.6% agar

MMS plates
See above
1.5% (w/v) agar

Protein purification:

Loading buffer
20 mM NaH_2PO_4 * H_2O
0.2 mM NaCl
pH 7.4

Elution buffers:
Loading buffer +
20mM imidazole
50mM imidazole
100 mM imidazole
250 mM imidazole

Extraction buffer (fungi):
25 mM Tris
0.15 M NaCl
50 % (v/v) glycerol
pH 7.2

Lysis buffer (bacteria):
10 mM Tris
1 mM EDTA
1 mM lysozyme

Appendix B:
Amino acid sequence of fungal expression plasmids

pMoj009_mCelurean

ctgacgcgccctgtagcggcgcattaagcgcggcgggtgtggtggttacgcgcagcgtgaccgctacacttgccagcgccctagc
gcccgctcctttcgctttcttcccttcctttctcgccacgttcgccggctttccccgtcaagctctaaatcgggggctcccttta
gggttccgatttagtgctttacggcacctcgaccccaaaaaacttgattagggtgatggttcacgtagtgggccatcgccctgat
agacggtttttcgccctttgacgttggagtccacgttctttaatagtggactcttgttccaaactggaacaacactcaaccctat
ctcggtctattcttttgatttataagggattttgccgatttcggcctattggttaaaaaatgagctgatttaacaaaaatttaac
gcgaattttaacaaaatattaacgcttacaatttccattcgccattcaggctgcgcaactgttgggaagggcgatcggtgcgggc
ctcttcgctattacgccagctggcgaaaggggatgtgctgcaaggcgattaagttgggtaacgccagggttttcccagtcacga
cgttgtaaaacgacggccagtgagcgcgcgtaatacgactcactatagggcgaattggagctcgtgaccggtgactctttctggc
atgcggagagacggacggacgcagagagaagggctgagtaataagccactggccagacagctctggcggctctgaggtgcagtgg
atgattattaatccgggaccggccgccctccgcccgaagtggaaaggctggtgtgcccctcgttgaccaagaatctattgcat
catcggagaatatggagcttcatcgaatcaccggcagtaagcgaaggagaatgtgaagccaggggtgtatagccgtcggcgaaat
agcatgccattaacctaggtacagaagtccaattgcttccgatctggtaaaagattcacgagatagtaccttctccgaagtaggt
agagcgagtacccggcgcgtaagctccctaattggcccatccggcatctgtagggcgtccaaatatcgtgcctctcctgctttgc
ccggtgtatgaaaccggaaaggccgctcaggagctggccagcggcgcagaccgggaacacaagctggcagtcgacccatccggtg
ctctgcactcgacctgctgaggtccctcagtccctggtaggcagctttgccccgtctgtccgcccggtgtgtcggcggggttgac
aaggtcgttgcgtcagtccaacatttgttgccatattttcctgctctccccaccagctgctcttttctttttctctttctttttccc
atcttcagtatattcatcttcccatccaagaacctttatttcccctaagtaagtactttgctacatccatactccatccttccca
tcccttattcctttgaaccttcagttcgagctttcccacttcatcgcagcttgactaacagctaccccgcttgagcagacatca
cccatggtgagcaagggcgaggagctgttcaccggggtggtgcccatcctggtcgagctggacggcgacgtaaacggccacaagt
tcagcgtgtccggcgagggcgagggcgatgccacctacggcaagctgaccctgaagttcatctgcaccaccggcaagctgcccgt
gccctggcccaccctcgtgaccaccctgacctggggcgtgcagtgcttcgcccgctaccccgaccacatgaagcagcacgacttc
ttcaagtccgccatgcccgaaggctacgtccaggagcgcaccatcttcttcaaggacgacggcaactacaagacccgcgccgagg
tgaagttcgagggcgacaccctggtgaaccgcatcgagctgaagggcatcgacttcaaggaggacggcaacatcctggggcacaa
gctggagtacaacgccatcagcgacaacgtctatatcaccgccgacaagcagaagaacggcatcaaggccaacttcaagatccgc
cacaacatcgaggacggcagcgtgcagctcgccgaccactaccagcagaacaccccatcggcgacggccccgtgctgctgcccg
acaaccactacctgagcacccagtccaagctgagcaaagaccccaacgagaagcgcgatcacatggtcctgctggagttcgtgac
cgccgccgggatcactctcggcatggacgagctgtacaagtaagaattctgaaagctttagtgatttaatagctccatgtcaaca
agaataaaacgcgttttcgggtttacctcttccagatacagctcatctgcaatgcattaatgcattgactgcaacctagtaacgc
cttncaggctccggcgaagagaagaatagcttagcagagctattttcattttcgggagacgagatcaagcagatcaacggtcgtc
aagagacctacgagactgaggaatccgctcttggctccacgcgactatatatttgtctctaattgtactttgacatgctcctctt
ctttactctgatagcttgactatgaaaattccgtcaccagcncctgggttcgcaaagataattgcatgtttcttccttgaactct
caagcctacaggacacacattcatcgtaggtataaacctcgaaatcanttcctactaagatggtatacaatagtaaccatgcatg
gttgcctagtgaatgctccgtaacacccaatacgccggcccgggtccctcgaggggggcccggtacccagcttttgttccctttt
agtgagggttaattgcgcgcttggcgtaatcatggtcatagctgtttcctgtgtgaaattgttatccgctcacaattccacacaa
catacgagccggaagcataaagtgtaaagcctggggtgcctaatgagtgagctaactcacattaattgcgttgcgctcactgccc
gctttccagtcgggaaacctgtcgtgccagctgcattaatgaatcggccaacgcgcggggagaggcggtttgcgtattgggcgct
cttccgcttcctcgctcactgactcgctgcgctcggtcgttcggctgcggcgagcggtatcagctcactcaaaggcggtaatacg
gttatccacagaatcaggggataacgcaggaaagaacatgtgagcaaaaggccagcaaaaggccaggaaccgtaaaaaggccgcg
ttgctggcgtttttccataggctccgcccccctgacgagcatcacaaaaatcgacgctcaagtcagaggtggcgaaacccgacag
gactataaagataccaggcgtttcccccctggaagctccctcgtgcgctctcctgttccgaccctgccgcttaccggatacctgtc
cgcctttctcccttcgggaagcgtggcgctttctcatagctcacgctgtaggtatctcagttcggtgtaggtcgttcgctccaag
ctgggctgtgtgcacgaacccccgttcagcccgaccgctgcgccttatccggtaactatcgtcttgagtccaacccggtaagac
acgacttatcgccactggcagcagccactggtaacaggattagcagagcgaggtatgtaggcggtgctacagagttcttgaagtg
gtggcctaactacggctacactagaaggacagtatttggtatctgcgctctgctgaagccagttaccttcggaaaaagagttggt
agctcttgatccggcaaacaaaccaccgctggtagcggtggtttttttgtttgcaagcagcagattacgcgcagaaaaaaaggat
ctcaagaagatcctttgatcttttctacggggtctgacgctcagtggaacgaaaactcacgttaagggattttggtcatgagatt
atcaaaaaggatcttcacctagatccttttaaattaaaaatgaagttttaaatcaatctaaagtatatatgagtaaacttggtct
gacagttaccaatgcttaatcagtgaggcacctatctcagcgatctgtctatttcgttcatccatagttgcctgactccccgtcg
tgtagataactacgatacgggagggcttaccatctggccccagtgctgcaatgataccgcgagacccacgctcaccggctccaga
tttatcagcaataaaccagccagccggaagggccgagcgcagaagtggtcctgcaactttatccgcctccatccagtctattaat
tgttgccgggaagctagagtaagtagttcgccagttaatagtttgcgcaacgttgttgccattgctacaggcatcgtggtgtcac
gctcgtcgtttggtatggcttcattcagctccggttcccaacgatcaaggcgagttacatgatcccccatgttgtgcaaaaaagc
ggttagctccttcggtcctccgatcgttgtcagaagtaagttggccgcagtgttatcactcatggttatggcagcactgcataat
tctcttactgtcatgccatccgtaagatgcttttctgtgactggtgagtactcaaccaagtcattctgagaatagtgtatgcggc
gaccgagttgctcttgcccggcgtcaatacgggataataccgcgccacatagcagaactttaaaagtgctcatcattggaaaacg
ttcttcggggcgaaaactctcaaggatcttaccgctgttgagatccagttcgatgtaacccactcgtgcacccaactgatcttca
gcatcttttactttcaccagcgtttctgggtgagcaaaaacaggaaggcaaaatgccgcaaaaaagggaataagggcgacacgga
aatgttgaatactcatactcttccttttcaatattattgaagcatttatcagggttattgtctcatgagcggatacatatttga
atgtatttagaaaaataaacaaatagggttccgcgcacatttccccgaaaagtgccac

pMoj009_Venus

ctgacgcgccctgtagcggcgcattaagcgcggcgggtgtggtggttacgcgcagcgtgaccgctacacttgccagcgccctagc
gcccgctccttttcgctttcttcccttcctttctcgccacgttcgccggctttccccgtcaagctctaaatcgggggctcccttta
gggttccgatttagtgctttacggcacctcgaccccaaaaaacttgattagggtgatggttcacgtagtgggccatcgccctgat
agacggtttttcgccctttgacgttggagtccacgttctttaatagtggactcttgttccaaactggaacaacactcaaccctat
ctcggtctattcttttgatttataagggattttgccgatttcggcctattggttaaaaaatgagctgatttaacaaaaatttaac
gcgaattttaacaaaatattaacgcttacaatttccattcgccattcaggctgcgcaactgttgggaagggcgatcggtgcgggc
ctcttcgctattacgccagctggcgaaaggggatgtgctgcaaggcgattaagttgggtaacgccagggttttcccagtcacga
cgttgtaaaacgacggccagtgagcgcgcgtaatacgactcactatagggcgaattggagctcgtgaccggtgactctttctggc
atgcggagagacggacggacgcagagagaagggctgagtaataagccactggccagacagctctggcggctctgaggtgcagtgg
atgattattaatccgggaccggccgcccctccgccccgaagtggaaaggctggtgtgcccctcgttgaccaagaatctattgcat
catcggagaatatggagcttcatcgaatcaccggcagtaagcgaaggagaatgtgaagccaggggtgtatagccgtcggcgaaat
agcatgccattaacctaggtacagaagtccaattgcttccgatctggtaaaagattcacgagatagtaccttctccgaagtaggt
agagcgagtacccggcgcgtaagctccctaattggcccatccggcatctgtagggcgtccaaatatcgtgcctctcctgctttgc
ccggtgtatgaaaccggaaaggccgctcaggagctggccagcggcgcagaccgggaacacaagctggcagtcgacccatccggtg
ctctgcactcgacctgctgaggtccctcagtccctggtaggcagctttgccccgtctgtccgcccggtgtgtcggcggggttgac
aaggtcgttgcgtcagtccaacatttgttgccatattttcctgctctccccaccagctgctcttttctttttctctttctttttccc
atcttcagtatattcatcttcccatccaagaacctttatttcccctaagtaagtactttgctacatccatactccatccttccca
tcccttattcctttgaaccttcagttcgagctttcccacttcatcgcagcttgactaacagctaccccgcttgagcagacatca
cccatggtgagcaagggcgaggagctgttcaccggggtggtgcccatcctggtcgagctggacggcgacgtaaacggccacaagt
tcagcgtgtccggcgagggcgagggcgatgccacctacggcaagctgaccctgaagttcatctgcaccaccggcaagctgcccgt
gccctggcccaccctcgtgaccaccttcggctacggcctgcagtgcttcgcccgctaccccgaccacatgaagcagcacgacttc
ttcaagtccgccatgcccgaaggctacgtccaggagcgcaccatcttcttcaaggacgacggcaactacaagacccgcgccgagg
tgaagttcgagggcgacaccctggtgaaccgcatcgagctgaagggcatcgacttcaaggaggacggcaacatcctggggcacaa
gctggagtacaactacaacagccacaacgtctatatcatggccgacaagcagaagaacggcatcaaggtgaacttcaagatccgc
cacaacatcgaggacggcagcgtgcagctcgccgaccactaccagcagaacaccccccatcggcgacggccccgtgctgctgcccg
acaaccactacctgagctaccagtccgccctgagcaaagaccccaacgagaagcgcgatcacatggtcctgctggagttcgtgac
cgccgccgggatcactctcggcatggacgagctgtacaagtaagaattctgaaagctttagtgatttaatagctccatgtcaaca
agaataaaacgcgttttcgggtttacctcttccagatacagctcatctgcaatgcattaatgcattgactgcaacctagtaacgc
cttncaggctccggcgaagagaagaatagcttagcagagctattttcattttcgggagacgagatcaagcagatcaacggtcgtc
aagagacctacgagactgaggaatccgctcttggctccacgcgactatatatttgtctctaattgtactttgacatgctcctctt
ctttactctgatagcttgactatgaaaattccgtcaccagcncctgggttcgcaaagataattgcatgtttcttccttgaactct
caagcctacaggacacacattcatcgtaggtataaacctcgaaatcanttcctactaagatggtatacaatagtaaccatgcatg
gttgcctagtgaatgctccgtaacacccaatacgccggcccgggtccctcgaggggggcccggtacccagcttttgttccctttt
agtgagggttaattgcgcgcttggcgtaatcatggtcatagctgtttcctgtgtgaaattgttatccgctcacaattccacacaa
catacgagccggaagcataaagtgtaaagcctggggtgcctaatgagtgagctaactcacattaattgcgttgcgctcactgccc
gctttccagtcgggaaacctgtcgtgccagctgcattaatgaatcggccaacgcgcggggagaggcggtttgcgtattgggcgct
cttccgcttcctcgctcactgactcgctgcgctcggtcgttcggctgcggcgagcggtatcagctcactcaaaggcggtaatacg
gttatccacagaatcaggggataacgcaggaaagaacatgtgagcaaaaggccagcaaaaggccaggaaccgtaaaaaggccgcg
ttgctggcgtttttccataggctccgcccccctgacgagcatcacaaaaatcgacgctcaagtcagaggtggcgaaacccgacag
gactataaagataccaggcgtttccccctggaagctccctcgtgcgctctcctgttccgaccctgccgcttaccggatacctgtc
cgcctttctcccttcgggaagcgtggcgctttctcatagctcacgctgtaggtatctcagttcggtgtaggtcgttcgctccaag
ctgggctgtgtgcacgaacccccgttcagcccgaccgctgcgccttatccggtaactatcgtcttgagtccaacccggtaagac
acgacttatcgccactggcagcagccactggtaacaggattagcagagcgaggtatgtaggcggtgctacagagttcttgaagtg
gtggcctaactacggctacactagaaggacagtatttggtatctgcgctctgctgaagccagttaccttcggaaaaagagttggt
agctcttgatccggcaaacaaaccaccgctggtagcggtggtttttttgtttgcaagcagcagattacgcgcagaaaaaaaggat
ctcaagaagatcctttgatcttttctacggggtctgacgctcagtggaacgaaaactcacgttaagggattttggtcatgagatt
atcaaaaaggatcttcacctagatccttttaaattaaaaatgaagttttaaatcaatctaaagtatatatgagtaaacttggtct
gacagttaccaatgcttaatcagtgaggcacctatctcagcgatctgtctatttcgttcatccatagttgcctgactccccgtcg
tgtagataactacgatacgggagggcttaccatctggccccagtgctgcaatgataccgcgagacccacgctcaccggctccaga
tttatcagcaataaaccagccagccggaagggccgagcgcagaagtggtcctgcaactttatccgcctccatccagtctattaat
tgttgccgggaagctagagtaagtagttcgccagttaatagtttgcgcaacgttgttgccattgctacaggcatcgtggtgtcac
gctcgtcgtttggtatggcttcattcagctccggttcccaacgatcaaggcgagttacatgatcccccatgttgtgcaaaaaagc
ggttagctccttcggtcctccgatcgttgtcagaagtaagttggccgcagtgttatcactcatggttatggcagcactgcataat
tctcttactgtcatgccatccgtaagatgcttttctgtgactggtgagtactcaaccaagtcattctgagaatagtgtatgcggc
gaccgagttgctcttgcccggcgtcaatacgggataataccgcgccacatagcagaactttaaaagtgctcatcattggaaaacg
ttcttcggggcgaaaactctcaaggatcttaccgctgttgagatccagttcgatgtaacccactcgtgcacccaactgatcttca
gcatcttttactttcaccagcgtttctgggtgagcaaaaacaggaaggcaaaatgccgcaaaaaagggaataagggcgacacgga
aatgttgaatactcatactcttccttttcaatattattgaagcatttatcagggttattgtctcatgagcggatacatatttga
atgtatttagaaaaataaacaaatagggggttccgcgcacatttccccgaaaagtgccac

pMoj009_mCitrin

ctgacgcgccctgtagcggcgcattaagcgcggcgggtgtggtggttacgcgcagcgtgaccgctacacttgccagcgccctagc
gcccgctccttttcgctttcttcccttcctttctcgccacgttcgccggctttccccgtcaagctctaaatcgggggctcccttta
gggttccgatttagtgctttacggcacctcgaccccaaaaaacttgattagggtgatggttcacgtagtgggccatcgccctgat
agacggtttttcgccctttgacgttggagtccacgttctttaatagtggactcttgttccaaactggaacaacactcaaccctat
ctcggtctattcttttgatttataagggattttgccgatttcggcctattggttaaaaaatgagctgatttaacaaaaatttaac
gcgaattttaacaaaatattaacgcttacaatttccattcgccattcaggctgcgcaactgttgggaagggcgatcggtgcgggc
ctcttcgctattacgccagctggcgaaaggggatgtgctgcaaggcgattaagttgggtaacgccagggttttcccagtcacga
cgttgtaaaacgacggccagtgagcgcgcgtaatacgactcactatagggcgaattggagctcgtgaccggtgactctttctggc
atgcggagagacggacggacgcagagagaagggctgagtaataagccactggccagacagctctggcggctctgaggtgcagtgg
atgattattaatccgggaccggccgcccctccgccccgaagtggaaaggctggtgtgcccctcgttgaccaagaatctattgcat
catcggagaatatggagcttcatcgaatcaccggcagtaagcgaaggagaatgtgaagccaggggtgtatagccgtcggcgaaat
agcatgccattaacctaggtacagaagtccaattgcttccgatctggtaaaagattcacgagatagtaccttctccgaagtaggt
agagcgagtacccggcgcgtaagctccctaattggcccatccggcatctgtagggcgtccaaatatcgtgcctctcctgctttgc
ccggtgtatgaaaccggaaaggccgctcaggagctggccagcggcgcagaccgggaacacaagctggcagtcgacccatccggtg
ctctgcactcgacctgctgaggtccctcagtccctggtaggcagctttgccccgtctgtccgcccggtgtgtcggcggggttgac
aaggtcgttgcgtcagtccaacatttgttgccatattttcctgctctccccaccagctgctcttttctttttctctttctttttccc
atcttcagtatattcatcttcccatccaagaacctttatttcccctaagtaagtactttgctacatccatactccatccttccca
tcccttattcctttgaaccttcagttcgagctttcccacttcatcgcagcttgactaacagctaccccgcttgagcagacatca
cccatggtgagcaagggcgaggagctgttcaccggggtggtgcccatcctggtcgagctggacggcgacgtaaacggccacaagt
tcagcgtgtccggcgagggcgagggcgatgccacctacggcaagctgaccctgaagttcatctgcaccaccggcaagctgcccgt
gccctggcccaccctcgtgaccaccttcggctacggcctgatgtgcttcgcccgctaccccgaccacatgaagcagcacgacttc
ttcaagtccgccatgcccgaaggctacgtccaggagcgcaccatcttcttcaaggacgacggcaactacaagacccgcgccgagg
tgaagttcgagggcgacaccctggtgaaccgcatcgagctgaagggcatcgacttcaaggaggacggcaacatcctggggcacaa
gctggagtacaactacaacagccacaacgtctatatcatggccgacaagcagaagaacggcatcaaggtgaacttcaagatccgc
cacaacatcgaggacggcagcgtgcagctcgccgaccactaccagcagaacaccccccatcggcgacggccccgtgctgctgcccg
acaaccactacctgagctaccagtccgccctgagcaaagaccccaacgagaagcgcgatcacatggtcctgctggagttcgtgac
cgccgccgggatcactctcggcatggacgagctgtacaagtaagaattctgaaagctttagtgatttaatagctccatgtcaaca
agaataaaacgcgttttcgggtttacctcttccagatacagctcatctgcaatgcattaatgcattgactgcaacctagtaacgc
cttncaggctccggcgaagagaagaatagcttagcagagctattttcattttcgggagacgagatcaagcagatcaacggtcgtc
aagagacctacgagactgaggaatccgctcttggctccacgcgactatatatttgtctctaattgtactttgacatgctcctctt
ctttactctgatagcttgactatgaaaattccgtcaccagcncctgggttcgcaaagataattgcatgtttcttccttgaactct
caagcctacaggacacacattcatcgtaggtataaacctcgaaatcanttcctactaagatggtatacaatagtaaccatgcatg
gttgcctagtgaatgctccgtaacacccaatacgccggcccgggtccctcgaggggggcccggtacccagcttttgttccctttt
agtgagggttaattgcgcgcttggcgtaatcatggtcatagctgtttcctgtgtgaaattgttatccgctcacaattccacacaa
catacgagccggaagcataaagtgtaaagcctggggtgcctaatgagtgagctaactcacattaattgcgttgcgctcactgccc
gctttccagtcgggaaacctgtcgtgccagctgcattaatgaatcggccaacgcgcggggagaggcggtttgcgtattgggcgct
cttccgcttcctcgctcactgactcgctgcgctcggtcgttcggctgcggcgagcggtatcagctcactcaaaggcggtaatacg
gttatccacagaatcaggggataacgcaggaaagaacatgtgagcaaaaggccagcaaaaggccaggaaccgtaaaaaggccgcg
ttgctggcgtttttccataggctccgcccccctgacgagcatcacaaaaatcgacgctcaagtcagaggtggcgaaacccgacag
gactataaagataccaggcgtttccccctggaagctccctcgtgcgctctcctgttccgaccctgccgcttaccggatacctgtc
cgcctttctcccttcgggaagcgtggcgctttctcatagctcacgctgtaggtatctcagttcggtgtaggtcgttcgctccaag
ctgggctgtgtgcacgaaccccccgttcagcccgaccgctgcgccttatccggtaactatcgtcttgagtccaacccggtaagac
acgacttatcgccactggcagcagccactggtaacaggattagcagagcgaggtatgtaggcggtgctacagagttcttgaagtg
gtggcctaactacggctacactagaaggacagtatttggtatctgcgctctgctgaagccagttaccttcggaaaaagagttggt
agctcttgatccggcaaacaaaccaccgctggtagcggtggtttttttgtttgcaagcagcagattacgcgcagaaaaaaaggat
ctcaagaagatcctttgatcttttctacggggtctgacgctcagtggaacgaaaactcacgttaagggattttggtcatgagatt
atcaaaaaggatcttcacctagatccttttaaattaaaaatgaagttttaaatcaatctaaagtatatatgagtaaacttggtct
gacagttaccaatgcttaatcagtgaggcacctatctcagcgatctgtctatttcgttcatccatagttgcctgactccccgtcg
tgtagataactacgatacgggagggcttaccatctggccccagtgctgcaatgataccgcgagacccacgctcaccggctccaga
tttatcagcaataaaccagccagccggaagggccgagcgcagaagtggtcctgcaactttatccgcctccatccagtctattaat
tgttgccgggaagctagagtaagtagttcgccagttaatagtttgcgcaacgttgttgccattgctacaggcatcgtggtgtcac
gctcgtcgtttggtatggcttcattcagctccggttcccaacgatcaaggcgagttacatgatcccccatgttgtgcaaaaaagc
ggttagctccttcggtcctccgatcgttgtcagaagtaagttggccgcagtgttatcactcatggttatggcagcactgcataat
tctcttactgtcatgccatccgtaagatgcttttctgtgactggtgagtactcaaccaagtcattctgagaatagtgtatgcggc
gaccgagttgctcttgcccggcgtcaatacgggataataccgcgccacatagcagaactttaaaagtgctcatcattggaaaacg
ttcttcggggcgaaaactctcaaggatcttaccgctgttgagatccagttcgatgtaacccactcgtgcacccaactgatcttca
gcatcttttactttcaccagcgtttctgggtgagcaaaaacaggaaggcaaaatgccgcaaaaaagggaataagggcgacacgga
aatgttgaatactcatactcttcctttttcaatattattgaagcatttatcagggttattgtctcatgagcggatacatatttga
atgtatttagaaaaataaacaaatagggggttccgcgcacatttccccgaaaagtgccac

pMoj009_CeVe

CTGACGCGCCCTGTAGCGGCGCATTAAGCGCGGCGGGTGTGGTGGTTACGCGCAGCGTGACCGCTACACT
TGCCAGCGCCCTAGCGCCCGCTCCTTTCGCTTTCTTCCCTTCCTTTCTCGCCACGTTCGCCGGCTTTCCC
CGTCAAGCTCTAAATCGGGGGCTCCCTTTAGGGTTCCGATTTAGTGCTTTACGGCACCTCGACCCCAAAA
AACTTGATTAGGGTGATGGTTCACGTAGTGGGCCATCGCCCTGATAGACGGTTTTTCGCCCTTTGACGTT
GGAGTCCACGTTCTTTAATAGTGGACTCTTGTTCCAAACTGGAACAACACTCAACCCTATCTCGGTCTAT
TCTTTTGATTTATAAGGGATTTTGCCGATTTCGGCCTATTGGTTAAAAAATGAGCTGATTTAACAAAAAT
TTAACGCGAATTTTAACAAAATATTAACGCTTACAATTTCCATTCGCCATTCAGGCTGCGCAACTGTTGG
GAAGGGCGATCGGTGCGGGCCTCTTCGCTATTACGCCAGCTGGCGAAAGGGGGATGTGCTGCAAGGCGAT
TAAGTTGGGTAACGCCAGGGTTTTCCCAGTCACGACGTTGTAAAACGACGGCCAGTGAGCGCGCGTAATA
CGACTCACTATAGGGCGAATTGGAGCTCGTGACCGGTGACTCTTTCTGGCATGCGGAGAGACGGACGGAC
GCAGAGAGAAGGGCTGAGTAATAAGCCACTGGCCAGACAGCTCTGGCGGCTCTGAGGTGCAGTGGATGAT
TATTAATCCGGGACCGGCCGCCCCTCCGCCCCGAAGTGGAAAGGCTGGTGTGCCCCTCGTTGACCAAGAA
TCTATTGCATCATCGGAGAATATGGAGCTTCATCGAATCACCGGCAGTAAGCGAAGGAGAATGTGAAGCC
AGGGGTGTATAGCCGTCGGCGAAATAGCATGCCATTAACCTAGGTACAGAAGTCCAATTGCTTCCGATCT
GGTAAAAGATTCACGAGATAGTACCTTCTCCGAAGTAGGTAGAGCGAGTACCCGGCGCGTAAGCTCCCTA
ATTGGCCCATCCGGCATCTGTAGGGCGTCCAAATATCGTGCCTCTCCTGCTTTGCCCGGTGTATGAAACC
GGAAAGGCCGCTCAGGAGCTGGCCAGCGGCGCAGACCGGGAACACAAGCTGGCAGTCGACCCATCCGGTG
CTCTGCACTCGACCTGCTGAGGTCCCTCAGTCCCTGGTAGGCAGCTTTGCCCCGTCTGTCCGCCCGGTGT
GTCGGCGGGGTTGACAAGGTCGTTGCGTCAGTCCAACATTTGTTGCCATATTTTCCTGCTCTCCCCACCA
GCTGCTCTTTTCTTTTCTCTTTCTTTTCCCATCTTCAGTATATTCATCTTCCCATCCAAGAACCTTTATT
TCCCCTAAGTAAGTACTTTGCTACATCCATACTCCATCCTTCCCATCCCTTATTCCTTTGAACCTTTCAG
TTCGAGCTTTCCCACTTCATCGCAGCTTGACTAACAGCTACCCCGCTTGAGCAGACATCACCCATGGTGA
GCAAGGGCGAGGAGCTGTTCACCGGGGTGGTGCCCATCCTGGTCGAGCTGGACGGCGACGTAAACGGCCA
CAAGTTCAGCGTGTCCGGCGAGGGCGAGGGCGATGCCACCTACGGCAAGCTGACCCTGAAGTTCATCTGC
ACCACCGGCAAGCTGCCCGTGCCCTGGCCCACCCTCGTGACCACCCTGACCTGGGGCGTGCAGTGCTTCG
CCCGCTACCCCGACCACATGAAGCAGCACGACTTCTTCAAGTCCGCCATGCCCGAAGGCTACGTCCAGGA
GCGCACCATCTTCTTCAAGGACGACGGCAACTACAAGACCCGCGCCGAGGTGAAGTTCGAGGGCGACACC
CTGGTGAACCGCATCGAGCTGAAGGGCATCGACTTCAAGGAGGACGGCAACATCCTGGGGCACAAGCTGG
AGTACAACGCCATCAGCGACAACGTCTATATCACCGCCGACAAGCAGAAGAACGGCATCAAGGCCAACTT
CAAGATCCGCCACAACATCGAGGACGGCAGCGTGCAGCTCGCCGACCACTACCAGCAGAACACCCCCATC
GGCGACGGCCCCGTGCTGCTGCCCGACAACCACTACCTGAGCACCCAGTCCAAGCTGAGCAAAGACCCCA
ACGAGAAGCGCGATCACATGGTCCTGCTGGAGTTCGTGACCGCCGCCCGCATGCATGGGGGCACCGGTGG
GTCCGAGCTCATGGTGAGCAAGGGCGAGGAGCTGTTCACCGGGGTGGTGCCCATCCTGGTCGAGCTGGAC
GGCGACGTAAACGGCCACAAGTTCAGCGTGTCCGGCGAGGGCGAGGGCGATGCCACCTACGGCAAGCTGA
CCCTGAAGTTCATCTGCACCACCGGCAAGCTGCCCGTGCCCTGGCCCACCCTCGTGACCACCTTCGGCTA
CGGCCTGCAGTGCTTCGCCCGCTACCCCGACCACATGAAGCAGCACGACTTCTTCAAGTCCGCCATGCCC
GAAGGCTACGTCCAGGAGCGCACCATCTTCTTCAAGGACGACGGCAACTACAAGACCCGCGCCGAGGTGA
AGTTCGAGGGCGACACCCTGGTGAACCGCATCGAGCTGAAGGGCATCGACTTCAAGGAGGACGGCAACAT
CCTGGGGCACAAGCTGGAGTACAACTACAACAGCCACAACGTCTATATCATGGCCGACAAGCAGAAGAAC
GGCATCAAGGTGAACTTCAAGATCCGCCACAACATCGAGGACGGCAGCGTGCAGCTCGCCGACCACTACC
AGCAGAACACCCCCATCGGCGACGGCCCCGTGCTGCTGCCCGACAACCACTACCTGAGCTACCAGTCCGC
CCTGAGCAAAGACCCCAACGAGAAGCGCGATCACATGGTCCTGCTGGAGTTCGTGACCGCCGCCGGGATC
ACTCTCGGCATGGACGAGCTGTACAAGTAAGAATTCAATTCTGAAAGCTTTAGTGATTTAATAGCTCCAT
GTCAACAAGAATAAAACGCGTTTCGGGTTTACCTCTTCCAGATACAGCTCATCTGCAATGCATTAATGCA
TTGGACCTCGCAACCCTAGTACGCCCTTCAGGCTCCGGCGAAGCAGAAGAATAGCTTAGCAGAGTCTATT
TTCATTTTCGGGAGACGAGATCAAGCAGATCAACGGTCGTCAAGAGACCTACGAGACTGAGGAATCCGCT
CTTGGCTCCACGCGACTATATATTTGTCTCTAATTGTACTTTGACATGCTCCTCTTCTTTACTCTGATAG
CTTGACTATGAAAATTCCGTCACCAGCCCCTGGGTTCGCAAAGATAATTGCACTGTTTCTTCCTTGAACT
CTCAAGCCTACAGGACACACATTCATCGTAGGTATAAACCTCGAAAATCATTCCTACTAAGATGGGTATA
CAATAGTAACCATGCATGGTTGCCTAGTGAATGCTCCGTAACACCCAATACGCGGCCGCTAACATCTCGA
GGGGGGGCCCGGTACCCAGCTTTTGTTCCCTTTAGTGAGGGTTAATTGCGCGCTTGGCGTAATCATGGTC
ATAGCTGTTTCCTGTGTGAAATTGTTATCCGCTCACAATTCCACACAACATACGAGCCGGAAGCATAAAG
TGTAAAGCCTGGGGTGCCTAATGAGTGAGCTAACTCACATTAATTGCGTTGCGCTCACTGCCCGCTTTCC
AGTCGGGAAACCTGTCGTGCCAGCTGCATTAATGAATCGGCCAACGCGCGGGGAGAGGCGGTTTGCGTAT
TGGGCGCTCTTCCGCTTCCTCGCTCACTGACTCGCTGCGCTCGGTCGTTCGGCTGCGGCGAGCGGTATCA
GCTCACTCAAAGGCGGTAATACGGTTATCCACAGAATCAGGGGATAACGCAGGAAAGAACATGTGAGCAA
AAGGCCAGCAAAAGGCCAGGAACCGTAAAAAGGCCGCGTTGCTGGCGTTTTTCCATAGGCTCCGCCCCCC
TGACGAGCATCACAAAAATCGACGCTCAAGTCAGAGGTGGCGAAACCCGACAGGACTATAAAGATACCAG
GCGTTTCCCCCTGGAAGCTCCCTCGTGCGCTCTCCTGTTCCGACCCTGCCGCTTACCGGATACCTGTCCG
CCTTTCTCCCTTCGGGAAGCGTGGCGCTTTCTCATAGCTCACGCTGTAGGTATCTCAGTTCGGTGTAGGT
CGTTCGCTCCAAGCTGGGCTGTGTGCACGAACCCCCCGTTCAGCCCGACCGCTGCGCCTTATCCGGTAAC
TATCGTCTTGAGTCCAACCCGGTAAGACACGACTTATCGCCACTGGCAGCAGCCACTGGTAACAGGATTA
GCAGAGCGAGGTATGTAGGCGGTGCTACAGAGTTCTTGAAGTGGTGGCCTAACTACGGCTACACTAGAAG
GACAGTATTTGGTATCTGCGCTCTGCTGAAGCCAGTTACCTTCGGAAAAAGAGTTGGTAGCTCTTGATCC
GGCAAACAAACCACCGCTGGTAGCGGTGGTTTTTTTGTTTGCAAGCAGCAGATTACGCGCAGAAAAAAAG
GATCTCAAGAAGATCCTTTGATCTTTTCTACGGGGTCTGACGCTCAGTGGAACGAAAACTCACGTTAAGG
GATTTTGGTCATGAGATTATCAAAAAGGATCTTCACCTAGATCCTTTTAAATTAAAAATGAAGTTTTAAA

TCAATCTAAAGTATATATGAGTAAACTTGGTCTGACAGTTACCAATGCTTAATCAGTGAGGCACCTATCT
CAGCGATCTGTCTATTTCGTTCATCCATAGTTGCCTGACTCCCCGTCGTGTAGATAACTACGATACGGGA
GGGCTTACCATCTGGCCCCAGTGCTGCAATGATACCGCGAGACCCACGCTCACCGGCTCCAGATTTATCA
GCAATAAACCAGCCAGCCGGAAGGGCCGAGCGCAGAAGTGGTCCTGCAACTTTATCCGCCTCCATCCAGT
CTATTAATTGTTGCCGGGAAGCTAGAGTAAGTAGTTCGCCAGTTAATAGTTTGCGCAACGTTGTTGCCAT
TGCTACAGGCATCGTGGTGTCACGCTCGTCGTTTGGTATGGCTTCATTCAGCTCCGGTTCCCAACGATCA
AGGCGAGTTACATGATCCCCCATGTTGTGCAAAAAAGCGGTTAGCTCCTTCGGTCCTCCGATCGTTGTCA
GAAGTAAGTTGGCCGCAGTGTTATCACTCATGGTTATGGCAGCACTGCATAATTCTCTTACTGTCATGCC
ATCCGTAAGATGCTTTTCTGTGACTGGTGAGTACTCAACCAAGTCATTCTGAGAATAGTGTATGCGGCGA
CCGAGTTGCTCTTGCCCGGCGTCAATACGGGATAATACCGCGCCACATAGCAGAACTTTAAAAGTGCTCA
TCATTGGAAAACGTTCTTCGGGGCGAAAACTCTCAAGGATCTTACCGCTGTTGAGATCCAGTTCGATGTA
ACCCACTCGTGCACCCAACTGATCTTCAGCATCTTTTACTTTCACCAGCGTTTCTGGGTGAGCAAAAACA
GGAAGGCAAAATGCCGCAAAAAAGGGAATAAGGGCGACACGGAAATGTTGAATACTCATACTCTTCCTTT
TTCAATATTATTGAAGCATTTATCAGGGTTATTGTCTCATGAGCGGATACATATTTGAATGTATTTAGAA
AAATAAACAAATAGGGGTTCCGCGCACATTTCCCCGAAAAGTGCCAC

pMoj009_CeCi

CTGACGCGCCCTGTAGCGGCGCATTAAGCGCGGCGGGTGTGGTGGTTACGCGCAGCGTGACCGCTACACT
TGCCAGCGCCCTAGCGCCCGCTCCTTTCGCTTTCTTCCCTTCCTTTCTCGCCACGTTCGCCGGCTTTCCC
CGTCAAGCTCTAAATCGGGGGCTCCCTTTAGGGTTCCGATTTAGTGCTTTACGGCACCTCGACCCCAAAA
AACTTGATTAGGGTGATGGTTCACGTAGTGGGCCATCGCCCTGATAGACGGTTTTTCGCCCTTTGACGTT
GGAGTCCACGTTCTTTAATAGTGGACTCTTGTTCCAAACTGGAACAACACTCAACCCTATCTCGGTCTAT
TCTTTTGATTTATAAGGGATTTTGCCGATTTCGGCCTATTGGTTAAAAAATGAGCTGATTTAACAAAAAT
TTAACGCGAATTTTAACAAAATATTAACGCTTACAATTTCCATTCGCCATTCAGGCTGCGCAACTGTTGG
GAAGGGCGATCGGTGCGGGCCTCTTCGCTATTACGCCAGCTGGCGAAAGGGGGATGTGCTGCAAGGCGAT
TAAGTTGGGTAACGCCAGGGTTTTCCCAGTCACGACGTTGTAAAACGACGGCCAGTGAGCGCGCGTAATA
CGACTCACTATAGGGCGAATTGGAGCTCGTGACCGGTGACTCTTTCTGGCATGCGGAGAGACGGACGGAC
GCAGAGAGAAGGGCTGAGTAATAAGCCACTGGCCAGACAGCTCTGGCGGCTCTGAGGTGCAGTGGATGAT
TATTAATCCGGGACCGGCCGCCCCTCCGCCCCGAAGTGGAAAGGCTGGTGTGCCCCTCGTTGACCAAGAA
TCTATTGCATCATCGGAGAATATGGAGCTTCATCGAATCACCGGCAGTAAGCGAAGGAGAATGTGAAGCC
AGGGGTGTATAGCCGTCGGCGAAATAGCATGCCATTAACCTAGGTACAGAAGTCCAATTGCTTCCGATCT
GGTAAAAGATTCACGAGATAGTACCTTCTCCGAAGTAGGTAGAGCGAGTACCCGGCGCGTAAGCTCCCTA
ATTGGCCCATCCGGCATCTGTAGGGCGTCCAAATATCGTGCCTCTCCTGCTTTGCCCGGTGTATGAAACC
GGAAAGGCCGCTCAGGAGCTGGCCAGCGGCGCAGACCGGGAACACAAGCTGGCAGTCGACCCATCCGGTG
CTCTGCACTCGACCTGCTGAGGTCCCTCAGTCCCTGGTAGGCAGCTTTGCCCCGTCTGTCCGCCCGGTGT
GTCGGCGGGGTTGACAAGGTCGTTGCGTCAGTCCAACATTTGTTGCCATATTTTCCTGCTCTCCCCACCA
GCTGCTCTTTTCTTTTCTCTTTCTTTTCCCATCTTCAGTATATTCATCTTCCCATCCAAGAACCTTTATT
TCCCCTAAGTAAGTACTTTGCTACATCCATACTCCATCCTTCCCATCCCTTATTCCTTTGAACCTTTCAG
TTCGAGCTTTCCCACTTCATCGCAGCTTGACTAACAGCTACCCCGCTTGAGCAGACATCACCCATGGTGA
GCAAGGGCGAGGAGCTGTTCACCGGGGTGGTGCCCATCCTGGTCGAGCTGGACGGCGACGTAAACGGCCA
CAAGTTCAGCGTGTCCGGCGAGGGCGAGGGCGATGCCACCTACGGCAAGCTGACCCTGAAGTTCATCTGC
ACCACCGGCAAGCTGCCCGTGCCCTGGCCCACCCTCGTGACCACCCTGACCTGGGGCGTGCAGTGCTTCG
CCCGCTACCCCGACCACATGAAGCAGCACGACTTCTTCAAGTCCGCCATGCCCGAAGGCTACGTCCAGGA
GCGCACCATCTTCTTCAAGGACGACGGCAACTACAAGACCCGCGCCGAGGTGAAGTTCGAGGGCGACACC
CTGGTGAACCGCATCGAGCTGAAGGGCATCGACTTCAAGGAGGACGGCAACATCCTGGGGCACAAGCTGG
AGTACAACGCCATCAGCGACAACGTCTATATCACCGCCGACAAGCAGAAGAACGGCATCAAGGCCAACTT
CAAGATCCGCCACAACATCGAGGACGGCAGCGTGCAGCTCGCCGACCACTACCAGCAGAACACCCCCATC
GGCGACGGCCCCGTGCTGCTGCCCGACAACCACTACCTGAGCACCCAGTCCAAGCTGAGCAAAGACCCCA
ACGAGAAGCGCGATCACATGGTCCTGCTGGAGTTCGTGACCGCCGCCCGCATGCATGGGGGCACCGGTGG
GTCCGAGCTCATGGTGAGCAAGGGCGAGGAGCTGTTCACCGGGGTGGTGCCCATCCTGGTCGAGCTGGAC
GGCGACGTAAACGGCCACAAGTTCAGCGTGTCCGGCGAGGGCGATGCCACCTACGGCAAGCTGACCCTGA
CCCTGAAGTTCATCTGCACCACCGGCAAGCTGCCCGTGCCCTGGCCCACCCTCGTGACCACCTTCGGCTA
CGGCCTGATGTGCTTCGCCCGCTACCCCGACCACATGAAGCAGCACGACTTCTTCAAGTCCGCCATGCCC
GAAGGCTACGTCCAGGAGCGCACCATCTTCTTCAAGGACGACGGCAACTACAAGACCCGCGCCGAGGTGA
AGTTCGAGGGCGACACCCTGGTGAACCGCATCGAGCTGAAGGGCATCGACTTCAAGGAGGACGGCAACAT
CCTGGGGCACAAGCTGGAGTACAACTACAACAGCCACAACGTCTATATCATGGCCGACAAGCAGAAGAAC
GGCATCAAGGTGAACTTCAAGATCCGCCACAACATCGAGGACGGCAGCGTGCAGCTCGCCGACCACTACC
AGCAGAACACCCCCATCGGCGACGGCCCCGTGCTGCTGCCCGACAACCACTACCTGAGCTACCAGTCCGC
CCTGAGCAAAGACCCCAACGAGAAGCGCGATCACATGGTCCTGCTGGAGTTCGTGACCGCCGCCGGGATC
ACTCTCGGCATGGACGAGCTGTACAAGTAAGAATTCCAATTCAATTCTGAAAGCTTTAGTGATTTAATAG
CTCCATGTCAACAAGAATAAAACGCGTTTCGGGTTTACCTCTTCCAGATACAGCTCATCTGCAATGCATT
AATGCATTGGACCTCGCAACCCTAGTACGCCCTTCAGGCTCCGGCGAAGCAGAAGAATAGCTTAGCAGAG
TCTATTTTCATTTTCGGGAGACGAGATCAAGCAGATCAACGGTCGTCAAGAGACCTACGAGACTGAGGAA
TCCGCTCTTGGCTCCACGCGACTATATATTTGTCTCTAATTGTACTTTGACATGCTCCTCTTCTTTACTC
TGATAGCTTGACTATGAAAATTCCGTCACCAGCCCCTGGGTTCGCAAAGATAATTGCACTGTTTCTTCCT

TGAACTCTCAAGCCTACAGGACACACATTCATCGTAGGTATAAACCTCGAAAATCATTCCTACTAAGATG
GGTATACAATAGTAACCATGCATGGTTGCCTAGTGAATGCTCCGTAACACCCAATACGCGGCCGCTAACA
TCTCGAGGGGGGGCCCGGTACCCAGCTTTTGTTCCCTTTAGTGAGGGTTAATTGCGCGCTTGGCGTAATC
ATGGTCATAGCTGTTTCCTGTGTGAAATTGTTATCCGCTCACAATTCCACACAACATACGAGCCGGAAGC
ATAAAGTGTAAAGCCTGGGGTGCCTAATGAGTGAGCTAACTCACATTAATTGCGTTGCGCTCACTGCCCG
CTTTCCAGTCGGGAAACCTGTCGTGCCAGCTGCATTAATGAATCGGCCAACGCGCGGGGAGAGGCGGTTT
GCGTATTGGGCGCTCTTCCGCTTCCTCGCTCACTGACTCGCTGCGCTCGGTCGTTCGGCTGCGGCGAGCG
GTATCAGCTCACTCAAAGGCGGTAATACGGTTATCCACAGAATCAGGGGATAACGCAGGAAAGAACATGT
GAGCAAAAGGCCAGCAAAAGGCCAGGAACCGTAAAAAGGCCGCGTTGCTGGCGTTTTTCCATAGGCTCCG
CCCCCCTGACGAGCATCACAAAAATCGACGCTCAAGTCAGAGGTGGCGAAACCCGACAGGACTATAAAGA
TACCAGGCGTTTCCCCCTGGAAGCTCCCTCGTGCGCTCTCCTGTTCCGACCCTGCCGCTTACCGGATACC
TGTCCGCCTTTCTCCCTTCGGGAAGCGTGGCGCTTTCTCATAGCTCACGCTGTAGGTATCTCAGTTCGGT
GTAGGTCGTTCGCTCCAAGCTGGGCTGTGTGCACGAACCCCCCGTTCAGCCCGACCGCTGCGCCTTATCC
GGTAACTATCGTCTTGAGTCCAACCCGGTAAGACACGACTTATCGCCACTGGCAGCAGCCACTGGTAACA
GGATTAGCAGAGCGAGGTATGTAGGCGGTGCTACAGAGTTCTTGAAGTGGTGGCCTAACTACGGCTACAC
TAGAAGGACAGTATTTGGTATCTGCGCTCTGCTGAAGCCAGTTACCTTCGGAAAAAGAGTTGGTAGCTCT
TGATCCGGCAAACAAACCACCGCTGGTAGCGGTGGTTTTTTTGTTTGCAAGCAGCAGATTACGCGCAGAA
AAAAAGGATCTCAAGAAGATCCTTTGATCTTTTCTACGGGGTCTGACGCTCAGTGGAACGAAAACTCACG
TTAAGGGATTTTGGTCATGAGATTATCAAAAAGGATCTTCACCTAGATCCTTTTAAATTAAAAATGAAGT
TTTAAATCAATCTAAAGTATATATGAGTAAACTTGGTCTGACAGTTACCAATGCTTAATCAGTGAGGCAC
CTATCTCAGCGATCTGTCTATTTCGTTCATCCATAGTTGCCTGACTCCCCGTCGTGTAGATAACTACGAT
ACGGGAGGGCTTACCATCTGGCCCCAGTGCTGCAATGATACCGCGAGACCCACGCTCACCGGCTCCAGAT
TTATCAGCAATAAACCAGCCAGCCGGAAGGGCCGAGCGCAGAAGTGGTCCTGCAACTTTATCCGCCTCCA
TCCAGTCTATTAATTGTTGCCGGGAAGCTAGAGTAAGTAGTTCGCCAGTTAATAGTTTGCGCAACGTTGT
TGCCATTGCTACAGGCATCGTGGTGTCACGCTCGTCGTTTGGTATGGCTTCATTCAGCTCCGGTTCCCAA
CGATCAAGGCGAGTTACATGATCCCCCATGTTGTGCAAAAAAGCGGTTAGCTCCTTCGGTCCTCCGATCG
TTGTCAGAAGTAAGTTGGCCGCAGTGTTATCACTCATGGTTATGGCAGCACTGCATAATTCTCTTACTGT
CATGCCATCCGTAAGATGCTTTTCTGTGACTGGTGAGTACTCAACCAAGTCATTCTGAGAATAGTGTATG
CGGCGACCGAGTTGCTCTTGCCCGGCGTCAATACGGGATAATACCGCGCCACATAGCAGAACTTTAAAAG
TGCTCATCATTGGAAAACGTTCTTCGGGGCGAAAACTCTCAAGGATCTTACCGCTGTTGAGATCCAGTTC
GATGTAACCCACTCGTGCACCCAACTGATCTTCAGCATCTTTTACTTTCACCAGCGTTTCTGGGTGAGCA
AAAACAGGAAGGCAAAATGCCGCAAAAAAGGGAATAAGGGCGACACGGAAATGTTGAATACTCATACTCT
TCCTTTTTCAATATTATTGAAGCATTTATCAGGGTTATTGTCTCATGAGCGGATACATATTTGAATGTAT
TTAGAAAAATAAACAAATAGGGGTTCCGCGCACATTTCCCCGAAAAGTGCCAC

pMoj009_CeVe 2.12

CTGACGCGCCCTGTAGCGGCGCATTAAGCGCGGCGGGTGTGGTGGTTACGCGCAGCGTGACCGCTACACT
TGCCAGCGCCCTAGCGCCCGCTCCTTTCGCTTTCTTCCCTTCCTTTCTCGCCACGTTCGCCGGCTTTCCC
CGTCAAGCTCTAAATCGGGGGCTCCCTTTAGGGTTCCGATTTAGTGCTTTACGGCACCTCGACCCCAAAA
AACTTGATTAGGGTGATGGTTCACGTAGTGGGCCATCGCCCTGATAGACGGTTTTTCGCCCTTTGACGTT
GGAGTCCACGTTCTTTAATAGTGGACTCTTGTTCCAAACTGGAACAACACTCAACCCTATCTCGGTCTAT
TCTTTTGATTTATAAGGGATTTTGCCGATTTCGGCCTATTGGTTAAAAAATGAGCTGATTTAACAAAAAT
TTAACGCGAATTTTAACAAAATATTAACGCTTACAATTTCCATTCGCCATTCAGGCTGCGCAACTGTTGG
GAAGGGCGATCGGTGCGGGCCTCTTCGCTATTACGCCAGCTGGCGAAAGGGGGATGTGCTGCAAGGCGAT
TAAGTTGGGTAACGCCAGGGTTTTCCCAGTCACGACGTTGTAAAACGACGGCCAGTGAGCGCGCGTAATA
CGACTCACTATAGGGCGAATTGGAGCTCGTGACCGGTGACTCTTTCTGGCATGCGGAGAGACGGACGGAC
GCAGAGAGAAGGGCTGAGTAATAAGCCACTGGCCAGACAGCTCTGGCGGCTCTGAGGTGCAGTGGATGAT
TATTAATCCGGGACCGGCCGCCCCTCCGCCCCGAAGTGGAAAGGCTGGTGTGCCCCTCGTTGACCAAGAA
TCTATTGCATCATCGGAGAATATGGAGCTTCATCGAATCACCGGCAGTAAGCGAAGGAGAATGTGAAGCC
AGGGGTGTATAGCCGTCGGCGAAATAGCATGCCATTAACCTAGGTACAGAAGTCCAATTGCTTCCGATCT
GGTAAAAGATTCACGAGATAGTACCTTCTCCGAAGTAGGTAGAGCGAGTACCCGGCGCGTAAGCTCCCTA
ATTGGCCCATCCGGCATCTGTAGGGCGTCCAAATATCGTGCCTCTCCTGCTTTGCCCGGTGTATGAAACC
GGAAAGGCCGCTCAGGAGCTGGCCAGCGGCGCAGACCGGGAACACAAGCTGGCAGTCGACCCATCCGGTG
CTCTGCACTCGACCTGCTGAGGTCCCTCAGTCCCTGGTAGGCAGCTTTGCCCCGTCTGTCCGCCCGGTGT
GTCGGCGGGGTTGACAAGGTCGTTGCGTCAGTCCAACATTTGTTGCCATATTTTCCTGCTCTCCCCACCA
GCTGCTCTTTTCTTTTCTCTTTCTTTTCCCATCTTCAGTATATTCATCTTCCCATCCAAGAACCTTTATT
TCCCCTAAGTAAGTACTTTGCTACATCCATACTCCATCCTTCCCATCCCTTATTCCTTTGAACCTTTCAG
TTCGAGCTTTCCCACTTCATCGCAGCTTGACTAACAGCTACCCCGCTTGAGCAGACATCACCCATGGTGA
GCAAGGGCGAGGAGCTGTTCACCGGGGTGGTGCCCATCCTGGTCGAGCTGGACGGCGACGTAAACGGCCA
CAAGTTCAGCGTGTCCGGCGAGGGCGAGGGCGATGCCACCTACGGCAAGCTGACCCTGAAGTTCATCTGC
ACCACCGGCAAGCTGCCCGTGCCCTGGCCCACCCTCGTGACCACCCTGACCTGGGGCGTGCAGTGCTTCG
CCCGCTACCCCGACCACATGAAGCAGCACGACTTCTTCAAGTCCGCCATGCCCGAAGGCTACGTCCAGGA
GCGCACCATCTTCTTCAAGGACGACGGCAACTACAAGACCCGCGCCGAGGTGAAGTTCGAGGGCGACACC
CTGGTGAACCGCATCGAGCTGAAGGGCATCGACTTCAAGGAGGACGGCAACATCCTGGGGCACAAGCTGG
AGTACAACGCCATCAGCGACAACGTCTATATCACCGCCGACAAGCAGAAGAACGGCATCAAGGCCAACTT

CAAGATCCGCCACAACATCGAGGACGGCAGCGTGCAGCTCGCCGACCACTACCAGCAGAACACCCCCATC
GGCGACGGCCCCGTGCTGCTGCCCGACAACCACTACCTGAGCACCCAGTCCAAGCTGAGCAAAGACCCCA
ACGAGAAGCGCGATCACATGGTCCTGCTGGAGTTCGTGACCGCCGCCCGCATGCATGACCAACTGACAGA
AGAGCAGATTGCAGAGTTCAAAGAAGCATTCTCATTATTCGACAAGGATGGGGATGGTACCATCACCACA
AAGGAACTTGGCACTGTTATGCGGTCGCTTGGACAAAACCCAACAGAAGCAGAATTGCAGGATATGATCA
ATGAAGTAGATGCTGATGGCAATGGAACAATTGACTTTCCTGAATTTCTGACTATGATGGCTAGAAAAAT
GAAAGACACAGACAGCGAAGAAGAAATCAGAGAAGCATTCCGTGTTTTTGACAAGGATGGCAATGGCTAT
ATCAGTGCTGCTGAATTACGTCATGTGATGACAAACCTTGGGGAGAAGTTAACAGATGAAGAAGTTGATG
AAATGATAAGGGAAGCAGATATTGATGGAGATGGCCAAGTAAACTATGAAGAGTTTGTACAAATGATGAC
AGCAAAGGGCGGCAAGAGGCGCTGGAAGAAAAACTTCATTGCCGTCAGCGCTGCCAACCGCTTCAAGAAG
ATCAGCAGCTCCGGGGCACTGGAGCTCATGGTGAGCAAGGGCGAGGAGCTGTTCACCGGGGTGGTGCCCA
TCCTGGTCGAGCTGGACGGCGACGTAAACGGCCACAAGTTCAGCGTGTCCGGCGAGGGCGAGGGCGATGC
CACCTACGGCAAGCTGACCCTGAAGTTCATCTGCACCACCGGCAAGCTGCCCGTGCCCTGGCCCACCCTC
GTGACCACCTTCGGCTACGGCCTGCAGTGCTTCGCCCGCTACCCCGACCACATGAAGCAGCACGACTTCT
TCAAGTCCGCCATGCCCGAAGGCTACGTCCAGGAGCGCACCATCTTCTTCAAGGACGACGGCAACTACAA
GACCCGCGCCGAGGTGAAGTTCGAGGGCGACACCCTGGTGAACCGCATCGAGCTGAAGGGCATCGACTTC
AAGGAGGACGGCAACATCCTGGGGCACAAGCTGGAGTACAACTACAACAGCCACAACGTCTATATCATGG
CCGACAAGCAGAAGAACGGCATCAAGGTGAACTTCAAGATCCGCCACAACATCGAGGACGGCAGCGTGCA
GCTCGCCGACCACTACCAGCAGAACACCCCCATCGGCGACGGCCCCGTGCTGCTGCCCGACAACCACTAC
CTGAGCTACCAGTCCGCCCTGAGCAAAGACCCCAACGAGAAGCGCGATCACATGGTCCTGCTGGAGTTCG
TGACCGCCGCCGGGATCACTCTCGGCATGGACGAGCTGTACAAGTAAGAATTCAATTCTGAAAGCTTTAG
TGATTTAATAGCTCCATGTCAACAAGAATAAAACGCGTTTCGGGTTTACCTCTTCCAGATACAGCTCATC
TGCAATGCATTAATGCATTGGACCTCGCAACCCTAGTACGCCCTTCAGGCTCCGGCGAAGCAGAAGAATA
GCTTAGCAGAGTCTATTTTCATTTTCGGGAGACGAGATCAAGCAGATCAACGGTCGTCAAGAGACCTACG
AGACTGAGGAATCCGCTCTTGGCTCCACGCGACTATATATTTGTCTCTAATTGTACTTTGACATGCTCCT
CTTCTTTACTCTGATAGCTTGACTATGAAAATTCCGTCACCAGCCCCTGGGTTCGCAAAGATAATTGCAC
TGTTTCTTCCTTGAACTCTCAAGCCTACAGGACACACATTCATCGTAGGTATAAACCTCGAAAATCATTC
CTACTAAGATGGGTATACAATAGTAACCATGCATGGTTGCCTAGTGAATGCTCCGTAACACCCAATACGC
GGCCGCTAACATCTCGAGGGGGGGCCCGGTACCCAGCTTTTGTTCCCTTTAGTGAGGGTTAATTGCGCGC
TTGGCGTAATCATGGTCATAGCTGTTTCCTGTGTGAAATTGTTATCCGCTCACAATTCCACACAACATAC
GAGCCGGAAGCATAAAGTGTAAAGCCTGGGGTGCCTAATGAGTGAGCTAACTCACATTAATTGCGTTGCG
CTCACTGCCCGCTTTCCAGTCGGGAAACCTGTCGTGCCAGCTGCATTAATGAATCGGCCAACGCGCGGGG
AGAGGCGGTTTGCGTATTGGGCGCTCTTCCGCTTCCTCGCTCACTGACTCGCTGCGCTCGGTCGTTCGGC
TGCGGCGAGCGGTATCAGCTCACTCAAAGGCGGTAATACGGTTATCCACAGAATCAGGGGATAACGCAGG
AAAGAACATGTGAGCAAAAGGCCAGCAAAAGGCCAGGAACCGTAAAAAGGCCGCGTTGCTGGCGTTTTTC
CATAGGCTCCGCCCCCCTGACGAGCATCACAAAAATCGACGCTCAAGTCAGAGGTGGCGAAACCCGACAG
GACTATAAAGATACCAGGCGTTTCCCCCTGGAAGCTCCCTCGTGCGCTCTCCTGTTCCGACCCTGCCGCT
TACCGGATACCTGTCCGCCTTTCTCCCTTCGGGAAGCGTGGCGCTTTCTCATAGCTCACGCTGTAGGTAT
CTCAGTTCGGTGTAGGTCGTTCGCTCCAAGCTGGGCTGTGTGCACGAACCCCCCGTTCAGCCCGACCGCT
GCGCCTTATCCGGTAACTATCGTCTTGAGTCCAACCCGGTAAGACACGACTTATCGCCACTGGCAGCAGC
CACTGGTAACAGGATTAGCAGAGCGAGGTATGTAGGCGGTGCTACAGAGTTCTTGAAGTGGTGGCCTAAC
TACGGCTACACTAGAAGGACAGTATTTGGTATCTGCGCTCTGCTGAAGCCAGTTACCTTCGGAAAAAGAG
TTGGTAGCTCTTGATCCGGCAAACAAACCACCGCTGGTAGCGGTGGTTTTTTTGTTTGCAAGCAGCAGAT
TACGCGCAGAAAAAAAGGATCTCAAGAAGATCCTTTGATCTTTTCTACGGGGTCTGACGCTCAGTGGAAC
GAAAACTCACGTTAAGGGATTTTGGTCATGAGATTATCAAAAAGGATCTTCACCTAGATCCTTTTAAATT
AAAAATGAAGTTTTAAATCAATCTAAAGTATATATGAGTAAACTTGGTCTGACAGTTACCAATGCTTAAT
CAGTGAGGCACCTATCTCAGCGATCTGTCTATTTCGTTCATCCATAGTTGCCTGACTCCCCGTCGTGTAG
ATAACTACGATACGGGAGGGCTTACCATCTGGCCCCAGTGCTGCAATGATACCGCGAGACCCACGCTCAC
CGGCTCCAGATTTATCAGCAATAAACCAGCCAGCCGGAAGGGCCGAGCGCAGAAGTGGTCCTGCAACTTT
ATCCGCCTCCATCCAGTCTATTAATTGTTGCCGGGAAGCTAGAGTAAGTAGTTCGCCAGTTAATAGTTTG
CGCAACGTTGTTGCCATTGCTACAGGCATCGTGGTGTCACGCTCGTCGTTTGGTATGGCTTCATTCAGCT
CCGGTTCCCAACGATCAAGGCGAGTTACATGATCCCCCATGTTGTGCAAAAAAGCGGTTAGCTCCTTCGG
TCCTCCGATCGTTGTCAGAAGTAAGTTGGCCGCAGTGTTATCACTCATGGTTATGGCAGCACTGCATAAT
TCTCTTACTGTCATGCCATCCGTAAGATGCTTTTCTGTGACTGGTGAGTACTCAACCAAGTCATTCTGAG
AATAGTGTATGCGGCGACCGAGTTGCTCTTGCCCGGCGTCAATACGGGATAATACCGCGCCACATAGCAG
AACTTTAAAAGTGCTCATCATTGGAAAACGTTCTTCGGGGCGAAAACTCTCAAGGATCTTACCGCTGTTG
AGATCCAGTTCGATGTAACCCACTCGTGCACCCAACTGATCTTCAGCATCTTTTACTTTCACCAGCGTTT
CTGGGTGAGCAAAAACAGGAAGGCAAAATGCCGCAAAAAAGGGAATAAGGGCGACACGGAAATGTTGAAT
ACTCATACTCTTCCTTTTTCAATATTATTGAAGCATTTATCAGGGTTATTGTCTCATGAGCGGATACATA
TTTGAATGTATTTAGAAAAATAAACAAATAGGGGTTCCGCGCACATTTCCCCGAAAAGTGCCAC

pMoj009_CeVe 6.1

CTGACGCGCCCTGTAGCGGCGCATTAAGCGCGGCGGGTGTGGTGGTTACGCGCAGCGTGACCGCTACACT
TGCCAGCGCCCTAGCGCCCGCTCCTTTCGCTTTCTTCCCTTCCTTTCTCGCCACGTTCGCCGGCTTTCCC
CGTCAAGCTCTAAATCGGGGGCTCCCTTTAGGGTTCCGATTTAGTGCTTTACGGCACCTCGACCCCAAAA
AACTTGATTAGGGTGATGGTTCACGTAGTGGGCCATCGCCCTGATAGACGGTTTTTCGCCCTTTGACGTT
GGAGTCCACGTTCTTTAATAGTGGACTCTTGTTCCAAACTGGAACAACACTCAACCCTATCTCGGTCTAT

TCTTTTGATTTATAAGGGATTTTGCCGATTTCGGCCTATTGGTTAAAAAATGAGCTGATTTAACAAAAAT
TTAACGCGAATTTTAACAAAATATTAACGCTTACAATTTCCATTCGCCATTCAGGCTGCGCAACTGTTGG
GAAGGGCGATCGGTGCGGGCCTCTTCGCTATTACGCCAGCTGGCGAAAGGGGGATGTGCTGCAAGGCGAT
TAAGTTGGGTAACGCCAGGGTTTTCCCAGTCACGACGTTGTAAAACGACGGCCAGTGAGCGCGCGTAATA
CGACTCACTATAGGGCGAATTGGAGCTCGTGACCGGTGACTCTTTCTGGCATGCGGAGAGACGGACGGAC
GCAGAGAGAAGGGCTGAGTAATAAGCCACTGGCCAGACAGCTCTGGCGGCTCTGAGGTGCAGTGGATGAT
TATTAATCCGGGACCGGCCGCCCCTCCGCCCCGAAGTGGAAAGGCTGGTGTGCCCCTCGTTGACCAAGAA
TCTATTGCATCATCGGAGAATATGGAGCTTCATCGAATCACCGGCAGTAAGCGAAGGAGAATGTGAAGCC
AGGGGTGTATAGCCGTCGGCGAAATAGCATGCCATTAACCTAGGTACAGAAGTCCAATTGCTTCCGATCT
GGTAAAAGATTCACGAGATAGTACCTTCTCCGAAGTAGGTAGAGCGAGTACCCGGCGCGTAAGCTCCCTA
ATTGGCCCATCCGGCATCTGTAGGGCGTCCAAATATCGTGCCTCTCCTGCTTTGCCCGGTGTATGAAACC
GGAAAGGCCGCTCAGGAGCTGGCCAGCGGCGCAGACCGGGAACACAAGCTGGCAGTCGACCCATCCGGTG
CTCTGCACTCGACCTGCTGAGGTCCCTCAGTCCCTGGTAGGCAGCTTTGCCCCGTCTGTCCGCCCGGTGT
GTCGGCGGGGTTGACAAGGTCGTTGCGTCAGTCCAACATTTGTTGCCATATTTTCCTGCTCTCCCCACCA
GCTGCTCTTTTCTTTTCTCTTTCTTTTCCCATCTTCAGTATATTCATCTTCCCATCCAAGAACCTTTATT
TCCCCTAAGTAAGTACTTTGCTACATCCATACTCCATCCTTCCCATCCCTTATTCCTTTGAACCTTTCAG
TTCGAGCTTTCCCACTTCATCGCAGCTTGACTAACAGCTACCCCGCTTGAGCAGACATCACCCATGGTGA
GCAAGGGCGAGGAGCTGTTCACCGGGGTGGTGCCCATCCTGGTCGAGCTGGACGGCGACGTAAACGGCCA
CAAGTTCAGCGTGTCCGGCGAGGGCGAGGGCGATGCCACCTACGGCAAGCTGACCCTGAAGTTCATCTGC
ACCACCGGCAAGCTGCCCGTGCCCTGGCCCACCCTCGTGACCACCCTGACCTGGGGCGTGCAGTGCTTCG
CCCGCTACCCCGACCACATGAAGCAGCACGACTTCTTCAAGTCCGCCATGCCCGAAGGCTACGTCCAGGA
GCGCACCATCTTCTTCAAGGACGACGGCAACTACAAGACCCGCGCCGAGGTGAAGTTCGAGGGCGACACC
CTGGTGAACCGCATCGAGCTGAAGGGCATCGACTTCAAGGAGGACGGCAACATCCTGGGGCACAAGCTGG
AGTACAACGCCATCAGCGACAACGTCTATATCACCGCCGACAAGCAGAAGAACGGCATCAAGGCCAACTT
CAAGATCCGCCACAACATCGAGGACGGCAGCGTGCAGCTCGCCGACCACTACCAGCAGAACACCCCCATC
GGCGACGGCCCCGTGCTGCTGCCCGACAACCACTACCTGAGCACCCAGTCCAAGCTGAGCAAAGACCCCA
ACGAGAAGCGCGATCACATGGTCCTGCTGGAGTTCGTGACCGCCGCCCGCATGCATGAGCAGATTGCAGA
GTTCAAAGAAGCCTTCTCATTATTCGACAAGGATGGGGACGGCACCATCACCACAAAGGAACTTGGCACT
GTTATGAGGTCGCTTGGACAAAACCCAACGGAAGCAGAATTGCAGGATATGATCAATGAAGTCGATGCTG
ATGGCAATGGAACGATTGACTTTCCTGAATTTCTTACTATGATGGCTAGAAAAATGAAGGACACAGGCGG
AGTGAAACTGATTCCGAGCTGGACCACCGTGATTCTGGTGAAATCTATGCTGCGTAAACGTAGCTTCGGC
AACCCGTTCGGCGGCGACAGCGAAGAGGAAATCCGAGAAGCATTCCGTGTTTTTGACAAGGATGGGAACG
GCTACATCAGCGCTGCTGAATTACGTCACGTCATGACAAACCTCGGGGAGAAGTTAACAGACGAAGAAGT
TGACGAAATGATAAGGGAAGCAGATATTGATGGTGACGGCCAAGTAAACTACGAAGAGTTTGTACAAATG
ATGACAGCAAAGGAGCTCATGGTGAGCAAGGGCGAGGAGCTGTTCACCGGGGTGGTGCCCATCCTGGTCG
AGCTGGACGGCGACGTAAACGGCCACAAGTTCAGCGTGTCCGGCGAGGGCGAGGGCGATGCCACCTACGG
CAAGCTGACCCTGAAGTTCATCTGCACCACCGGCAAGCTGCCCGTGCCCTGGCCCACCCTCGTGACCACC
TTCGGCTACGGCCTGCAGTGCTTCGCCCGCTACCCCGACCACATGAAGCAGCACGACTTCTTCAAGTCCG
CCATGCCCGAAGGCTACGTCCAGGAGCGCACCATCTTCTTCAAGGACGACGGCAACTACAAGACCCGCGC
CGAGGTGAAGTTCGAGGGCGACACCCTGGTGAACCGCATCGAGCTGAAGGGCATCGACTTCAAGGAGGAC
GGCAACATCCTGGGGCACAAGCTGGAGTACAACTACAACAGCCACAACGTCTATATCATGGCCGACAAGC
AGAAGAACGGCATCAAGGTGAACTTCAAGATCCGCCACAACATCGAGGACGGCAGCGTGCAGCTCGCCGA
CCACTACCAGCAGAACACCCCCATCGGCGACGGCCCCGTGCTGCTGCCCGACAACCACTACCTGAGCTAC
CAGTCCGCCCTGAGCAAAGACCCCAACGAGAAGCGCGATCACATGGTCCTGCTGGAGTTCGTGACCGCCG
CCGGGATCACTCTCGGCATGGACGAGCTGTACAAGTAAGAATTCAATTCTGAAAGCTTTAGTGATTTAAT
AGCTCCATGTCAACAAGAATAAAACGCGTTTCGGGTTTACCTCTTCCAGATACAGCTCATCTGCAATGCA
TTAATGCATTGGACCTCGCAACCCTAGTACGCCCTTCAGGCTCCGGCGAAGCAGAAGAATAGCTTAGCAG
AGTCTATTTTCATTTTCGGGAGACGAGATCAAGCAGATCAACGGTCGTCAAGAGACCTACGAGACTGAGG
AATCCGCTCTTGGCTCCACGCGACTATATATTTGTCTCTAATTGTACTTTGACATGCTCCTCTTCTTTAC
TCTGATAGCTTGACTATGAAAATTCCGTCACCAGCCCCTGGGTTCGCAAAGATAATTGCACTGTTTCTTC
CTTGAACTCTCAAGCCTACAGGACACACATTCATCGTAGGTATAAACCTCGAAAATCATTCCTACTAAGA
TGGGTATACAATAGTAACCATGCATGGTTGCCTAGTGAATGCTCCGTAACACCCAATACGCGGCCGCTAA
CATCTCGAGGGGGGGCCCGGTACCCAGCTTTTGTTCCCTTTAGTGAGGGTTAATTGCGCGCTTGGCGTAA
TCATGGTCATAGCTGTTTCCTGTGTGAAATTGTTATCCGCTCACAATTCCACACAACATACGAGCCGGAA
GCATAAAGTGTAAAGCCTGGGGTGCCTAATGAGTGAGCTAACTCACATTAATTGCGTTGCGCTCACTGCC
CGCTTTCCAGTCGGGAAACCTGTCGTGCCAGCTGCATTAATGAATCGGCCAACGCGCGGGGAGAGGCGGT
TTGCGTATTGGGCGCTCTTCCGCTTCCTCGCTCACTGACTCGCTGCGCTCGGTCGTTCGGCTGCGGCGAG
CGGTATCAGCTCACTCAAAGGCGGTAATACGGTTATCCACAGAATCAGGGGATAACGCAGGAAAGAACAT
GTGAGCAAAAGGCCAGCAAAAGGCCAGGAACCGTAAAAAGGCCGCGTTGCTGGCGTTTTTCCATAGGCTC
CGCCCCCCTGACGAGCATCACAAAAATCGACGCTCAAGTCAGAGGTGGCGAAACCCGACAGGACTATAAA
GATACCAGGCGTTTCCCCCTGGAAGCTCCCTCGTGCGCTCTCCTGTTCCGACCCTGCCGCTTACCGGATA
CCTGTCCGCCTTTCTCCCTTCGGGAAGCGTGGCGCTTTCTCATAGCTCACGCTGTAGGTATCTCAGTTCG
GTGTAGGTCGTTCGCTCCAAGCTGGGCTGTGTGCACGAACCCCCCGTTCAGCCCGACCGCTGCGCCTTAT
CCGGTAACTATCGTCTTGAGTCCAACCCGGTAAGACACGACTTATCGCCACTGGCAGCAGCCACTGGTAA
CAGGATTAGCAGAGCGAGGTATGTAGGCGGTGCTACAGAGTTCTTGAAGTGGTGGCCTAACTACGGCTAC
ACTAGAAGGACAGTATTTGGTATCTGCGCTCTGCTGAAGCCAGTTACCTTCGGAAAAAGAGTTGGTAGCT
CTTGATCCGGCAAACAAACCACCGCTGGTAGCGGTGGTTTTTTTGTTTGCAAGCAGCAGATTACGCGCAG
AAAAAAAGGATCTCAAGAAGATCCTTTGATCTTTTCTACGGGGTCTGACGCTCAGTGGAACGAAAACTCA
CGTTAAGGGATTTTGGTCATGAGATTATCAAAAAGGATCTTCACCTAGATCCTTTTAAATTAAAAATGAA

GTTTTAAATCAATCTAAAGTATATATGAGTAAACTTGGTCTGACAGTTACCAATGCTTAATCAGTGAGGC
ACCTATCTCAGCGATCTGTCTATTTCGTTCATCCATAGTTGCCTGACTCCCCGTCGTGTAGATAACTACG
ATACGGGAGGGCTTACCATCTGGCCCCAGTGCTGCAATGATACCGCGAGACCCACGCTCACCGGCTCCAG
ATTTATCAGCAATAAACCAGCCAGCCGGAAGGGCCGAGCGCAGAAGTGGTCCTGCAACTTTATCCGCCTC
CATCCAGTCTATTAATTGTTGCCGGGAAGCTAGAGTAAGTAGTTCGCCAGTTAATAGTTTGCGCAACGTT
GTTGCCATTGCTACAGGCATCGTGGTGTCACGCTCGTCGTTTGGTATGGCTTCATTCAGCTCCGGTTCCC
AACGATCAAGGCGAGTTACATGATCCCCCATGTTGTGCAAAAAAGCGGTTAGCTCCTTCGGTCCTCCGAT
CGTTGTCAGAAGTAAGTTGGCCGCAGTGTTATCACTCATGGTTATGGCAGCACTGCATAATTCTCTTACT
GTCATGCCATCCGTAAGATGCTTTTCTGTGACTGGTGAGTACTCAACCAAGTCATTCTGAGAATAGTGTA
TGCGGCGACCGAGTTGCTCTTGCCCGGCGTCAATACGGGATAATACCGCGCCACATAGCAGAACTTTAAA
AGTGCTCATCATTGGAAAACGTTCTTCGGGGCGAAAACTCTCAAGGATCTTACCGCTGTTGAGATCCAGT
TCGATGTAACCCACTCGTGCACCCAACTGATCTTCAGCATCTTTTACTTTCACCAGCGTTTCTGGGTGAG
CAAAAACAGGAAGGCAAAATGCCGCAAAAAAGGGAATAAGGGCGACACGGAAATGTTGAATACTCATACT
CTTCCTTTTTCAATATTATTGAAGCATTTATCAGGGTTATTGTCTCATGAGCGGATACATATTTGAATGT
ATTTAGAAAAATAAACAAATAGGGGTTCCGCGCACATTTCCCCGAAAAGTGCCAC

pMoj009_TN-L15mCer

CTGACGCGCCCTGTAGCGGCGCATTAAGCGCGGCGGGTGTGGTGGTTACGCGCAGCGTGACCGCTACACT
TGCCAGCGCCCTAGCGCCCGCTCCTTTCGCTTTCTTCCCTTCCTTTCTCGCCACGTTCGCCGGCTTTCCC
CGTCAAGCTCTAAATCGGGGGCTCCCTTTAGGGTTCCGATTTAGTGCTTTACGGCACCTCGACCCCAAAA
AACTTGATTAGGGTGATGGTTCACGTAGTGGGCCATCGCCCTGATAGACGGTTTTTCGCCCTTTGACGTT
GGAGTCCACGTTCTTTAATAGTGGACTCTTGTTCCAAACTGGAACAACACTCAACCCTATCTCGGTCTAT
TCTTTTGATTTATAAGGGATTTTGCCGATTTCGGCCTATTGGTTAAAAAATGAGCTGATTTAACAAAAAT
TTAACGCGAATTTTAACAAAATATTAACGCTTACAATTTCCATTCGCCATTCAGGCTGCGCAACTGTTGG
GAAGGGCGATCGGTGCGGGCCTCTTCGCTATTACGCCAGCTGGCGAAAGGGGGATGTGCTGCAAGGCGAT
TAAGTTGGGTAACGCCAGGGTTTTCCCAGTCACGACGTTGTAAAACGACGGCCAGTGAGCGCGCGTAATA
CGACTCACTATAGGGCGAATTGGAGCTCGTGACCGGTGACTCTTTCTGGCATGCGGAGAGACGGACGGAC
GCAGAGAGAAGGGCTGAGTAATAAGCCACTGGCCAGACAGCTCTGGCGGCTCTGAGGTGCAGTGGATGAT
TATTAATCCGGGACCGGCCGCCCCTCCGCCCCGAAGTGGAAAGGCTGGTGTGCCCCTCGTTGACCAAGAA
TCTATTGCATCATCGGAGAATATGGAGCTTCATCGAATCACCGGCAGTAAGCGAAGGAGAATGTGAAGCC
AGGGGTGTATAGCCGTCGGCGAAATAGCATGCCATTAACCTAGGTACAGAAGTCCAATTGCTTCCGATCT
GGTAAAAGATTCACGAGATAGTACCTTCTCCGAAGTAGGTAGAGCGAGTACCCGGCGCGTAAGCTCCCTA
ATTGGCCCATCCGGCATCTGTAGGGCGTCCAAATATCGTGCCTCTCCTGCTTTGCCCGGTGTATGAAACC
GGAAAGGCCGCTCAGGAGCTGGCCAGCGGCGCAGACCGGGAACACAAGCTGGCAGTCGACCCATCCGGTG
CTCTGCACTCGACCTGCTGAGGTCCCTCAGTCCCTGGTAGGCAGCTTTGCCCCGTCTGTCCGCCCGGTGT
GTCGGCGGGGTTGACAAGGTCGTTGCGTCAGTCCAACATTTGTTGCCATATTTTCCTGCTCTCCCCACCA
GCTGCTCTTTTCTTTTCTCTTTCTTTTCCCATCTTCAGTATATTCATCTTCCCATCCAAGAACCTTTATT
TCCCCTAAGTAAGTACTTTGCTACATCCATACTCCATCCTTCCCATCCCTTATTCCTTTGAACCTTTCAG
TTCGAGCTTTCCCACTTCATCGCAGCTTGACTAACAGCTACCCCGCTTGAGCAGACATCACCCATGGTGA
GCAAGGGCGAGGAGCTGTTCACCGGGGTGGTGCCCATCCTGGTCGAGCTGGACGGCGACGTAAACGGCCA
CAAGTTCAGCGTGTCCGGCGAGGGCGAGGGCGATGCCACCTACGGCAAGCTGACCCTGAAGTTCATCTGC
ACCACCGGCAAGCTGCCCGTGCCCTGGCCCACCCTCGTGACCACCCTGACCTGGGGCGTGCAGTGCTTCG
CCCGCTACCCCGACCACATGAAGCAGCACGACTTCTTCAAGTCCGCCATGCCCGAAGGCTACGTCCAGGA
GCGCACCATCTTCTTCAAGGACGACGGCAACTACAAGACCCGCGCCGAGGTGAAGTTCGAGGGCGACACC
CTGGTGAACCGCATCGAGCTGAAGGGCATCGACTTCAAGGAGGACGGCAACATCCTGGGGCACAAGCTGG
AGTACAACGCCATCAGCGACAACGTCTATATCACCGCCGACAAGCAGAAGAACGGCATCAAGGCCAACTT
CAAGATCCGCCACAACATCGAGGACGGCAGCGTGCAGCTCGCCGACCACTACCAGCAGAACACCCCCATC
GGCGACGGCCCCGTGCTGCTGCCCGACAACCACTACCTGAGCACCCAGTCCAAGCTGAGCAAAGACCCCA
ACGAGAAGCGCGATCACATGGTCCTGCTGGAGTTCGTGACCGCCGCCCGCATGCTCAGCGAGGAGATGAT
TGCTGAGTTCAAAGCTGCCTTTGACATGTTTGATGCGGACGGTGGTGGGGACATCAGCACCAAGGAGTTG
GGCACGGTGATGAGGATGCTGGGCCAGAACCCCACCAAAGAGGAGCTGGATGCCATCATCGAGGAGGTGG
ACGAGGATGGCAGCGGCACCATCGACTTCGAGGAGTTCCTGGTGATGATGGTGCGCCAGATGAAAGAGGA
CGCCAAGGGCAAGTCTGAGGAGGAGCTGGCCAACTGCTTCCGCATCTTCGACAAGAACGCTGATGGGTTC
ATCGACATCGAGGAGCTGGGTGAGATTCTCAGGGCCACTGGGGAGCACGTCATCGAGGAGGACATAGAAG
ACCTCATGAAGGATTCAGACAAGAACAATGACGGCCGCATTGACTTCGATGAGTTCCTGAAGATGATGGA
GGGTGTGCAGGAGCTCATGGTGAGCAAGGGCGAGGAGCTGTTCACCGGGGTGGTGCCCATCCTGGTCGAG
CTGGACGGCGACGTAAACGGCCACAAGTTCAGCGTGTCCGGCGAGGGCGAGGGCGATGCCACCTACGGCA
AGCTGACCCTGAAGTTCATCTGCACCACCGGCAAGCTGCCCGTGCCCTGGCCCACCCTCGTGACCACCTT
CGGCTACGGCCTGATGTGCTTCGCCCGCTACCCCGACCACATGCGCCAGCACGACTTCTTCAAGTCCGCC
ATGCCCGAAGGCTACGTCCAGGAGCGCACCATCTTCTTCAAGGACGACGGCAACTACAAGACCCGCGCCG
AGGTGAAGTTCGAGGGCGACACCCTGGTGAACCGCATCGAGCTGAAGGGCATCGACTTCAAGGAGGACGG
CAACATCCTGGGGCACAAGCTGGAGTACAACTACAACAGCCACAACGTCTATATCATGGCCGACAAGCAG
AAGAACGGCATCAAGGCCAACTTCAAGATCCGCCACAACATCGAGGACGGCAGCGTGCAGCTCGCCGACC
ACTACCAGCAGAACACCCCCATCGGCGACGGCCCCGTGCTGCTGCCCGACAACCACTACCTGAGCTACCA
GTCCGCCCTGAGCAAAGACCCCAACGAGAAGCGCGATCACATGGTCCTGCTGGAGTTCGTGACCGCCGCC

GGGATCACTCTCGGCATGGACGAGCTGTACAAGTAAGAATTCAATTCTGAAAGCTTTAGTGATTTAATAG
CTCCATGTCAACAAGAATAAAACGCGTTTCGGGTTTACCTCTTCCAGATACAGCTCATCTGCAATGCATT
AATGCATTGGACCTCGCAACCCTAGTACGCCCTTCAGGCTCCGGCGAAGCAGAAGAATAGCTTAGCAGAG
TCTATTTTCATTTTCGGGAGACGAGATCAAGCAGATCAACGGTCGTCAAGAGACCTACGAGACTGAGGAA
TCCGCTCTTGGCTCCACGCGACTATATATTTGTCTCTAATTGTACTTTGACATGCTCCTCTTCTTTACTC
TGATAGCTTGACTATGAAAATTCCGTCACCAGCCCCTGGGTTCGCAAAGATAATTGCACTGTTTCTTCCT
TGAACTCTCAAGCCTACAGGACACACATTCATCGTAGGTATAAACCTCGAAAATCATTCCTACTAAGATG
GGTATACAATAGTAACCATGCATGGTTGCCTAGTGAATGCTCCGTAACACCCAATACGCGGCCGCTAACA
TCTCGAGGGGGGGCCCGGTACCCAGCTTTTGTTCCCTTTAGTGAGGGTTAATTGCGCGCTTGGCGTAATC
ATGGTCATAGCTGTTTCCTGTGTGAAATTGTTATCCGCTCACAATTCCACACAACATACGAGCCGGAAGC
ATAAAGTGTAAAGCCTGGGGTGCCTAATGAGTGAGCTAACTCACATTAATTGCGTTGCGCTCACTGCCCG
CTTTCCAGTCGGGAAACCTGTCGTGCCAGCTGCATTAATGAATCGGCCAACGCGCGGGGAGAGGCGGTTT
GCGTATTGGGCGCTCTTCCGCTTCCTCGCTCACTGACTCGCTGCGCTCGGTCGTTCGGCTGCGGCGAGCG
GTATCAGCTCACTCAAAGGCGGTAATACGGTTATCCACAGAATCAGGGGATAACGCAGGAAAGAACATGT
GAGCAAAAGGCCAGCAAAAGGCCAGGAACCGTAAAAAGGCCGCGTTGCTGGCGTTTTTCCATAGGCTCCG
CCCCCCTGACGAGCATCACAAAAATCGACGCTCAAGTCAGAGGTGGCGAAACCCGACAGGACTATAAAGA
TACCAGGCGTTTCCCCCTGGAAGCTCCCTCGTGCGCTCTCCTGTTCCGACCCTGCCGCTTACCGGATACC
TGTCCGCCTTTCTCCCTTCGGGAAGCGTGGCGCTTTCTCATAGCTCACGCTGTAGGTATCTCAGTTCGGT
GTAGGTCGTTCGCTCCAAGCTGGGCTGTGTGCACGAACCCCCCGTTCAGCCCGACCGCTGCGCCTTATCC
GGTAACTATCGTCTTGAGTCCAACCCGGTAAGACACGACTTATCGCCACTGGCAGCAGCCACTGGTAACA
GGATTAGCAGAGCGAGGTATGTAGGCGGTGCTACAGAGTTCTTGAAGTGGTGGCCTAACTACGGCTACAC
TAGAAGGACAGTATTTGGTATCTGCGCTCTGCTGAAGCCAGTTACCTTCGGAAAAAGAGTTGGTAGCTCT
TGATCCGGCAAACAAACCACCGCTGGTAGCGGTGGTTTTTTTGTTTGCAAGCAGCAGATTACGCGCAGAA
AAAAAGGATCTCAAGAAGATCCTTTGATCTTTTCTACGGGGTCTGACGCTCAGTGGAACGAAAACTCACG
TTAAGGGATTTTGGTCATGAGATTATCAAAAAGGATCTTCACCTAGATCCTTTTAAATTAAAAATGAAGT
TTTAAATCAATCTAAAGTATATATGAGTAAACTTGGTCTGACAGTTACCAATGCTTAATCAGTGAGGCAC
CTATCTCAGCGATCTGTCTATTTCGTTCATCCATAGTTGCCTGACTCCCCGTCGTGTAGATAACTACGAT
ACGGGAGGGCTTACCATCTGGCCCCAGTGCTGCAATGATACCGCGAGACCCACGCTCACCGGCTCCAGAT
TTATCAGCAATAAACCAGCCAGCCGGAAGGGCCGAGCGCAGAAGTGGTCCTGCAACTTTATCCGCCTCCA
TCCAGTCTATTAATTGTTGCCGGGAAGCTAGAGTAAGTAGTTCGCCAGTTAATAGTTTGCGCAACGTTGT
TGCCATTGCTACAGGCATCGTGGTGTCACGCTCGTCGTTTGGTATGGCTTCATTCAGCTCCGGTTCCCAA
CGATCAAGGCGAGTTACATGATCCCCCATGTTGTGCAAAAAAGCGGTTAGCTCCTTCGGTCCTCCGATCG
TTGTCAGAAGTAAGTTGGCCGCAGTGTTATCACTCATGGTTATGGCAGCACTGCATAATTCTCTTACTGT
CATGCCATCCGTAAGATGCTTTTCTGTGACTGGTGAGTACTCAACCAAGTCATTCTGAGAATAGTGTATG
CGGCGACCGAGTTGCTCTTGCCCGGCGTCAATACGGGATAATACCGCGCCACATAGCAGAACTTTAAAAG
TGCTCATCATTGGAAAACGTTCTTCGGGGCGAAAACTCTCAAGGATCTTACCGCTGTTGAGATCCAGTTC
GATGTAACCCACTCGTGCACCCAACTGATCTTCAGCATCTTTTACTTTCACCAGCGTTTCTGGGTGAGCA
AAAACAGGAAGGCAAAATGCCGCAAAAAAGGGAATAAGGGCGACACGGAAATGTTGAATACTCATACTCT
TCCTTTTTCAATATTATTGAAGCATTTATCAGGGTTATTGTCTCATGAGCGGATACATATTTGAATGTAT
TTAGAAAAATAAACAAATAGGGGTTCCGCGCACATTTCCCCGAAAAGTGCCAC

Appendix C: Plasmidmaps

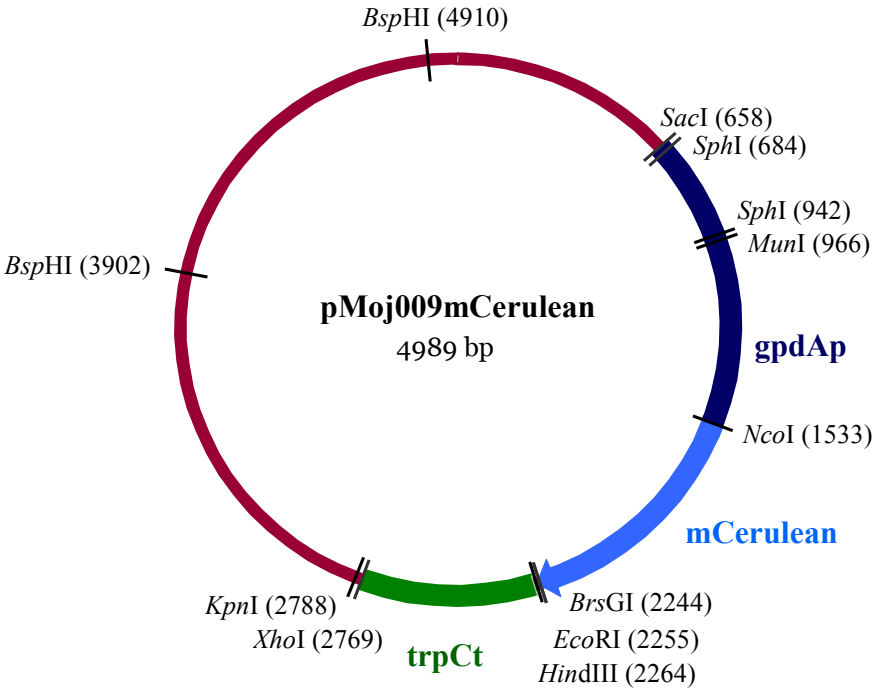

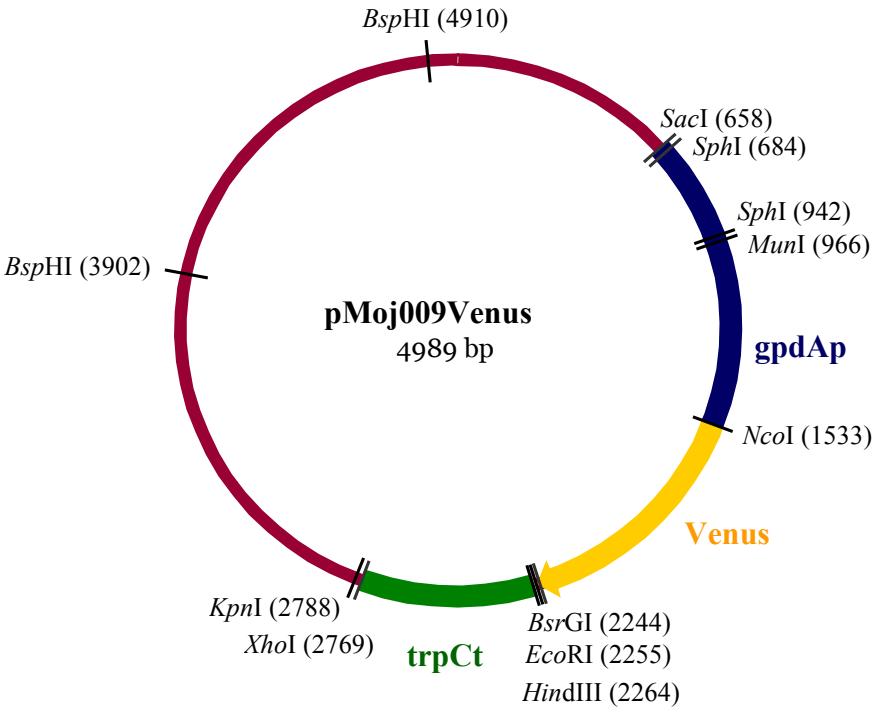
BspHI (4910)
SacI (658)
SphI (684)
SphI (942)
MunI (966)
BspHI (3902)
pMoj009Venus
4989 bp
gpdAp
NcoI (1533)
Venus
KpnI (2788)
XhoI (2769)
trpCt
BsrGI (2244)
EcoRI (2255)
HindIII (2264)

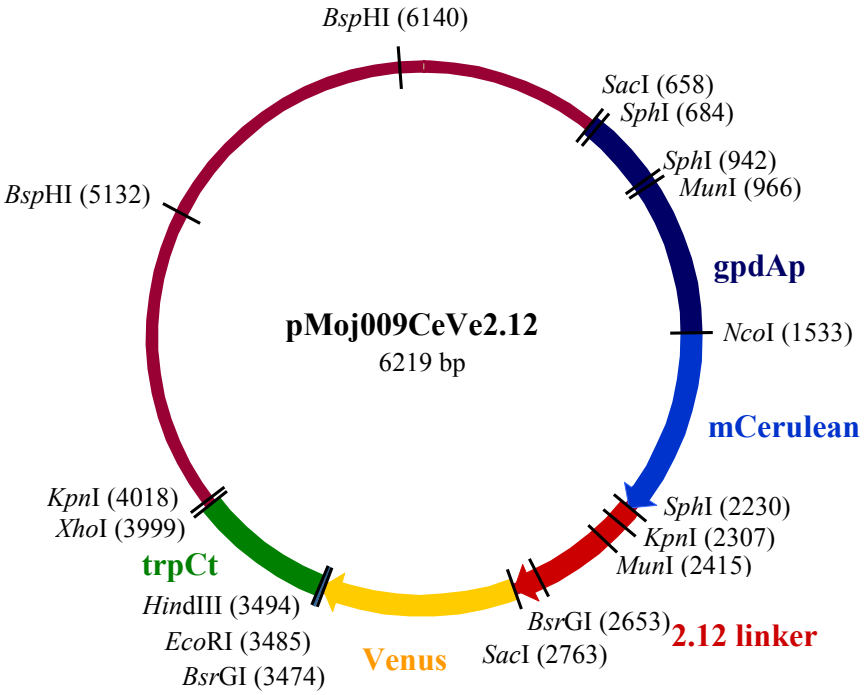
BspHI (6140)
SacI (658)
SphI (684)
SphI (942)
MunI (966)
BspHI (5132)
gpdAp
pMoj009CeVe2.12
6219 bp
NcoI (1533)
mCerulean
SphI (2230)
KpnI (2307)
MunI (2415)
KpnI (4018)
XhoI (3999)
trpCt
HindIII (3494)
EcoRI (3485)
BsrGI (3474)
Venus
BsrGI (2653)
SacI (2763)
2.12 linker

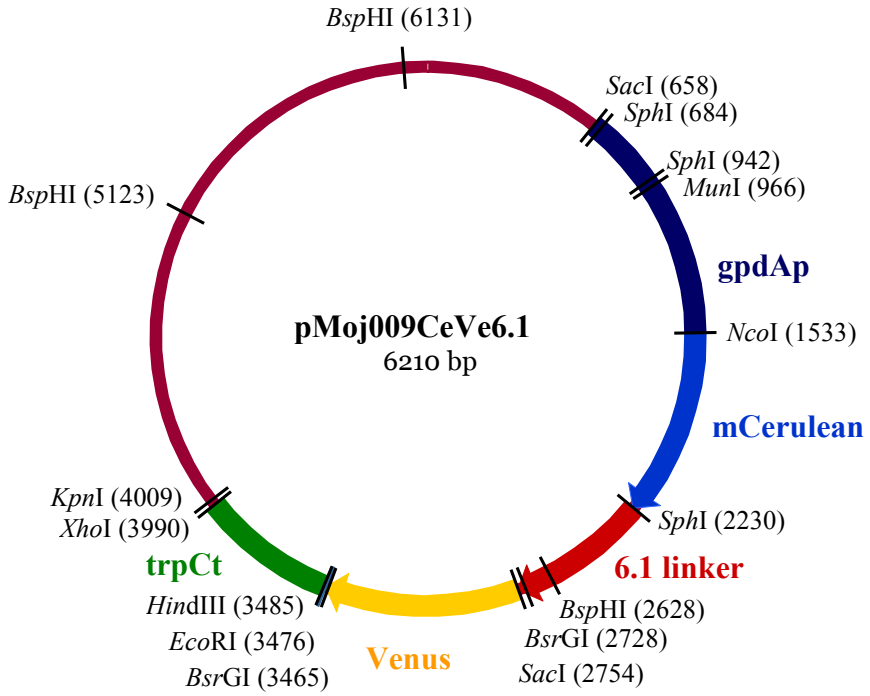
BspHI (6131)
SacI (658)
SphI (684)
SphI (942)
MunI (966)
BspHI (5123)
gpdAp
pMoj009CeVe6.1
6210 bp
NcoI (1533)
mCerulean
KpnI (4009)
XhoI (3990)
SphI (2230)
trpCt
6.1 linker
HindIII (3485)
EcoRI (3476)
BsrGI (3465)
BspHI (2628)
BsrGI (2728)
Venus
SacI (2754)

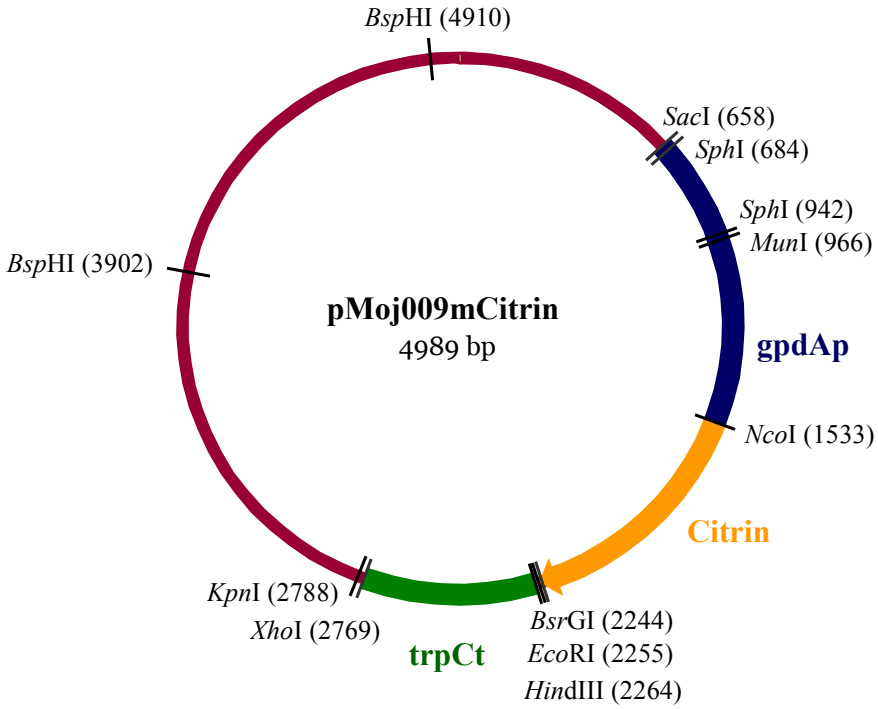
BspHI (4910)
SacI (658)
SphI (684)
SphI (942)
MunI (966)
BspHI (3902)
pMoj009mCitrin
4989 bp
gpdAp
NcoI (1533)
Citrin
KpnI (2788)
XhoI (2769)
BsrGI (2244)
EcoRI (2255)
trpCt
HindIII (2264)

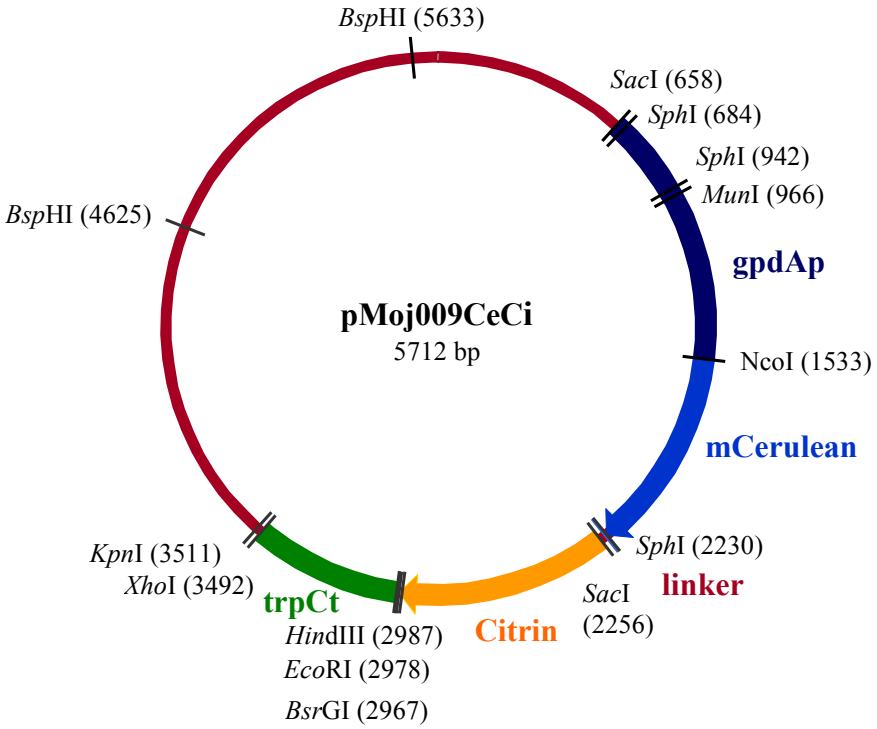
BspHI (5633)
SacI (658)
SphI (684)
SphI (942)
MunI (966)
gpdAp
BspHI (4625)
pMoj009CeCi
5712 bp
NcoI (1533)
mCerulean
SphI (2230)
linker
KpnI (3511)
XhoI (3492)
trpCt
SacI
(2256)
Citrin
HindIII (2987)
EcoRI (2978)
BsrGI (2967)

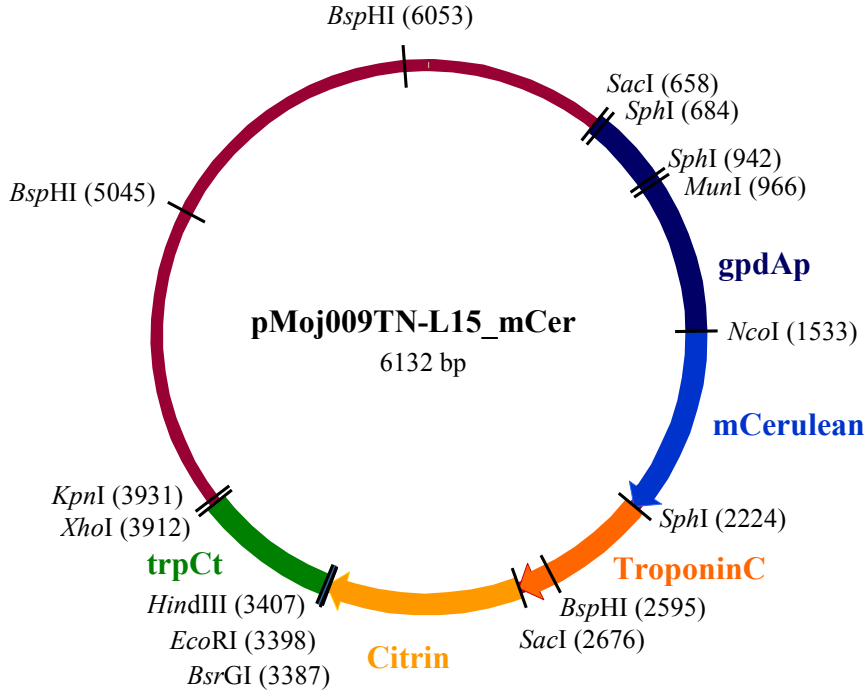
BspHI (6053)
SacI (658)
SphI (684)
SphI (942)
MunI (966)
BspHI (5045)
gpdAp
pMoj009TN-L15_mCer
6132 bp
NcoI (1533)
mCerulean
KpnI (3931)
XhoI (3912)
SphI (2224)
trpCt
TroponinC
HindIII (3407)
BspHI (2595)
EcoRI (3398)
SacI (2676)
Citrin
BsrGI (3387)

Appendix D: Publications

Bagar T, Altenbach K, Read ND, Benčina M (2009) Live-cell imaging and measurement of intracellular pH in filamentous fungi using a genetically encoded ratiometric probe**.** *Eukaryotic cell* **8**: 703-712

Harvey AR, Fletcher-Holmes DW, Gorman A, Altenbach K, Arlt J, Read ND (2005) Spectral imaging in a snapshot. *Proceedings of SPIE – Spectral Imaging: Instrumentation, Applications, and Analysis III* **5694**: 110-119

Millington M, Grindlay GJ, Altenbach K, Neely RK, Kolch W, Bencina M, Read ND, Jones AC, Dryden DTF, Magennis SW (2007) High-precision FLIM-FRET in fixed and living cells reveals heterogeneity in a simple CFP-YFP fusion protein. *Biophysical Chemistry* **127**: 155-164

Bibliography

Allen GJ, Kwak JM, Chu SP, Llopis J, Tsien RY, Harper JF, Schroeder JI (1999) Cameleon calcium indicator reports cytoplasmic calcium dynamics in *Arabidopsis* guard cells. *Plant J.* **19**: 735-747

Anand S and Prasad R (1989) Rise in intracellular pH is concurrent with 'start' progression of *Saccharomyces cerevisiae. J. Gen. Microbiol.* **135**: 2173-2179

Bagar T (2009) Spremljanje znotrajceličnih sprememb prostih kalcijevih ionov in vrednosti pH pri glivi *Aspergillus niger. Doctoral thesis*, University of Ljubljana

Bagar T, Altenbach K, Read ND, Benčina M (2009). Live-cell imaging and measurement of intracellular pH in filamentous fungi using a genetically encoded ratiometric probe**.** *Eukaryot. Cell* **8**: 703-712

Baird GS, Zacharias DA, Tsien RY (1999): Circular permutations and receptor insertion within green fluorescent proteins. *PNAS* **96**: 11241-11246

Barton JK, Den Hollander JA, Lee TM, Maclaughlin A, Shulman RG (1980) Measurement of the internal pH of yeast spores by ^{31}P nuclear magnetic resonance. *PNAS* **77**: 2470-2473

Benčina M, Bagar T, Lah L and Krasevec N (2009) A comparative genomic analysis of calcium and proton signalling/homeostasis in *Aspergillus* species. *Fungal Genet. Biol.* **46**: 93-104

Becker W, Bergmann A, Hink MA, König K, Benndorf K, Biskup K (2004) Fluorescence lifetime maging by time-correlated single-photon counting. *Microscop. Res. Tech.* **63**:58-66.

Bennet JW (1998) Mycotechnology: the role of fungi in biotechnology. *J Biotech* **66**: 101-107

Berridge MJ, Lipp P, Bootman MD (2000) The versatility and universatility of calcium signalling. *Nat. Rev. Mol. Cell Biol.* **1**: 11-21

Berridge MJ, Bootman MD, Roderick HL (2003) Calcium Signalling: Dynamics, Homeostasis and Remodelling. *Nat. Rev. Mol. Cell Biol.* **4**, 517-592

Bootman MD, Berridge MJ, Roderick HL (2001) Calcium signalling: more messengers, more channels more complexity. *Curr. Biol.* 12: R563-R565

Breje K, Sixma TK, Kitts PA, Kain SR, Tsien RY, Ormö M, Remington SJ (1997) Structural basis for dual excitation and photoisomerization of the *Aequorea victoria* green fluorescent protein. *PNAS* **94**:2306-2311

Brownlee (2000) Cellular calcium imaging: so, what's new? *Trends Cell Biol.* **10**: 451-457

Chattoraj M, King B, Bublitz G, Boxer S (1996) Ultra-fast excited state dynamics in green fluorescnet protein: Multiple states and proton transfer. *PNAS* **93**: 8362-8367

Cobbold PH and Rink TJ (1987) Fluorescence and bioluminescence measurement of cytoplasmic free calcium. *Biochem. J.* **248**: 313-328

Den Hollander JA, Ugurbil K, Brown TR, Shulman RG (1981) Phosphorus-31 nuclear magnetic resonance studies of the effect of oxygen upon glycolysis in yeast. *Biochem.* **20**: 5871-580

Duncan RR, Bergmann A, Cousin MA, Apps DK, Shipston MJ (2003) Multi-dimensional time-correlated single photon counting (TCSPC) fluorescence lifetime imaging microscopy (FLIM) to detect FRET in living cells. *J. Microscop.* **215**:1-12.

Edlind T, Smith L, Henry K, Katiyar S, Nickels J (2002) Antifungal activity in Saccaromyces cerevisiae is modulated by calcium signalling *Mol. Microbiol.* **46**(1): 257-268

Ehrig T, O'Kane D, Prendergast F (1995) Green-fluorescent protein mutants with altered fluorescence excitation spectra. *FEBS Letters* **367**: 163-166

Elson D, Webb S, Siegel J, Suhling K, Davis D, Lever J, Phillip D, Wallace A, French P (2002) Biomedical Applications of Fluorescence Lifetime Imaging. *Opt. Photonics News* 26-32

Feige JN, Sage D, Wahli W, Desvergne B, Gelman L (2005) PixFRET, an ImageJ plug-in for FRET calculation that can accommodate variations in spectral bleed-throughs. *Microsc. Res. Tech.* **68**:51-88

Fricker MD, Parsons A, Tlalka M, Blancaflor E, Gilroy S, Meyer A, Plieth RY (2001) Fluorescent probes for living plant cells, p. 35-84. In C Hawes and B Satiai-Jeunemaitre (ed.), *Plant Cell Biology*: A Practical Approach, 2nd ed. University Press Oxford, Oxford, UK

Förster T (1948) Zwischenmolekulare Energiewanderung und Fluoreszenz. *Ann. Phys.* **2**: 55-75

Gadd GM (1994) The growing fungus, *Signal Transd. Fungi* 183-210

Gadella TWJ, Van der Krogt GNM, Bisseling T (1999) GFP-based FRET microscopy in living plant cells. *Trends Plant Sci. update* **4**: 287-29

Galagan JE, Calvo SE, Borkovich KA, Selker EU, Read ND, Jaffe D, Fitzhugh W, Ma L, Smirnov S, Purcell S, Rehman B, Elkins T, Engels T, Wang S, Nielsen CB, Butler J, Endrizzi M, Qui D, Ianakiev P, Bell-Pedersen D, Nelson MA, Werner-Washburne M, Selitrennikoff CP, Kinsey JA, Braun EL, Zelter A, Schulte U, Kothe GO, Jedd G, Mewes W, Staben C, Marcotte E, Greenberg, D, Roy A, Foley K, Naylor J, Stange-Thomann N, Barrett R, Gnerre S, Kamal M, Kamvysselis M, Mauceli E, Bielke C, Rudd S, Frishman D, Krystofova S, Rasmussen C, Metzenberg RL, Perkins DD, Kroken S, Cogoni C, Macino, G., Catcheside D, Li W, Pratt RJ, Osmani SA, DeSouza CPC, Glass L, Orbach MJ, Berglund JA, Voelker R, Yarden O, Plamann M, Seiler S, Dunlap J., Radford A, Aramayo R, Natvig DO, Alex LA, Mannhaupt G, Ebbole DJ, Freitag M, Paulsen I, Sachs MS, Lander ES, Nusbaum C, Birren B (2003). The genome sequence of the filamentous fungus *Neurospora crassa. Nature* 422: 859-868

Gao DJ, Knight MR, Trewavas AJ, Sattelmacher B, Plieth C (2004) Self-reporting Arabidopsis expressing pH and [Ca^{2+}] indicators unveil ion dynamics in the cytoplasm and in the apoplast under abiotic stress. *Plant Phys.* **134**: 898-908

Gerritsen HC, de Grauw K (2001) One- and two-photon confocal fluorescence lifetime imaging and its applications. *Meth. Cell. Imaging*, Oxford University Press, New York. 309–323

Gerson DF and Burton AC (1976) The relation of cycling of intracellular pH to mitosis in the acellular slime mould Physarum polycephalum. *J. Cell Physiol.* **91**: 297-304

Gillies RJ and Deamer DW (1979) Intracellular pH changes during the cell cycle in *Tetrahymena. J. Cell Physiol.* **100**: 23-32

Grynkiewicz G, Poenie M, Tsien RY (1985) A new generation of Ca2+ indicators with greatly improved fluorescence properties. *J. Biol. Chem*. **260**:3440-3450

Harvey AR, Fletcher-Holmes DW, Gorman A, Altenbach K, Arlt J, Read ND (2005) Spectral imaging in a snapshot. *Proceedings of SPIE – Spectral Imaging: Instrumentation, Applications, and Analysis III* **5694**: 110-119

Haworth RS and Fliegel L (1993) Intracellular pH in *Schizosaccharomyces pombe* – comparison with *Saccharomyces cerevisiae. Mol. Cell. Biochem.* **124**: 131-140

Heim R, Prasher DC, Tsien RY (1994) Wavelength mutations and post translations autooxidation of green fluorescent protein. *PNAS* **91**: 12501-12504

Heim R, Tsien RY (1996) Engineering green fluorescent protein for improved brightness, longer wavelengths and fluorescence resonance energy transfer. *Curr. Biol.* **6**: 178-182

Hesse SJA, Ruijter GJG, Dijkema C, Visser J (2000) Measurement of intracellular (compartmental) pH by ^{31}P NMR in *Aspergillus niger*. *J. Biotech.* **77**: 5-15

Hesse SJA, Ruijter GJG, Dijkema C, Visser J (2002) Intracellular pH homeostasis in the filamentous fungus *Aspergillus niger*. *Eur. J. Biochem.* **269**: 3485-3494

Inouye S, Noguchi M, Sakaki Y, Takagi Y, Miyata T, Iwanaga S, Miyata T, Tsuji FI (1985) Cloning and sequence analysis of cDNA for luminescent protein aequorin. *PNAS* **82**: 3154-3158

Jankowski A, Kim JH, Collins RF, Daneman R, Walton P, Grinstein S (2001): In situ measurements of the pH of mammalian peroxisomes using the fluorescent protein pHluorin. *J. Biol. Chem.* **276**: 48748-48753

Jernejc K and Legiša M (2004) A drop of intracellular pH stimulates citric acid accumulation by some strains of *Aspergillus niger*. *J. Biotech.* **112**: 289-297

Jose M, Nair DK, Altrock WD, Dresbach T, Gundelfinger ED, Zuschratter W (2008) Investigating interactions mediated by the presynaptic protein bassoon in living cells by Foerster's resonance energy transfer and fluorescence lifetime imaging microscopy. *Biophys J* **94**, 1483-1496.

Karagiannis J, Young PG (2001): Intracellular pH homeostasis during cell –cycle progression and growth state transition in *Schizosacccharomyces pombe*. *J. Cell Sci.* **114**: 2929-2941

Kemnitz K, Pfeifer l, Ainbund MR (1997) Detector for multichannel spectroscopy and fluorescence lifetime imaging on the picosecond timescale. *Nucl. Intrum. Methods Phys. Res.* **397**: 86-87

Lakowicz JR, Szmacinski H (1996) Imaging Applications of Time-Resolved Fluorescence Spectroscopy. *Fluoresc. Imaging Spectrosc. Microsc.* **137**: 273-311

Leica Microsystems (2006) Spectral fluorescence lifetime imaging microscopy:

new dimensions with Leica TCS SP5. *Nat. Methods, Application note*

Li CJ, Heim R, Lu P, Tsien RY, Chang DC (1999) Dynamic redistribution of calmodulin in HeLa cells during cell division as revealed by a GFP-calmodulin fusion protein technique. *J. Cell Sci.* **112**: 1567-1577

Lyot B (1933) Optical apparatus with wide field using interference of polarized light. *C. R. Acad. Sci.* (Paris) **197**: 1593
Lyot B (1944) Filter monochromatique polarisant et ses applications en physique solaire. *Annu. Astrophys.* **7**: 32

Machen TE, Leigh MJ, Taylor C, Kimura T, Asano S, Moore HPH (2003) pH of TGN and recycling endosomes of H^+/K^+-ATPase-transfected HEK-293 cells: implications for pH regulation in the secretory pathway *Am. J. Physiol. – Cell Physiol.* **285** (1): C205 - C214

Miesenböck G, De Angelis DA, Rothman JE (1998) Visualizing secretion and synaptic transmission with pH-sensitive green fluorescent proteins. *Nature* **394**: 192-195

Miyawaki A, Griesbeck O, Heim R, Tsien RY (1999) Dynamic and quantitative Ca^{2+} measurements using improved cameleons. *Cell Biol.* **96**: 2135-2140

Miyawaki A, Llopis J, Heim R, McCafferty JM, Adams JA, Ikura M, Tsien RY (1997) Fluorescenct indicators for Ca^{2+} based on green fluorescent proteins and calmodulin. *Nature* **388**: 882-887

Millington M, Grindlay GJ, Altenbach K, Neely RK, Kolch W, Bencina M, Read ND, Jones AC, Dryden DTF, Magennis SW (2007) High-precision FLIM-FRET in fixed and living cells reveals hetgerogehneity in a simple CFP-YFP fusion protein. *Biophys. Chem.* **127**: 155-164

Moser MJ, Flory MR, Davis TN (1997) Calmodulin localizes to the spindle pole body of *Schizosaccharomyces pombe* and performs an essential function in chromosome segregation. *J. Cell Sci.* **110**: 1805-1812

Nagai T, Ibata K, Park ES, Kubota M, Mikoshiba K, Miyawaki A (2002): A variant of yellow fluorescent protein with fast and efficient maturation for cell-biological applications. *Nat. Biotech.* **20:** 87-90

Ohman Y (1938) A new monochromator. *Nature* **41**: 157, 291

Ohman Y (1958) On some new birefringent filter for solar research. *Ark. Astron.* **2**: 165

Okorokova Facanha LA, Appelgren H, Tabish M, Okorokov L, Ekwall K (2002) The endoplasmic reticulum cation P-type ATPase Cta4p is required for control of cell shape and microtubule dynamics. *J. Cell Biol.* **157**: 1029-1039

Ormö M, Cubitt A, Kallio K, Gross L, Tsien R, Remington S (1996) Crystal structure of the *Aequorea victoria* green fluorescent protein. *Science* **273**: 1392-1395

Parton RM, Fischer S, Malho R, Papasouliotis O, Jelitto TC, Leonard T, Read ND (1997) Pronounced cytoplasmic pH gradients are not required for tip growth in plant and fungal cells. *J. Cell Sci.* **110**: 1187-1198

Pel HJ et al. (2007) Genome sequencing and analysis of the versatile cell factory Aspergillus niger CBS 513.88. *Nat. Biotech.* **25**: 221-231.

Pena A, Ramirez J, Rosas G, Calahorra M (1995) Proton pumping and the internal pH of yeast cells, measured with pyranine introduced by electroporation. *J. Bact.* **177**: 1017-1022

Peterka et al (2005) Characterisation of metal-chelate methacrylate monoliths. *J. Chrom. A*

Piston DW and Kremers G (2007) Fluorescent protein FRET: the good, the bad and the ugly. *Trends Biochem. Sci.* **32**, 9-12

Plumridge A, Hesse SJA, Watson AJ, Lowe KC, Stratford M, Archer DB (2004) The Weak Acid Preservative Sorbic Acid Inhibits Conidial Germination and Mycelial Growth of *Aspergillus niger* Through Intracellular Acidification. *Appl. Environ. Microbiol.* **70**(6): 3506-3511

Pollok BA, Heim R (1999) Using GFP in FRET-based applications. *Trends Cell Biol.* **9**: 57-60

Rizzo MA, Springer GH, Granada B, Piston DW (2004) An improved cyan fluorescent protein variant useful for FRET. *Nat. Biotech.* **22** (4): 445-449

Ruijter GJG, Panneman H, Visser J (1997) Overexpression of phosphofructokinase and pyruvate kinase in citric acid-producing *Aspergillus niger*. *Biochim. Biophys. Acta* **1334**: 317-326

Sanders D, Pelloux J, Brownlee C, Harper JF (2002) Calcium at the Crossroads of Signalling. *The Plant Cell*: S401-S417

Schuldiner S and Rozengurt E (1982) Na+/H+ antiport in Swiss 3T3 cells:

mitogenic stimulation leads to cytoplasmic alkalinization. *PNAS* **79**: 7778-7782

Sekar RB, Periasamy A (2003) Fluorescence resonance energy transfer (FRET) microscopy imaging of live cell protein localizations. *J. Cell Biol.* **160**: 629-633 Additional: Online Supplemental Material 1-5

Serrano R, Ruiz A, Bernal D, Chambers JR, Ariño J (2002)The transcriptional response to alkaline pH in *Saccharomyces cerevisiae*: evidence for calcium-mediated signalling. *Mol. Microbiol.* **46**(5), 1319-1333

Shaw BD, Hoch HC (2001) Ions as Regulators of Growth and Development, *The Mycota VIII, Biology of the Fungal Cell*, Springer-Verlag Berlin Heidelberg

Shimomura O, Jhonson FH, Saiga Y (1963) Microdetermination of calcium by aequorin luminescence. *Science* **140**: 1339-1340

Shimomura O, Musickl B, Kishi Y (1988) Semi-synthetic aequorin: an improved tool for the measurement of calcium ion concentration. *Biochem. J.* **251**: 405-410

Stauffer TP, Ahn S, Meyer T (1998) Receptor-induced transient reduction in plasma membrane PtdIns(4,5)P_2 concentration monitored in living cells. *Curr. Biol.* **8:** 343–346

Tramier M, Gautier I, Piolot T, Ravalet S, Kemnitz K, Coppey JC, Durieux C, Mignotte V, Coppey-Moisan M (2002) Picosecond-hetero-FRET microscopy to probe protein-protein interactions in live cells. *Biophys. J.* **83**:3570-3577.

Truong K, Sawano A, Mizuno H, Hama H, Tong KI, Mal TK, Miyawaki A, Ikura M (2001) FRET-based *in vivo* Ca^{2+} imaging by a new calmodulin-GFP fusion molecule. *Nat. Struct. Biol.* **8**: 1069-1073

Tsien RY (1998) The Green Fluorescent Protein. *Ann. Rev. Biochem.* **67**: 509-544

Ward WW (1981) Properties of the coelenterate green-fluorescent proteins. *Bioluminescence and chemiluminescence*, Academic Press, New York: 235-242

Ward WW, Prentice HJ, Roth AF, Cody CW, Reeves SC (1982) Spectral perturbations of the *Aequorea* green-fluorescent protein. *Photochem. Photobiol.* **35**: 803-808

Webb SED(2003) Development and Application of Widefield Fluorescence Lifetime Imaging. *PhD thesis:* Imperial College of Science, Technology and Medicine, University of London

Xu X, Gerard ALV, Huang BCB, Anderson DC, Payan DG , Luo Y (1998) Detection of programmed cell death using fluorescence energy transfer. *Nucleic Acids Res.* **26**: 2034-2035

Yang F, Moss LG, Phillips GN (1996) The molecular structure of green fluorescent protein. *Nat. Biotech.* **14**: 1246-1251

Yoshida T, Toda T, Yanagida M (1994) A calcineurin-like gene *ppb1*$^{+}$ in fission yeast, mutant defects in cytokinesis, cell polarity, mating and spindle pole body positioning. *J. Cell Sci.* **107**: 1725-1735

Youvan DC et al (1997) Calibration of fluorescence resonance energy transfer in microscopy using genetically engineered GFP derivatives on nickel chelating beads. Biotechnol. et al. **3**: 1-18

Zaccolo M, De Giorgi F, Cho CY, Feng L, Knapp T, Negulescu PA, Taylor SS, Tsien RY, Pozzan T (2000) A genetically encoded, fluorescent indicator for cyclic AMP in living cells. *Nat. Cell Biol.* **2**: 25−29

Zaccolo M, Pozzan T (2000) Imaging signal transduction in living cells with GFP-based probes. *IUBM Life* **49**: 375-379

Zapata-Hommer O and Griesbeck O (2003) Efficiently folding and circularly permuted variants of the Sapphire mutant of GFP. *BMC Biotechnol*. **3**, 5

Zelter A, Benčina M, Bowman BJ, Yarden O, Read ND (2004) A comparative genomic analysis of the calcium signaling machinery in *Neurospora crassa*, *Magnaporthe grisea* and *Saccharomyces cerevisiae. Fungal Gen. Biol.* **41**: 827-841